Strahlungsmessungen und synoptische Beobachtungen
in Ny-Ålesund

Radiation Measurements and Synoptic Observations at Ny-Ålesund

Heike Kupfer, Andreas Herber, Gert König-Langlo

This data report is a continuing work basing of the diploma thesis
„Variation der Strahlungsgrößen und meteorologischen Parameter an der BSRN-Station Ny-Ålesund/ Spitzbergen 1993 - 2002“ (Variation of the Radiation and Meteorological Parameters of the BSRN-Station Ny-Ålesund/ Spitsbergen 1993 – 2002)
by Heike Kupfer, which was submitted at the Department of Geography of the Friedrich-Schiller-University in Jena.

Dieser Datenreport ist eine weiterführende Arbeit basierend auf der Diplomarbeit
„Variation der Strahlungsgrößen und meteorologischen Parameter an der BSRN-Station Ny-Ålesund/ Spitzbergen 1993 - 2002“
von Heike Kupfer, die 2003 am Institut für Geographie der Friedrich-Schiller-Universität Jena vorgelegt wurde.

Heike Kupfer

Freie Universität Berlin
Institut für Meteorologie
Carl-Heinrich-Becker-Weg 6-10
12165 Berlin

Tel.: (030) 838 71152
Email: Heike_Kupfer@yahoo.de

Index

Zusammenfassung

Das weltweite Baseline Surface Radiation Network (BSRN) dient der Erforschung des Klimawandels. Die deutsch - französische Forschungsbasis AWIPEV Ny-Ålesund/ Spitzbergen gehört seit 1992 zum BSRN- Netzwerk. An ihr werden meteorologische- und Strahlungsmessungen durchgeführt. Die synoptischen Beobachtungen werden vom Norwegischen Polarinstitut (NPI) übernommen.
Diese Arbeit ist die erste ausführliche Analyse von Strahlungs – und meteorologischen Daten, die an dieser BSRN- Station aufgenommen wurden.
Durch die Unterstützung des NPI und des Norwegischen Meteorologischen Institutes (DNMI) war eine Erweiterung der Koldewey-Reihe (1993-2002) in einem größeren Zeitraum möglich.
Für eine solche Trendanalyse standen Strahlungsdaten von 1974 bis 1992 sowie meteorologische WMO Standardwerte von 1931-60 und 1961-90 zur Verfügung. Diese Langzeit-Datenreihen waren nötig um gesicherte Aussagen über die klimatische Entwicklung in Ny-Ålesund zu treffen.
In den Wintermonaten übten die großen Druck- und Temperaturunterschiede von warmen Luftmassen im Süden und kalten Luftmassen im Norden einen erheblichen Einfluss auf das Wettergeschehen in Ny-Ålesund aus. Kalte, polare Luft wird mit Hochdruckgebieten vom Polarmeer nach Spitzbergen transportiert. Der Energieverlust im Winter ist leicht niedriger als der Energiegewinn im Sommer. Somit liegt die Strahlungsbilanz mit 1.4 W/m² im leicht positiven Bereich.
In der Polarnacht traten starke Temperaturschwankungen zwischen 7°C und -35°C auf, während in den Sommermonaten relativ konstante Temperaturen um 5°C herrschten. Das Jahresmittel der Koldewey-Reihe beträgt -5.1°C und ist damit um 0.8K niedriger als das Jahresmittel der Standardreihe von 1931-60 und um 0.7K höher als das Jahresmittel der Standardreihe von 1961–90. Der leichte Temperaturanstieg im Untersuchungszeitraum kann jedoch nicht mit der Strahlungsbilanz erklärt werden, da diese im Zeitraum 1974-2001 deutlich abnahm. Mögliche Ursachen für die Erwärmung können dynamische Prozesse, wie der verstärkte Transport von warmen Luft- oder Wassermassen nach Spitzbergen oder der länger eisfrei bleibende Kongsfjord sein.
Während der letzten Jahre konnte ein deutlicher Temperaturanstieg im Winter verzeichnet werden; vor allem im Januar mit einem Anstieg von 5.9K. Zwischen 1915 und Mitte der 20er Jahre war ein Anstieg der Wintertemperatur von 8K zu beobachten. Seit den 30er Jahren konnten dekadische Temperaturschwankungen der Jahresmittel festgestellt werden.
Diese periodischen Temperaturschwankungen können auf der unterschiedlichen Ausprägung der Arktischen Oszillation (AO) beruhen. Positive und negative Phase der AO wechseln sich in unregelmäßigen Intervallen von wenigen Tagen bis einigen Monaten ab. Wenn aber das Phänomen über Jahre und Jahrzehnte betrachtet wird, dominiert immer nur eine Phase, womit sich auch die dekadischen Temperaturschwankungen in Ny-Ålesund erklären lassen. Diese dekadischen Schwankungen der Phasen der AO stehen nach SCHULZ (2001) im signifikanten Zusammenhang mit dem 11-jährigen Sonnenfleckenzyklus.
Eine Auswertung der meteorologischen Größen und Strahlungsparametern in einem Zeitraum von 8 bzw. 9 Jahren ist für eine ausführliche Klimaanalyse zu kurz, es können jedoch Trends aufgezeichnet werden. Mit Hilfe historischer Daten des DNMI sowie des NPI war es möglich, klimatische Tendenzen zu erkennen.

Abstract

The global Baseline Surface Radiation Network (BSRN) serves for the detection of climate change. Since 1992 the German – French Research Base AWIPEV Ny-Ålesund/Spitsbergen belongs to the BSRN. Measurements of radiation and meteorological parameters and synoptic observations (Norwegian Polar Institute NP) are carried out. This is the first extensive analysis of radiation and meteorologic data of this station.
An extension of the Koldewey data series (1993-2002) with long-term means could be realized by the assistance of the NPI and the Norwegian Meteorological Institute (DNMI).
For such a trend analysis the long-term radiation data were available from 1974-1992 and the meteorological WMO normals 1931-60 and 1961-90. These long-term data series are required for secured statements about the climatic development in Ny-Ålesund.
In winter the differences between warm air masses from the south and cold air masses from the north influence the weather in Ny-Ålesund. Cold and dry air is brought to Spitsbergen by high-pressure areas from the polar sea. The energy loss in winter is slightly less than the energy gain in summer. The annual mean energy budget is positive with 1.4 W/m².
During the polar night, the temperature showed variations between 7°C and -35°C, while in the summer months the temperatures were constant about 5°C. The yearly mean temperature of the Koldewey data series is -5.1°C. It is 0.7K higher than the mean of the 1961–90 normal and 0.8K lower than the mean of the 1931-60 normal. A significance of this temperature trend could not be found. The budget decreased during the years 1974-2001 and cannot be the reason of this slight temperature rise. Possible causes for the warming could be dynamic processes like an extended warm air- and water transport. ´
A clear temperature rise during the winter months of the latest years was found while especially in January where the averages increased for 5.9K. Between 1915 and the mid 1920ies a rise of the winter temperatures of 8K was observed. The decadic variations of the temperature trends are obvious since the 1930ies.
These periodic temperature fluctuations may be based on the different extend of the Arctic Oscillation (AO). These phases alternate in irregular intervals reaching from a few days to some months. But when the phenomenon is watched over years and decades, there is always one of the states dominating, which may explain the decadal fluctuations of the temperature. These decadal variations of the phases of the AO are standing in significant relationship with the 11-year cycle of high and low intensity of solar activity.
The evaluation of the meteorologic - and radiation parameters in the observation period of 8 and 9 years gives some trends but it is too short for a detailed climatologic analysis. Nevertheless, by using historical data of the DNMI and the NPI, climatologic trends could be estimated.

Acknowledgements

This data report extends my diploma thesis. For the help and assistance I thank to K. Dethloff, R. Neuber, S. Debatin and K. Benkenstein from the Alfred-Wegener-Institute as well as R. Mäusbacher of the Friedrich-Schiller-University Jena. I would also like to thank M. Wolff, H. Poetschik, J. Kube, Y. Kramer and S. Luetzenkirchen who provided me with informations, pictures and GPS-data and supported me during my stay in Ny-Ålesund. Many thanks also to the administrators H. Gericke from the AWI Potsdam, H. Liegmahl-Piper from the AWI-Bremerhaven and M. Kuhne from the MFPA Weimar for making connection with the database MISAWI in Bremerhaven. I am especially thankful to J. Børre-Ørbaek, V. Hisdal, T. Vinje and T. Villinger of the Norwegian Polar Institute as well as I. Hanssen-Bauer, M. Skogh and G .A. Dalsbø of the DNMI for providing me with so much helpful literature and data which made a long-term trend analysis and a comparison with the BSRN data possible.

Berlin, May 2006

Heike Kupfer

Acronyms

Ac	=	cloudtype - Altocumulus
AWI	=	Alfred-Wegener-Institut for Polar and Marine Research
AO	=	Arctic Oscillation
BSRN	=	Baseline Surface Radiation Network
Cb	=	cloudtype – Cumulunimbus
C_H	=	high clouds
C_L	=	low clouds
C_M	=	medium-high clouds
Cu	=	cloudtype - Cumulus
DIN	=	German Institute for Standardisation
DNMI	=	Det Norske Meteorologiske Institutt (Norwegian Meteorological Institute)
DWD	=	Deutscher Wetterdienst (German Weather Service)
E	=	treeless polar climates (climate zone)
ECC	=	electrochemical-concentration-cell
ED	=	European Date
EF	=	Ice-climates (climate zone)
ESRO	=	European Space Research Organisation
ETHZ	=	Eidgenössische Technische Hochschule Zürich (Technical University Zurich)
ET	=	Tundra-climates (climate zone)
FTP	=	File Transfer Protocol
GPS	=	Global Positioning System
ICSU	=	International Council of Scientific Unions
IOC	=	Intergovernmental Oceanographic Commission
IR	=	infrarred
LIDAR	=	Light Detection and Ranging
MISAWI	=	Meteorological Information System of the AWI
MISU	=	Meterologiscal Institute of the University of Stockholm
NDSC	=	Network for Detection of Stratospheric Change
NIP	=	Normal Incidence Pyrheliometer
NPI	=	Norsk Polarinstitutt (Norwegian Polar Institute)
OG	=	orange glass
PIR	=	Precision Infrared Radiometer
r.H.	=	relative Humidity
RG	=	red glass
SA	=	sunrise
Sc	=	cloudtype - Stratocumulus
SQL	=	Structured Query Language
St	=	cloudtype - Stratus
SU	=	sunset
UTC	=	Universal Time Coordinated
UV	=	ultraviolett
VDI	=	Vereinigung Deutscher Ingenieure (Unity of German Engineers)
WCRP	=	World Climate Research Programme
WMO	=	World Meteorological Organization
WRMC	=	World Radiation Monitoring Center

1 Introduction

The German polar science was founded in 1868/69 with the first arctic scientific voyage by Carl Koldewey with the Norwegian vessel „Greenland“. During his voyage he was able to reach the west-coast of Spitsbergen at a latitude of 81°05’ north (LANGE 2001). Ny-Ålesund (78°55’ N, 11°56’ E) was used as the point of departure for Roald Amundsens, Umberto Nobiles and Lincoln Ellsworths flight over the Northpole with the Zeppelin „Norge“ in 1926, which made the place world famous. The Norwegian Kings Bay Kull Komp. started coal mining activity (HISDAL 1998) in 1916. Since the mid 20ies meteorological observations have been undertaken, but not on a regular basis. Two scientific excursions to Ny-Ålesund and its surroundings were performed by the Nationalkommitee für Geodäsie und Geophysik (“National Committee for Geodesy and Geophysics” of the Academy of sciences of the GDR) Berlin in 1962-66. During these scientific missions, several meteorological, glaciological, cartographical and radiation measurements were done around the glaciers Kongsbreen and Midre Lovenbreen. (National Committee for Geodesy and Geophysics of the GDR 1962, 1965/66). However, the recordings were only taken over a short period and could not be used for this evaluation. Irregular meteorological measurements were also taken by the Kings Bay Kull Komp. and ESRO (European Space Research Organisation) Telemetry Station between the years 1950 and 1953, as well as in 1961 and 1968 respectively. Since 1969 regular meteorological observations were taken by the Norwegian ESRO-station, situated about 1,7 km southeast of Ny-Ålesund. The measurement programme was continued in 1974 by the Norsk Polarinstitutt (Norwegian Polarinstitute) which maintains a permanent station in Ny-Ålesund since 1968 (FØRLAND et al. 1997). In 1988 the German arctic station in Ny-Ålesund was set up. It was named after the first German arctic polar scientist, Carl Koldewey. Since 2003 the station is called German – French Research Base AWIPEV. At this station, atmospheric, biologic and geophysical research is carried out within the scope of continious observations or short-termed campaigns. The station pays special concentration to the research of the atmosphere by launching rawin- and ozone sondes, performing radiation measurements and the spectroscopic detection of aerosols and trace gases. Two global networks for the exploration of the global change are a central for the atmospheric long-term observations: the NDSC (Network for Detection of Stratospheric Change) and the BSRN (Baseline Surface Radiation Network) (LANGE 2001).

The decrease of the polar ozone layer, the melting of polar ice, the anthropogenic influence of the atmosphere with aerosols and greenhouse gases are only a few of the topics in climate research, which can be studied in international cooperation only. In order to make global comparisons the evaluations for the instruments and measurement methods global standards have been created. Therefore the World Climate Research Programme (WCRP) in cooperation with the World Meteorological Organization (WMO), the International Council of Scientific Unions (ICSU) and the Intergovernmental Oceanographic Commission (IOC) of the UNESCO founded the Baseline Surface Radiation Network (BSRN) in the field of radiation research at the end of the 80s. The concept of BSRN was developed for the observation of climatic change and for the validation of satellite data. Special interest is focussed to the net radiation balance at the earth’s surface and the radiation transfer through the atmosphere. The network guarantees a homogeneous, continuous and long-term measurement of meteorological parameters and radiation data as well as it gives the possibility to record the global radiation field and to detect its changes.

Another aim of BSRN is to monitor local and regional tendencies in the radiation flux at the earth’s surface. Many climatic changes can be explained with changes in the radiation

field. In 2004 the network includes 36 operating stations, 4 pending stations and 2 candidating stations. The stations are distributed all over the world in all climate zones 79° north to 90° south and from 157° west up to 168° east. The 16 operational stations regularly measure meteorological parameters and radiation data in high temporal resolution.

All of the data collected by the stations are archieved in the BSRN- data base, currently maintained by the WCRP at the ETH Zürich (McARTHUR 2000). The BSRN-website (http://bsrn.ethz.ch) gives a good overview over every single station and provides some more general information of the network, the organisations behind and its publications. It also offers the chance to order data from the network for analysis.

The German – French Research Base AWIPEV at Ny-Ålesund, Svalbard joined the BSRN in 1992. The instruments, recording frequencies and data control, are determined by guidelines defined by a coordination group of the BSRN and the WMO. The Koldewey-Station data is firstly included in the databank of the Meteorological Information System of the Alfred-Wegener-Institutes (MISAWI) where the data are tested and validated with WMO-standards, before it is transferred to the BSRN-data base (s. Chapter 3.2).

This work is based on the data of the BSRN-station in Ny-Ålesund. It is aimed to examine the changes of the meteorological parameters and the radiation data between the years 1993 and 2002. Long-term data rows were included in order to detect climatic changes in Ny-Ålesund. The analysis is carried out with the help of the meteorological data base of the Alfred Wegener Institute „MISAWI“.

2 Regional Climate of Svalbard

2.1 Geographic Location

Spitsbergen is the biggest island of the Svalbard archipelago which is politically controlled by Norway. Svalbard has an extension between 74° - 81° northern latitude and 10° - 35° eastern longitude (s. Fig. 2.1).

Spitsbergens landscape is dominated by glaciers and the continuous permafrost. The changes of polar day and polar night determine its climate. The ecology of these regions is very sensitive towards climatic change; therefore the climate research of the polar regions is of special interest.

Fig. 2.1: Overview over the Svalbard archipelago ([Web1] source: CIA World Factbook 2001)

2.2 Climate of Svalbard

According to the definition by KÖPPEN a polar climate is given when the mean temperature of the warmest month is less than 10°C. Within the „treeless polar climates" (E) he has made more differentiations with the ice climate (EF), where the temperature sinks under the freezing point and the tundra climate (ET), where the mean temperature of at least one month is above 0°C. Svalbard is situated far within the 10°C July-Isotherm, still the temperature rises in one month at least above the freezing point. Svalbard is assigned to the polar tundra climate zone (ET) according the KÖPPEN-classification (FØRLAND et al. 1997, LAUER 1993).

2.3 Ocean Currents, Air-mass Transport and Polar Sea-ice

The climate of Spitsbergen is determined by the high air pressure areas of Greenland and the Arctic Ocean as well as by a deep pressure area near Iceland (FØRLAND et al. 1997). Westerly and south-westerly winds dominate between Iceland and Norway which bring mild air towards Svalbard. In the Northeast of Svalbard the air masses are transported anti-cyclonically with easterly and north-easterly winds. This is the reason for high temperature differences of up to 30°C at Svalbard in winter. (HISDAL 1998).
The most important ocean current that influences Svalbard is the warm „West-Spitsbergen current", a side-arm of the Gulf stream, which is coming from the south and determines the climate especially in the west of Svalbard. It creates the northernmost pack-ice free place of the world northwest of Svalbard. Cold Arctic Ocean currents pass Spitsbergen on their way to the south in the west along the coast of Greenland and at the eastern coast of Svalbard.

The warm „West-Spitsbergen current", a side-arm of the Gulf-stream, and the mild air masses cause a relative warm climate in Svalbard. The mean winter temperature of the western Svalbard station Isfjord Radio is about 20°C higher than the one at the Canadian station Isachsen, which is situated at the same latitude (HISDAL 1998).

The course of the polar sea ice rim shows an obvious shift northwards in April of the years 1866, 1966 und 1995 (s. Fig. 2.2).

The sea-ice conditions in front of the west-coast of Spitsbergen depend on the influence of the warm and cold ocean currents in the seasonal change. The sea-ice rim reaches its maximum extension in April and its minimum extension in September (VINJE 1984). Between February and April the Fjords of the west-coast regularly freeze and cause a slight continental climate in the „inner-fjord-areas“(HANSSEN-BAUER et al. 1990, HISDAL 1985).

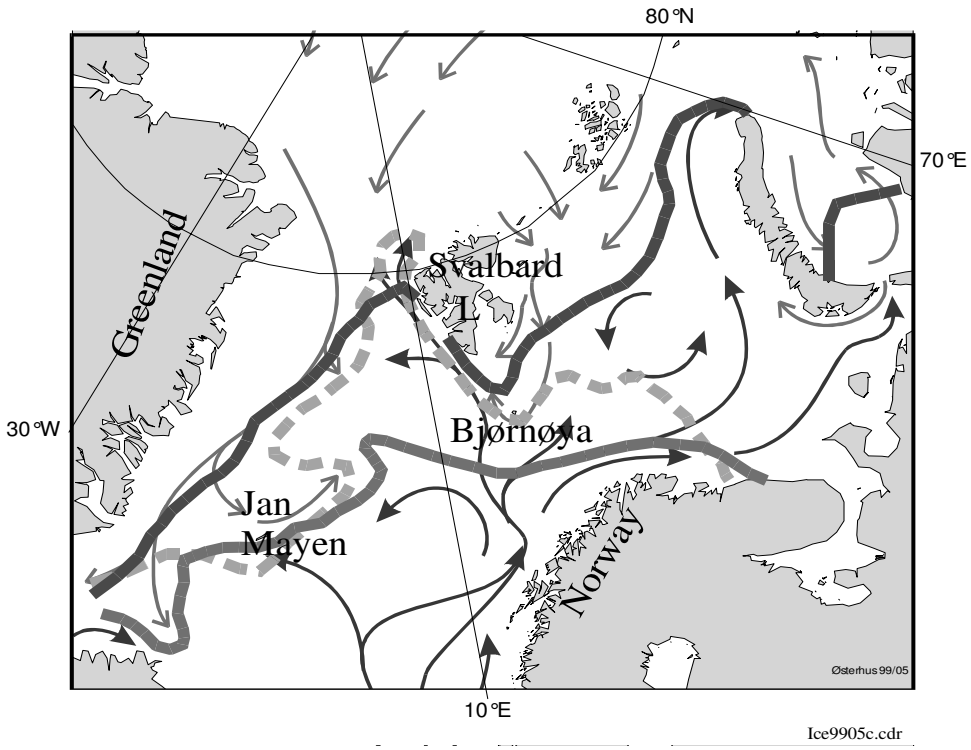

Fig. 2.2: Ocean currents and polar sea-ice rim (April) grey line: 1866, dashed: 1966, dark: 1996) in the Svalbard region (VINJE 2000)

2.4 Local Climate of Ny-Ålesund

Ny-Ålesund is located at 78°55' northern latitude and 11°56' eastern longitude and is the northernmost steady settlement of the earth. The village is situated in the north of the Brøggerhalvøya (Brøgger peninsula) and borders directly on the Kongsfjorden (Kingsfjord) in the north (s. Appendix A2). In the south of the village the 554 m high Zeppelin mountain shades the place for several weeks in spring and fall.

In the southwest the name-giving glacier of the peninsula, the Brøggerbreen (norw.: Breen = glacier) mouths over the Bayelva-runoff in the Kongsfjord. The Zeppelin mountain covers the village from the influence of the Brøggerbreen. About 15 km east, at the end of the Kongsfjorden the Kongsbreen calves into the fjord in a length of 10 kms. This glacier has with the fjord the most important climatic influence on Ny-Ålesund. Cold catabatic winds with mainly high velocities carry snow, dust and saltwater particles towards the mouth of the fjord. Solid snow dunes in N-S-direction around Ny-Ålesund and low snow heights close to the glacier show the evidence of these winds.

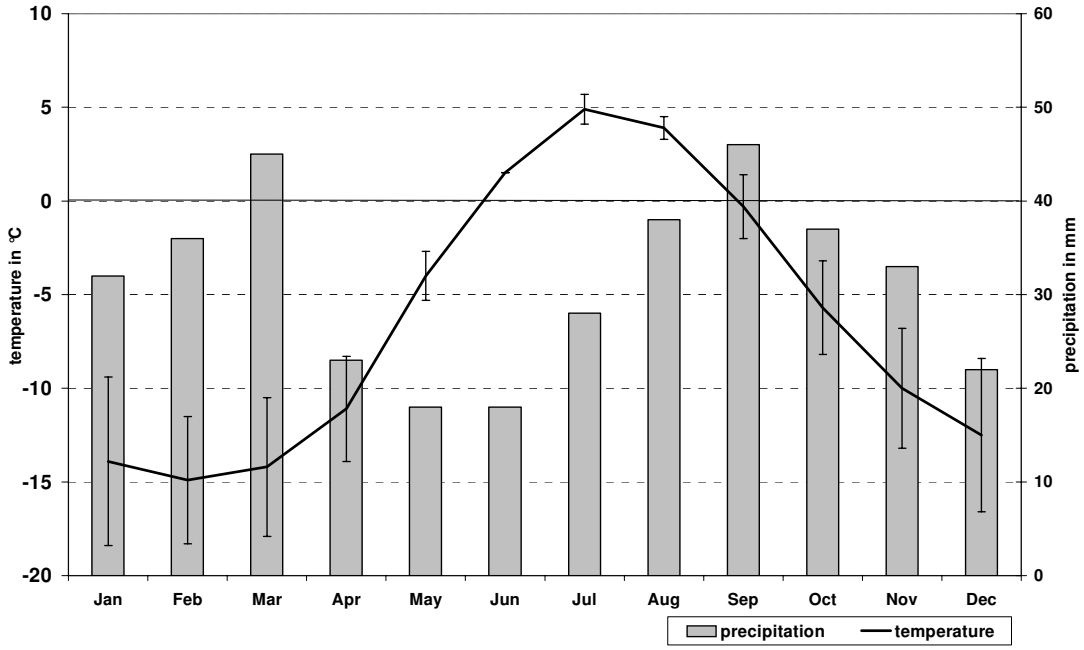

Fig. 2.3: Climate (temperature and precipitation) of Ny-Ålesund according the WMO normals of 1961-1990

On the Kongsfjord a thick and closed ice crust is only developed rarely, mainly caused by the warming of the „West-Spitsbergen current". The winterly snow cover of about 1 m is totally melting during only a few weeks in June. The soil is characterized by a thaw layer from a few decimetres to a meter in the summer months (ROTH and BOIKE 2001). Still the soil keeps frozen until a depth of a few 100 m all year round (LIESØL in BOIKE 2003). The highest temperatures in Ny-Ålesund according the WMO (1961 - 1990) normals were reached in July and the lowest in February (s. Fig. 2.3). In this period the average annual temperature was at -6,3 °C and the mean annual precipitation at 385 mm/a. The months with the most precipitation are March and September with 45 and 46 mm, which mainly falls as snow. The lowest amounts of precipitation were measured in May and June with 18 mm average, which is mainly rain. Between 1975 and 1996 have been observed: 25 % rain, 44 % snow and 31 % a mixture of snow and rain. Rain and snow can occur in every month of the year. According BLÜMEL, EBERLE (2001) and the WMO normals for Ny-Ålesund between 1961 - 1990 an even precipitation balance could be found between the summer months (May – October) with 185 mm and the winter months (November - April) with 191mm. The evaporation is much higher than the precipitation during the summer months. An exact precipitation measurement is very complicated in these latitudes, because snowfall and snowdrift often occurs together (FØRLAND et al. 1997, 2000).

3 BSRN Site Ny-Ålesund

3.1 Measured Quantities

The BSRN-station (Baseline Surface Radiation Network) Ny-Ålesund records radiation and meteorological data within the worldwide network organized by the WMO. The components of the station are the radiation station, a ceilometer, a meteorological tower and the launching facility for rawin and ozone sondes. The location of the measuring stations is shown in Appendix 3.

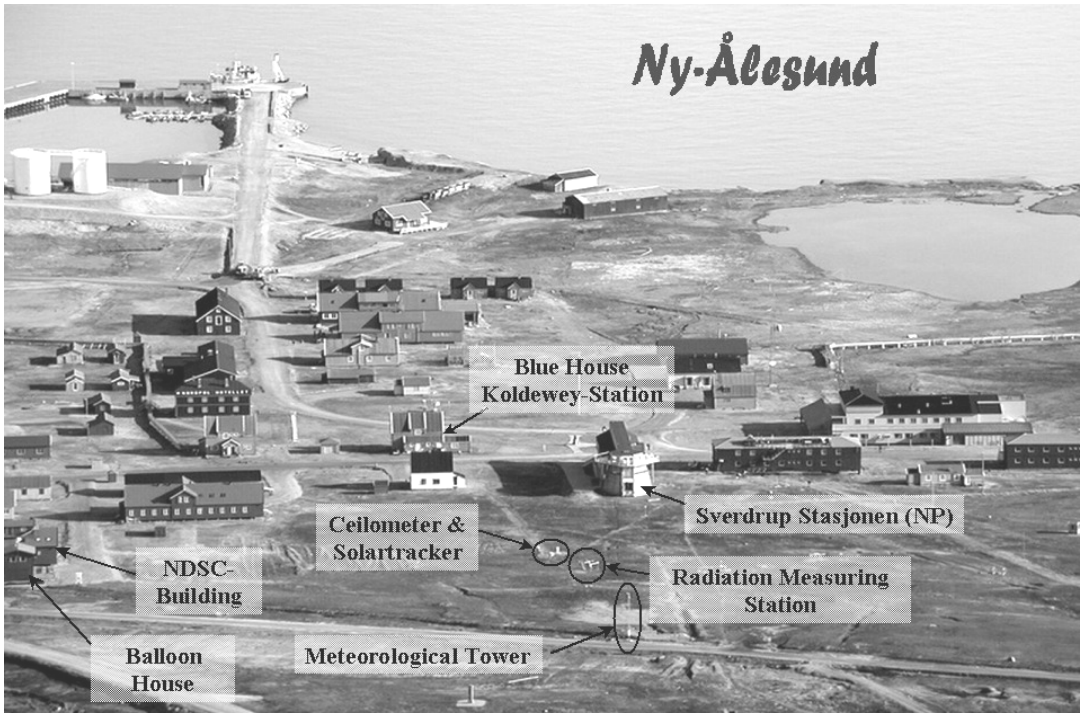

Fig. 3.1: The position of the BSRN station within the village Ny-Ålesund

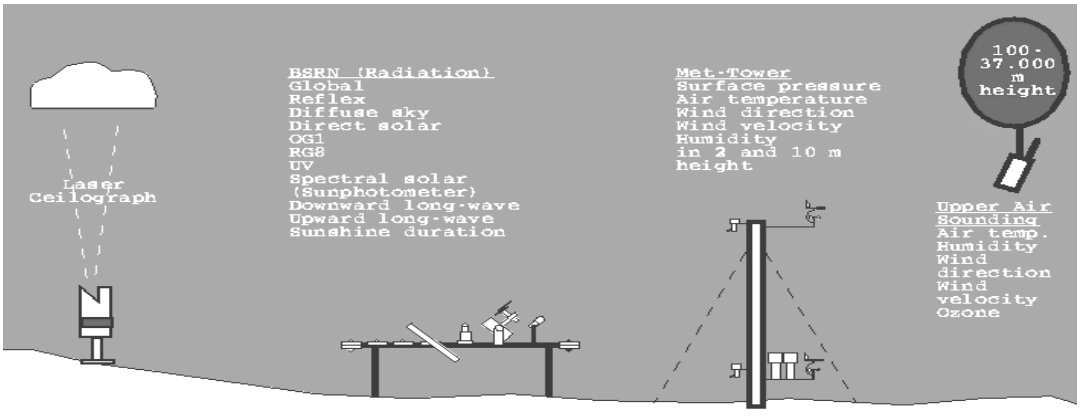

Fig. 3.2: Measuring instruments and measured values of the the BSRN-Station in Ny-Ålesund (KOENIG-LANGLO 2002)

The radiation data are recorded since 30th August 1992. The measurements of the meteorological tower with sensors for temperature, air pressure, relative humidity and wind started one year later in summer 1993. In the first phase the measurements were recorded with a time resolution of one-minute and data storage as 5-minute averages. Since 1998 a new data acquisition system made a sample time of 2 seconds and an

averaging period of one minute possible. The instruments of the BSRN-station and their relevant measurement parameters are shown in Fig. 3.2.

3.1.1 Radiation Measurements

The radiation site (see Fig. 3.3) accommodates upward and downward directed pyranometer to measure the global radiation, short wave reflex radiation as well as filtered short wave radiation (that contains the wavelength range from 530 to 2800 nm [OG8-orange glass filter] and the range from 695 to 2800 nm [RG1-red glass filter]). The instruments for the filtered short wave radiation do not belong to the BSRN network; their data are used by the Alfred-Wegener-Institute for specific computations only. Furthermore, the radiation site includes a pyrgeometer[2)] (directed downward) to measure of long wave thermal outgoing radiation of the earth surface, a Solar 111[3)] to measure the sunshine duration as well as an UV measuring instrument. An upward directed pyranometer for the measurement of the diffuse short wave radiation and a upward directed pyrgeometer to measure the long wave incomming radiation (counter radiation) (see Fig. 3.4) are installed at the solar tracker. Both instruments are protected by shading balls from direct solar radiation.

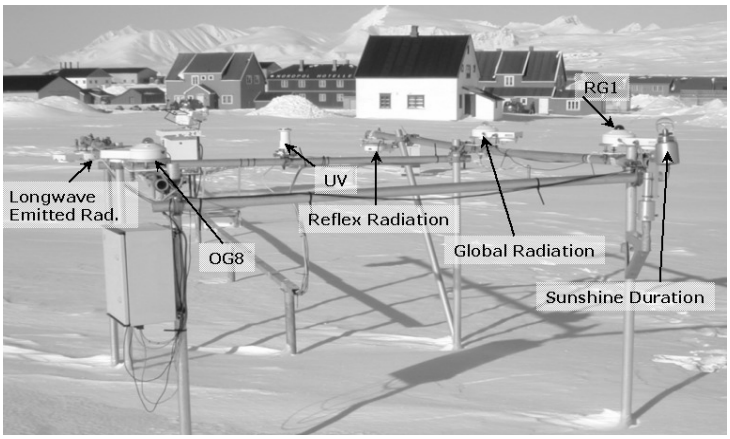

Fig. 3.3: Radiation site in Ny-Ålesund

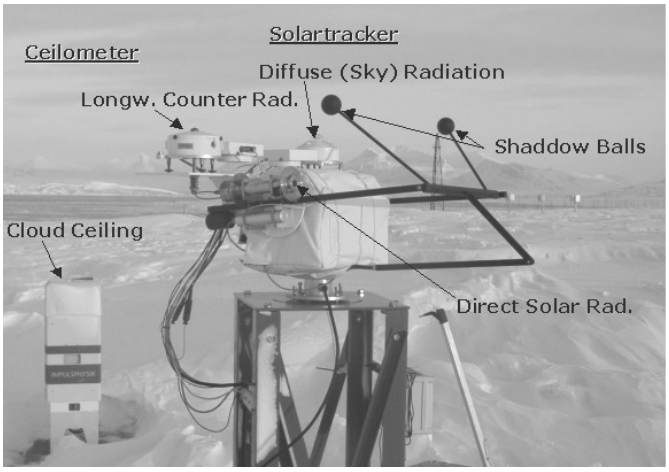

Fig. 3.4: Solartracker and ceilometer

The direct solar radiation is measured by the Normal Incidence Pyrheliometer (NIP), which is installed laterally at the solar tracker. The adjustment of the biaxial solar tracker is calculated by computations of the sun position (passive mode).

Small deviations from the computed sun position can be corrected with a 4-quadranten-diode (active mode) (McARTHUR 2000²). A sun photometer is installed at the solar tracker in order to measure the optical thickness of atmospheric aerosol. The data of the sun photometer do not enter the BSRN database yet, although they are part of the BSRN strategy.

Pyranometer (Fig. 3.5): Pyranometers are used to measure diffuse radiation, reflex radiation and global radiation fluxes. The radiation heats a blackened receiving area, which is protected against weather influences by a glass dome (McARTHUR 2000[2]). The pyranometer CM11 converts the temperature rise at the black surface versus the instrument body using a thermopile into a thermo voltage.

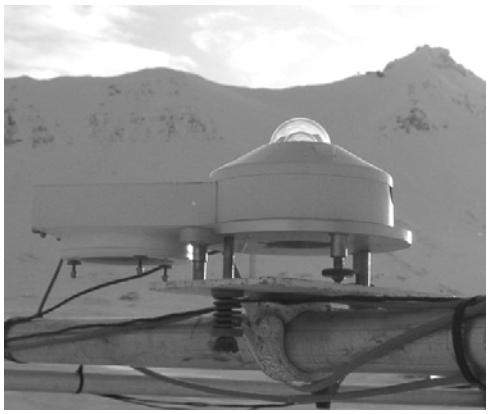

Fig. 3.5: Pyranometer (global radiation)

The CM11 is spectrally sensitive within the range of 0.3 – 3 µm which covers the full solar spectrum. A white screen prevents an overheat of the equipment. Additionally, a fan is mounted in the instrument to avoid the deposition of hoarfrost and dew as well as the heating of the dome. The instruments for the measurement of the diffuse radiation and global radiation set up in an upward direction. A downward directed pyranometer for the measurement of the short-wave reflex radiation, is installed at the radiation station. The measuring deviation of the instrument is indicated with approx. ± 2 % (Kipp & Zonen CM11 technical manual, VDI 3786/5) .

Pyrgeometer (Fig. 3.6): The Precision Infrared radiometer (PIR) is used for the separate measurement of long-wave emitted radiation and counter radiation. The long-wave rate of radiation penetrates through the dome, and is measured by absorption of the radiation on a black surface with a thermopile. The pyrgeometer operates in a wavelength range of 4 – 50 µm where the measuring devation is approx. ±1 % (Eppley PIR technical manual, McARTHUR 2000). The long wave emitted radiation is measured with a downward directed pyrgeometer (see Fig. 3.3) while the counter radiation is measured at the solar tracker with an upward directed pyrgeometer that is shaded against direct sunshine (see Fig. 3.4).

Fig.3.6: Pyrgeometer (longwave emitted radiation)

Sunshine detector (Fig. 3.7): The sunshine detector Solar 111 is adjusted in a way that the instrument axes corresponds with the geographical latitude of Ny-Ålesund (78.92°). The instrument contains 6 solar cells, around which an aperture rotates. Because of this rotation the aperture always covers a small section of the sky, and the solar cell output within this section is reduced. During sunless days the changes in the output signal are small. Is the sun located in the covered segment, the output signal of the solar cells is reduced to the

Fig.3.7: Sunshine detector

entire portion of the direct irradiation. The amplitude of the resulting impulse is the unit for the direct insolation power and can be compared with an adjustable threshold value (Haenni Solar 111 technical manual). The Solar 111 is equipped with a heating and a thermostat, to protect the instrument from freezing under these harsh Arctic conditions; the measuring deviation lies at ± 2 %.

Normal Incidence Pyrheliometer (NIP) (Fig. 3.8): The Normal Incidence Pyrheliometer measures the direct solar radiation in the incidence angle of the sun within a spectral range of 0.3 – 3 µm. The radiation penetrates the instrument through a 1 mm thick infrasil window (quartz glass) in an aperture-tube and is absorbed by a black receiving area. The increase of temperature in opposition to the instrument temperature is converted into a thermovoltage by a thermopile and recorded as a measuring signal. The incident radiation is measured within an entry angle of 5°. At both sides of the tubus flanges are mounted, which make an exact alignment towards the sun possible. Malfunctions may arise by contamination of the window as well as by deposits of dew and hoar frost. The NIP at the station in Ny-Ålesund belongs to the WMO first-class standards with a measuring devation of ± 2 %. Because of the temperature sensitivity of the NIP (temperature range <-20 – +40°C), it is removed from the solar tracker during the polar night and only reinstalled with return of the sun (see Fig. 3.4) (Eppley technical manual, VDI 3786/5).

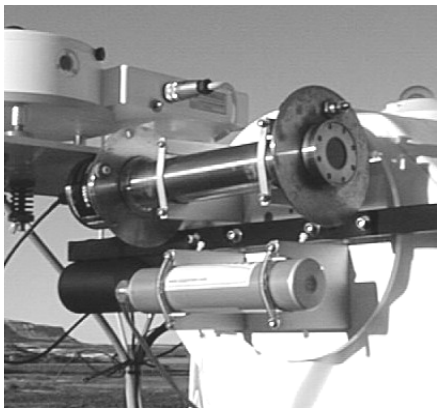

Fig.3.8: Normal Incidence Pyrheliometer (NIP)

3.1.2 Meteorological Measurements

Temperature, wind direction and wind velocity are measured at the meteorological tower in a height of 2 m and 10 m, while the relative humidity is only measured in 2 m height. The sensors are installed on instrument holders in a way that they are not influenced or shaded by the tower. The meteorological tower is located approximately 100 m southwest of the radiation site (see Fig. 3.9).

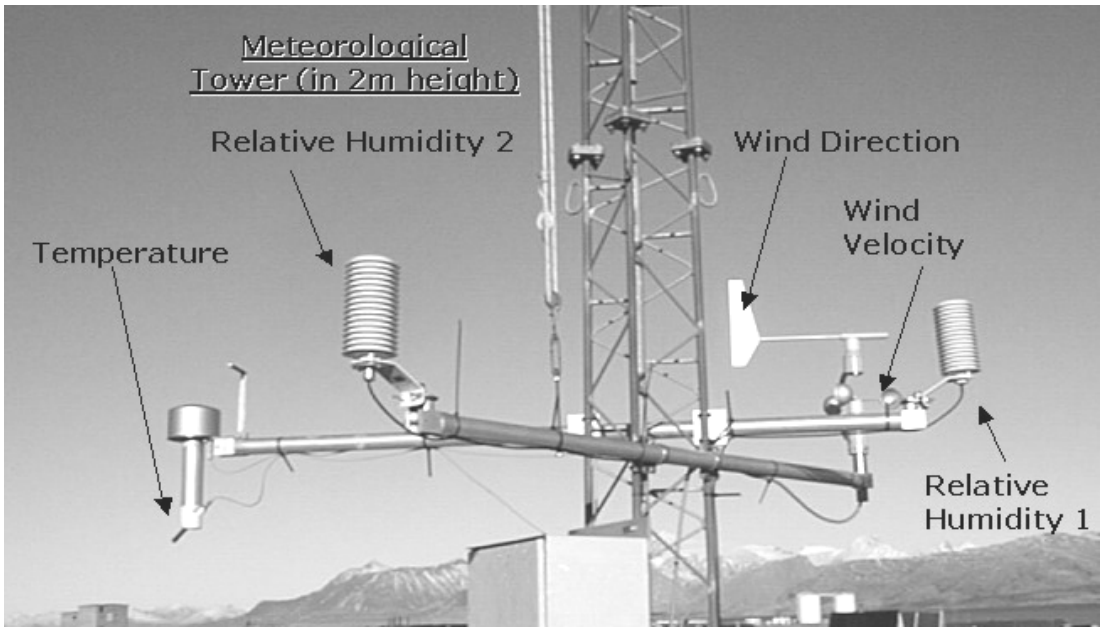

Fig. 3.9: Measuring sensors at the meteorological tower in 2 m height (Ny-Ålesund in summer 2002)

Temperature: The temperatures of the BSRN station are measured by resistance thermometers PT-100 (Thies 2.1265.10), which are protected from direct insolation. Air is sucked in by a fan and directed towards the measuring resistor. The measuring range of the PT-100 is from <-30 °C to +80 with a devation of approximately ± 0,1°C (Thies 2.1265.10 technical manual).

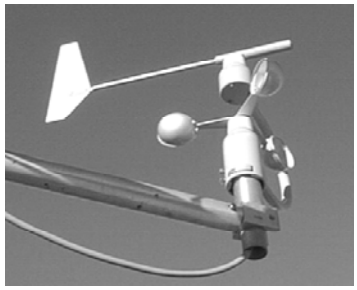

Fig. 3.10: Anemometer and wind vane in 2 m height

Wind: The wind sensor is a combined equipment of an anemometer and a wind vane (see Fig. 3.10). The rotations of the anemometer are transfered over the ball-bearing axle of the 3 arm cup anemometer into a slotted cylinder. The optically scanned signal produce an impulse frequency, which is proportional to the wind velocity; it is recorded with a counter. The measuring range of the anemometer amounts 0.3 - 50 m/sec The internal measuring deviation of the set up is about ±0.3 m/sec The wind direction is measured with an low-inertia metal vane, whose ball-bearing axle is connected with a potentiometer. The measured value of the resistor depends on the position of the potentiometer. The measuring deviation of the wind vane amounts ± 2 degrees (Thies 4.3323.21 technical manual). In this work the wind data of the set up are analyzed in a height of 10 m.

Relative humidity: The relative humidity (r.H.) can be measured with hair-hygrometers or with capacitive humidity sensors. During the installation of the meteorological tower two hair-hygrometers were mounted at the 2-m-level, which were meanwhile substituted by 2 humicap sensors. (The hair-hygrometer of the position 1 (NE exposition) was exchanged by a humicap on 25th October 1999. The exchange of the second hair-hygrometer (position 2: SE exposition) with another humicap was realized on July 28, 2002. The time between these changes the second hair-hygrometer was used to validate the measured data of the humicap sensor.) A big rise of measuring precesion could be reached after the installation of the humicap sensors. To determine the relative humidity in this report data were used basing on the measuring values of the humidity sensor in position 1. The values of the instument in position 2 are only used for comparisons.

Hair-hygrometer: The sensor of the hair-hygrometer consists of a few hairs that are streched to a harp. The length of the hairs alters with temperature changes. Natural hair used in this instrument degenerates under the dry air conditions. Therefore, the instrument has to be recalibrated in saturated humid air on a regular basis. The hair-hygrometers have been regenerated once per month. The values of the hair-hygrometers are regularly controlled with a Assmann-psychrometer. The measuring range of the hair-hygrometers amounts 10 - 100 % r.H. in an environment temperature of –35 – +70 °C with a measuring devation of ± 2 % r.H. (Thies 1.1000.50 technical manual).

Humicap-H-Sensor: This capacitive microprocessor-controlled humidity sensor (HMP 233) can be applied in a range of 0 - 100 % r.H. with environmental temperatures –40 $\pm$ 80 °C. This instrument has in the range of 0 - 90 % r.H. a measuring deviation of ± 1 % and within a range of 90 – 100 % r.H a measuring deviationof ± 2 %. The measuring principle is based on a capacity changes by the absorption of water molecules in a polymer-thin-film, which aims a thermodynamical balance with its environment (VAISALA technical manual).

Cloud Ceiling: The cloud ceiling is measured by a LIDAR (Light Detection and Ranging) with a wavelength of 862 nm. This LIDAR is a laser based ceilograph LD-40 and is located about 5 m next to the solar tracker (Fig. 3.4). It measures in a ceiling

range between 23 m and 12 650 m height with a measuring deviation of ± 23 m (at solid objects). Before the installation of the LD-40 Ceilometer on 1st July 1998 the cloud height was measured with a wavelength of 911 nm by a LD-WHX Ceilometer situated about 150 m further north. Its range was limited to 3600 m. The increase of the range could be obtained by an improvement of optics, electronics and the selection of the wavelength. The measuring range of the ceilometer can be limited by precipitation, vapor, dust or particles in the atmosphere (Impulsphysik LD-25/LD-40 technical manual).

Air Pressure: The air pressure is measured by a digital Digiquarz barometer (Paroscientific 740-16B), attached in the Blue House of the Koldewey station in 11 m height over the sea level. At a quarz barometer the oscillation frequency of a crystal quartz resonator in a vacuum is changed by the air pressure. The measured pressure is led into a springy high-grade steel chamber or into a spring tube which transmits a power to the resonator and changes the oscillation frequency proportional to the pressure. Characteristic values for the digital quartz barometer are indicated in a pressure measuring range of 0 – 1050 hPa, a measuring deviation of ± 0,01 % and a resolution of $0 - 5 \cdot 10^{-8}$ hPa (PAROSCIENTIFIC 2002, VDI 3786/16).

3.1.3 Synoptic Observations

Synoptic observations are regular weather observations at certain time standards by international valid regulation key. Wind-, visibility- and cloud characteristics, air pressure, dew point and temperature are determined with synoptic observations. The clouds and visibility are observed by the Norwegian Polar Institute in Ny-Ålesund daily at 6, 12 and 18 o'clock. Wind and temperature measurements are performed in a three hour rhythm. From these synoptic observations data for cloud ceiling, fog and dew point temperature were taken for this evaluation (KOENIG-LANGLO 1992).

3.2 Data Archiving and Data Processing

3.2.1 The Meteorological Information System of the Alfred Wegener Institute (MISAWI)

The meteorological information system of the Alfred Wegener Institute „MISAWI“ is used for archiving and evaluation of radiation and meteoroligical data. It is based on the relational database Sybase. The database contains the radiation and meteorological data from the Koldewey Station since 1992/93, data from synoptical observations of the Norwegian Polar Institute Ny-Ålesund since 30th September 1990 as well as data from all rawin sondes since 3rd June 1991. Furthermore, all data of the research vessel Polarstern (since December 1982) and the Neumayer Station (since 28th January 1981) are collected in MISAWI too (see Fig. 3.11). Radiation- and meteoroligical data are firstly stored in a so-called RAD-file at the local workstation and get tested for any obvious mistakes or failures. Later on, they pass through different testing methods to examine the quality and tolerances of the data. Most parameters have an upper and lower limits, like the wind direction have a range from 0° - 360°. Special limits are used for parameters without fixed limits, like air pressure and temperature. Moreover some data are tested for plausibility (global radiation > reflex radiation, wind velocity (10 m) > wind velocity (2 m) etc.. Questionable values are flagged, listed in error logs and manually checked. After the first validation at the station, the data are sent to the AWI Potsdam via FTP (File Transfer Protocol) where they get controlled again. Later, the data are imported into the MISAWI (KOENIG-LANGLO and HERBER 1996). In the MISAWI the measured

data gets completed by calculated values such as solar altitude (h_S) and extraterrestrial solar radiation using equations of IQBAL (1983) (see Chapter 3.2.3).

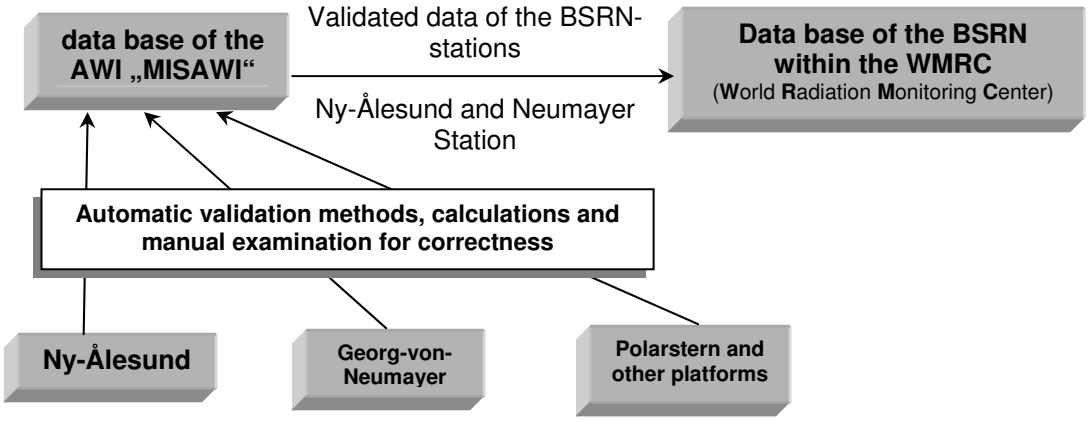

Fig. 3.11: Scheme of the data recording with the MISAWI

Within the MISAWI the data get automatically validated, manual corrected and outstanding values filled up with –9999. After the validation the data are sent to the World Radiation Monitoring Center (WRMC) via FTP, see Fig. 3.11.

The data of the MISAWI can be queried with SQL (Structured Query Language). Also a special user-interface for querying data is provided for users without SQL knowledge at the homepage of the Alfred Wegener Institute (www.awi-bremerhaven.de). A more detailed description of the MISAWI is given by KOENIG-LANGLO and MARX (1997), KOENIG-LANGLO (1992) as well as KOENIG-LANGLO and HERBER (1996).

3.2.2 Statistic Methods

Measurements took place with a time resolution of approximately one measurement per minute and an avaraging for five minutes during the period of January 1994 until July 1998. Starting from 14th July 1998 the time resolution of the measurement and measurement transmission could be substantially increased by new technology. Since sufficient measured values were present and could be transfered, it was possible to realize the demand of the BSRN (1998) for one-minute-averaging.

These different means were considered in the analysis by weighting means and standard deviations. Seven day running means were used for the presentation of the meteorological data of the exemplary year 2001 in order to eliminate extreme weather situations (see Fig. 4.36). The running mean is a series of average values, which helps to smooth fluctuations in a dataset, so that the trend becomes better visible. Nevertheless, with this method it is not possible to indicate the smoothing values for the beginning and the end of the time series (MONKA and VOSS 2002). Regression curves were used for the evaluations of measuring values and trend analysis for short- and long-term data sets.

3.2.3 Observation Periods

For the meteorological data the observation period has been selected from January 1994 to December 2001. While a period from winter 1993/1994 till summer 2002 has been used for the seasonal analysis. Radiation analysis started in January 1993. The year 2001 was choosen to show a daily course during a year. That is why the daily means were recorded for all values (see Fig. 4.36).

Examples for the daily course are given for two days with different weather conditions: a clear day with 24 h sun on 25th May 2002 and a covered day without a single minute of sunshine on 29th May 2002.

3.2.4 Systematical Devations of the Solar Altitude

For the MISAWI the calculation of the solar altitude was done using the approximation of the solar declination *(δ)* by M.IQBAL (1983). During the evaluations a divergence could be detected from the data that was determined with the following approximation equation:

$$\delta = (0{,}006918 - 0{,}399912\cos\varphi + 0{,}070257\sin\varphi - 0{,}006758\cos 2\varphi + 0{,}000907\sin 2\varphi - 0{,}002697\cos 3\varphi + 0{,}00148\sin 3\varphi)(180/\pi) \quad (3.11)$$

where δ - solar declination, φ - latitude

The isopleth-diagramm of the solar altitude in Ny-Ålesund (Fig. 3.16) shows a maximum before June 21 (solid line). The data calculated with this equation reaches its maximum at the beginning of June already. With the help of the following equation,

$$\sin h_S = \sin\varphi \cdot \sin\delta + \cos\varphi \cdot \cos\omega \cdot \cos\delta \quad (3.12)$$

where h_S – solar height, ω - hourly angle (WMO 1981) and the solar calculation programme „XEphem“ it was possible to determine the size of the divergence with about 13 to 16 days. A correction of this systematical error in the database could not be managed until the end of this thesis. The divergence as it is shown in Fig. 3.12 bases on monthly and hourly means. The daily means of the solar height are equal with the values calculated according IQBALs equation and can be used for further calculations.

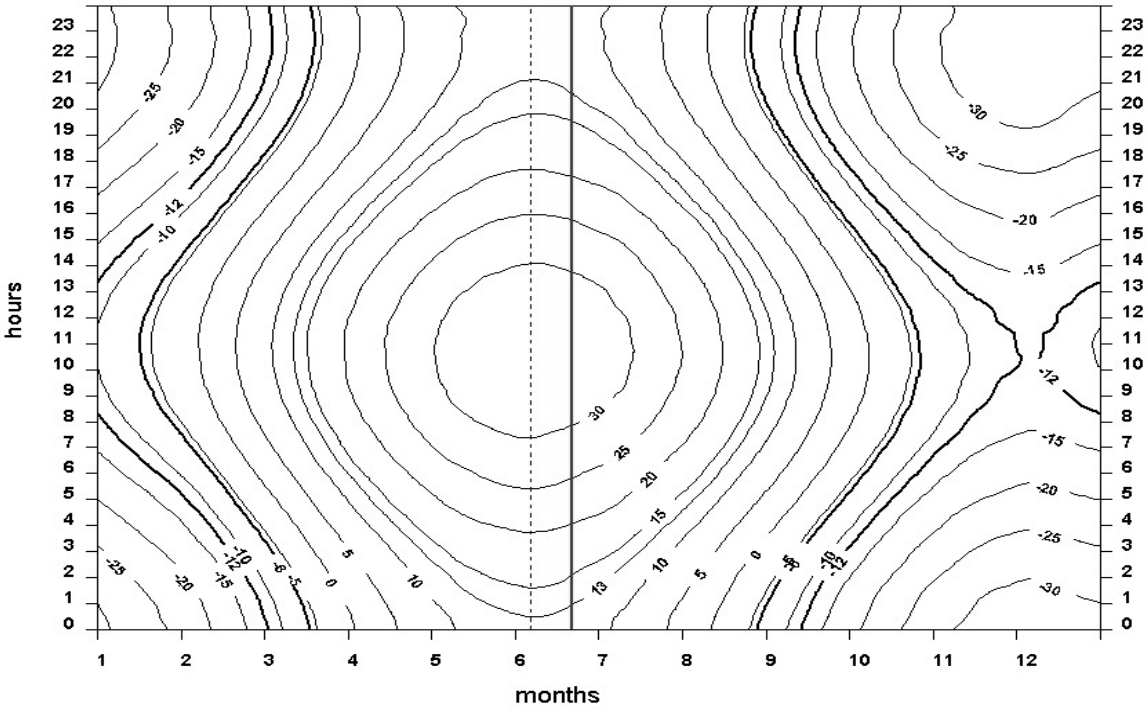

Fig. 3.12: Isopleth-diagramm of the solar altitude and solar maximum according IQBAL (dashed line) theoretical solar maximum on 21st June (solid line)

4 Evaluation and Results

4.1 Radiation Field

Radiation measurements are influenced by the radiation field, sunshine duration and cloud coverage. The solar height h_s during the year is shown in Fig. 4.1 where the refraction is not taken into account. It is shown that the transitional period from the polar night to polar day starts when the maximum daily height of the sun (noon) reaches the horizon. The polar day begins when the minimum solar height (midnight) is obtained above the horizon as well. On 21st June the maximum height of $h_s = 34.5°$ is reached. The minimum height is to be noticed with $h_s = –34.5°$ in 21st December. During the equinocts the mean solar elevation is reached at 11.2°. The polar night starts when the maximum solar elevation per day stays below the horizon. From middle to the end of December the sun does not even rise during noon above the -12° where the nautical twilight-zone begins.

The lighting conditions are characterized by the the solar position and the orography. The daily course of the sun dependend on the orography of Ny-Ålesund is schematically presented in Fig. 4.2 for selected days of the year. After the sun reached the horizon at noon around the 19th February[1)] (see Tab. 4.1), the diffuse radiation wins importance and some days later the direct sun radiation as well.

The direct sun radiation will be reduced by the shadow effect of the Zeppelin mountain up to the end of March. For the first time of the year the sun can be seen approximately on 6th March. The oro-graphy of the mountains has the consequence that in this time the sun appears each morning between Slatto- and Haavimbfjellet in the southeast (SE) for a short time only. A few days later the sun can be observed between the mountain summits of the Brøggerbreen in the southwest (SW) also in the afternoon. The sun stays constantly above the horizon in the time from 16th (20th) April until 23rd (26th) August

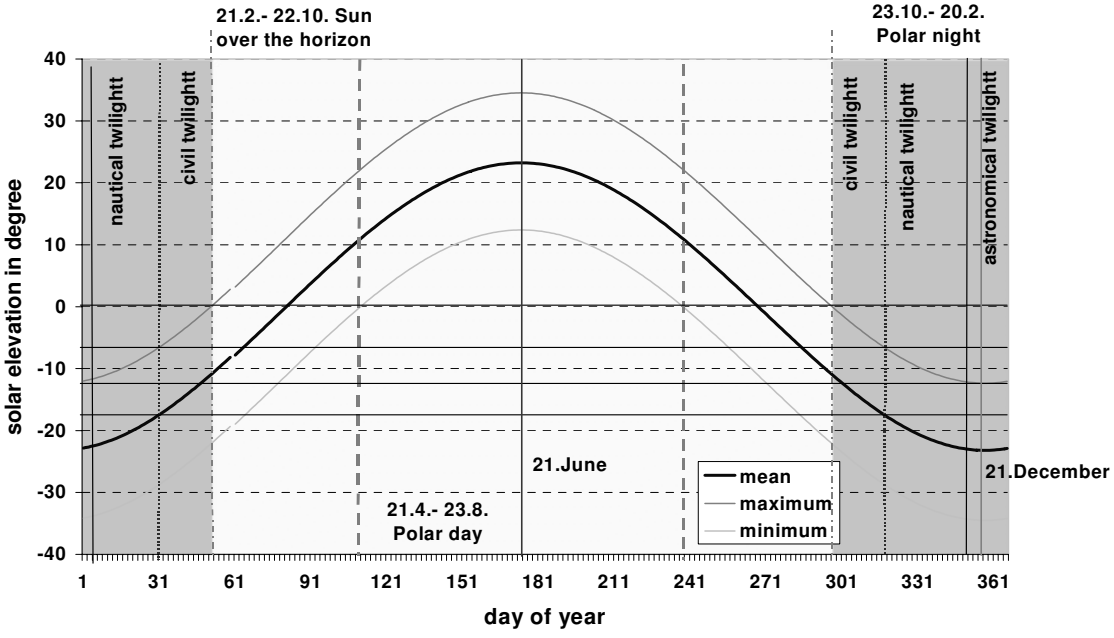

Fig. 4.1: Daily mean, -maxima and -minima of the solar elevation, acc. IQBAL (1983) for 2001

[1)] first value with refraction acc. US Naval Observatory for Ny-Ålesund, second value acc. the calculations in the database by IQBAL (1983)

The polar day in Ny-Ålesund is about 131 or 132 nights long. From the beginning of October there cannot be detected any solar radiation anymore. The sun sets finally for the polar night around 22nd and 24th October, which stays there for about 116 or 124 days (see Appendix 4.1 Fig. 1 – 12).

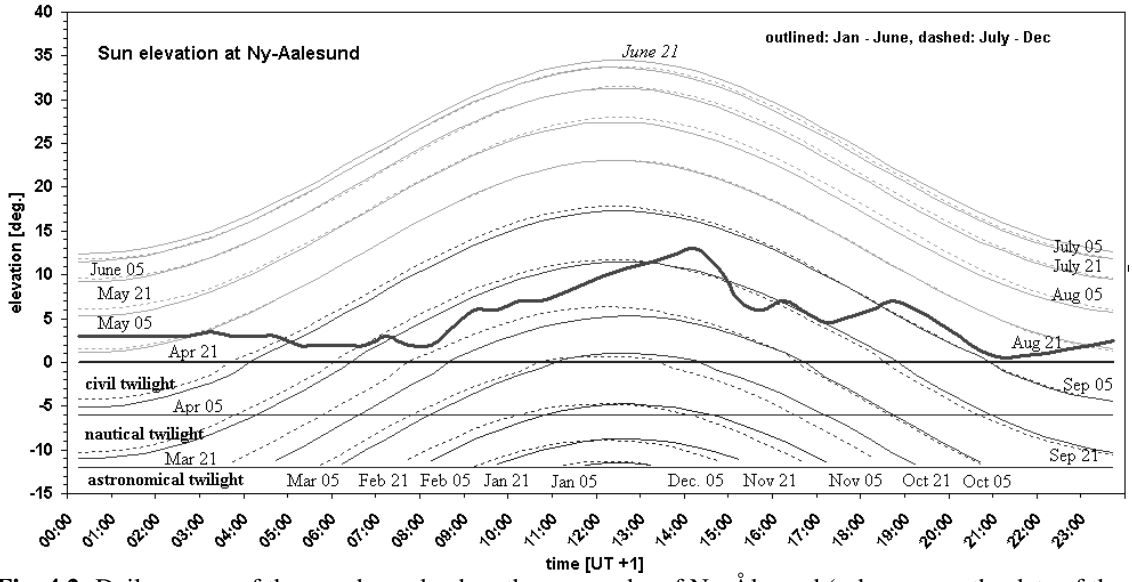

Fig. 4.2: Daily course of the sun dependend on the orography of Ny-Ålesund (schema acc. the data of the US Naval Observatory with refraction)

Tab. 4.1: Important solar data relating the horizon (zero horizon, NN) for Ny-Ålesund acc.: US Naval Observatory; HISDAL and FINNEKÅSA (1996); IQBAL (1983)

source	first sunrise	last sunset	polar day		polar night	
			begin	end	begin	end
acc. US Naval Obs.	18. Februar	24. Oktober	16. Apr	26. Aug	25. Okt.	17. Feb.
acc. HISDAL, et al.	18. Februar	24. Oktober	17. Apr	27. Aug	25. Okt.	17. Feb.
acc. IQBAL (1983)	21. Februar	22. Oktober	20. Apr	23. Aug	23. Okt.	20. Feb.

Because of the different calculation methods, the dates for polar day and polar night according the MISAWI differ in some days from the dates of the U.S. Naval Observatory, The calculation of the U.S. Naval Observatory bases on the upper rim of the sun as well as it includes the refraction, that can take up to 0.6° in Arctic regions (HISDAL et al. 1992). The sun position calculation according IQBAL (1983), used in the database, does not take into account (consider) the refraction (see Fig. 4.1). Strongly varying dates for the sun phases are refered in the literature (STONEHOUSE 1989, HISDAL 1998). The dates specified by HISDAL and FINNEKÅSA (1996) match relatively good with the dates determined by the U.S. Naval Observatory. Calculations which include the refraction are more exact (in order) to determine the times for the beginning and end of the transitional phases. That is why the data of the U.S. Naval Observatory were used in Fig. 4.2.

Slight fluctuations of these dates from year to year may result from the variation of the refraction and the temporal near to leap years (HISDAL et al. 1992). However, this data only were provided in rougher temporal distances (hourly means, sunrise and sunset times). In this paper data of daily means, sun maximum and minimum are still based on the computations of the database MISAWI because of higher resolution.

4.2 Sunshine Duration

The radiation parameter of sunshine duration is measured at the BSRN-Station with a sunshine detector Solar 111 since 1992 (see Chapter 3). For the analysis data was used within the period between 1st January 1993 to 31st December 2001. The sunshine duration depends on the position of the Sun and on the cloud coverage. A longer sunshine duration can be expected under clear sky conditions and rising sun. During the months of February/March as well as October the mountains of the Brøgger peninsula have a strong influence on the sunshine duration in Ny-Ålesund. Especially the shadow effect of the Zeppelin mountain decreases with the rising sun (see Fig. 4.3).

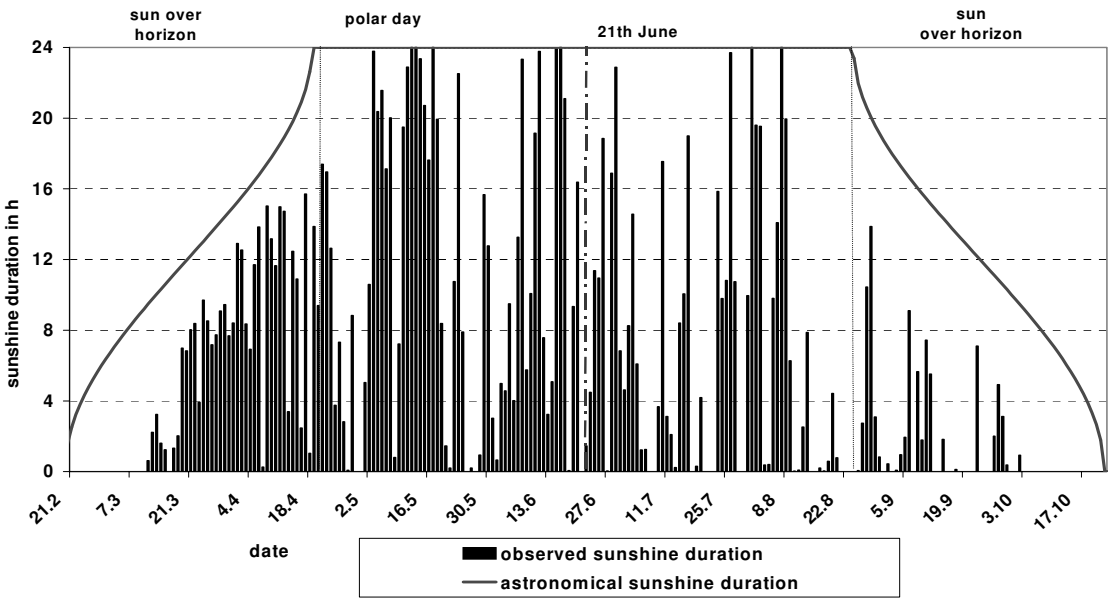

Fig. 4.3: Daily cumulative parameter of the observed and astronomical sunshine duration (21st Feb.- 22nd Oct. 2001)

The first solar observations of the year (direct solar radiation >120 W/m²) were typically executed in the period between 9th March (1995) and 13rd March (1996 and 1999), see Tab. 4.2). The latest measurements of sunshine have been recorded between 28th September (1993) and 5th October (1998). The village is shaded from direct solar radiation from 2nd October until 11th March. It cannot be determined exactly if the first sunrise over the mountains falls together with the first direct solar radiation record. At a covered sky, the first sunshine reaches the village some days later. The last sunset cannot be determined exactly because of the higher cloud coverage in autumn.

Tab. 4.2: Day of the first and the last observed sunshine (E_I >120 W/m²)

	93	**94**	**95**	**96**	**97**	**98**	**99**	**00**	**01**
First day	10.3.	11.3.	9.3.	13.3.	12.3.	12.3	13.3.	9.3.	11.3.
Last day	28.9.	3.10.	3.10.	1.10.	22.9.	5.10.	3.10.	1.10.	2.10.

The connection between the daily cumulative parameter of the astronomical and the observed sunshine duration for the year 2001 is represented in Fig. 4.3. It can be noted that the difference between the astronomical and observed sunshine duration is smallest in March/April and May. In the year 2001 a predominance of sunshine duration was observed for the phase where the sun rises from the horizon to the zenith compared with the phase where the sun sets towards the horizon. In the first half of April numerous sun days are

recorded with (still) a relatively small sunshine duration, (because the sun does not yet stand for 24 h over the horizon). In May the sunshine duration per day is substantially longer than in April, the number of sun days however is smaller because of the increasing cloudiness. The relationship of the sunshine duration observed on the earth's surface (*S)* and the astronomical duration of sunshine (S_0) is called relative sunshine duration (S_{rel}).

$$S_{rel} = \frac{S}{S_0} \tag{4.1}$$

The observed, the astronomical and the relative sunshine duration are represented in Tab. 4.3 for the investigation period as well as for the year 2001. It is to be recognized that 2001 the relative sunshine duration was the highest from April to June.

Tab. 4.3: Observed, astronomical and relative sunshine duration for the Koldewey row (1993 – 2001) and the exemplary year 2001

	Feb	**Mar**	**Apr**	**May**	**Jun**	**Jul**	**Aug**	**Sep**	**Oct**	**year**
1993 - 2001										
Observed sunshine in h	---	81.1	280.3	300.7	218.6	183.5	136.1	71.6	0.9	1272.8
Astronomical sunshine in h	38.5	337.0	618.5	744.0	720.0	744.0	715.3	417.9	133.2	4468.4
Relative sunshine in %	---	24.1	45.3	40.4	30.4	24.7	19.0	17.1	0.7	28.5
2001										
Observed sunshine in h	---	114.1	275.0	406.3	323.5	209.4	161.5	52.3	0.9	1542.9
Astronomical sunshine in h	37.1	335.0	616.6	744.0	720.0	744.0	716.5	419.8	135.4	4468.4
Relative sunshine in %	---	34.1	44.6	54.6	44.9	28.1	22.5	12.5	0.7	34.5

April and May are typically the sunniest months. In most years the relative sunshine duration has the highest values in April. The sunniest year of the investigation period was 2001 with a sunshine duration of 1542 h, while the sun in 1994 was shining only 907 h. The average annual sunshine duration of the observation period of 1993 - 2001 amounts to 1273 h. For Ny-Ålesund the observed and the astronomical sunshine duration are represented in Appendix 4.2, Fig. 1 for the period 1993 - 2001. The cumulative daily observed sunshine duration lies at a maximum value of 24 hours at approximately 1 to 4 days per year. One of these days is the 25th of May 2002 that is described in chapter 4.6 and compared with an overcast day (29th May 2002).

4.3 Cloud Ceiling

At the Koldewey station the cloud ceiling is measured with a ceilometer that only detect the respective lowest cloud layer. The laser beam of the first ceilometer (1993 - 1998) reached only a height of maximally 3600 m. According to the WMO organization the ceiling is classified in the polar zone in low clouds (0 - 2 km), medium high clouds (2 - 4 km) and high clouds (3 - 8 km) (see Chapter 2.1.2.3). Some of the medium high clouds as well as the high clouds could not be recorded by this ceilometer. Improvements of the distances up to 13000 m result from implementing a new laser ceilometer Ld-40 in 1998. The evaluation of the measured values according the WMO classes was difficult, because overlappings appeared in the transient range from middle to high clouds. Therefore the values between 4 and 8 km were used for the class of the high clouds.

Fig. 4.4 shows the monthly frequency of the occurrence for low, middle and high clouds as well as for clear sky in the year 2001. The biggest percentage of low clouds of more than 60% arises in the months of January and July until September. In September the percentage of low clouds even rises up to 76 %. Their lowest frequency appears in March with 30 %. Medium high clouds arise the whole year over with a percentage between 5 and 10 %.

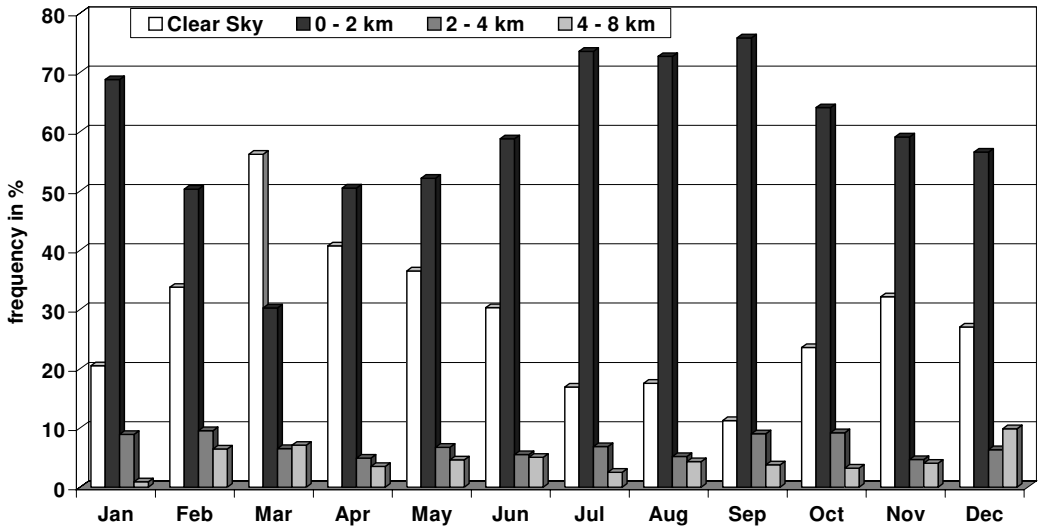

Fig. 4.4: Monthly percentage of low (0 - 2 km), middle-high (2 - 4 km) and high (4 - 8 km) clouds as well as clear sky for 2001

The percentage of the cloudless sky during the year 2001 rises from 20 % in January to 56 % in March and drops thereafter towards July down to 17 %. Most rarely clear sky appears July until September but this percentage increases again during the polar night. High clouds appear the whole year 2001 with percentages from 1 to 10 % only.

Ceiling recordings are not easy to be compared with the coverage, since the ceiling is only measured punctually. The degree of coverage is provided by Norwegian Polar Institute in context of the synoptic observations. According the synoptic key the degree of coverage is estimated in eighths: class 0 stands for cloudless sky; class 8 stands for a completely covered sky (DWD 1982). The synoptic observations of cloud ceiling and coverage are accomplished in Ny-Ålesund only three times on the day. Therefore, it was not possible to give any statements about average daily conditions. To get an overall view, all observations within one class were set into relation to all possible observations (see Fig. 4.5). The figure shows the frequency of the classes 0 - 8 in the observation period 1993 - 2001 compared with those of the year 2001. It is to be stated that the classes 1, 7 and 8 appear most frequently in both in the observation period 1993 - to 2001 and in 2001. The sky is covered completely with clouds to 33 % of yearly average, a percentage (class 8) that only reached 23 % in the year 2001. The classes 3 - 6 appear in both time series relatively evenly between 4 to 9 %. The degree of the coverage of the sky is represented in Fig. 4.5; from this the direct ceiling cannot be recognized.

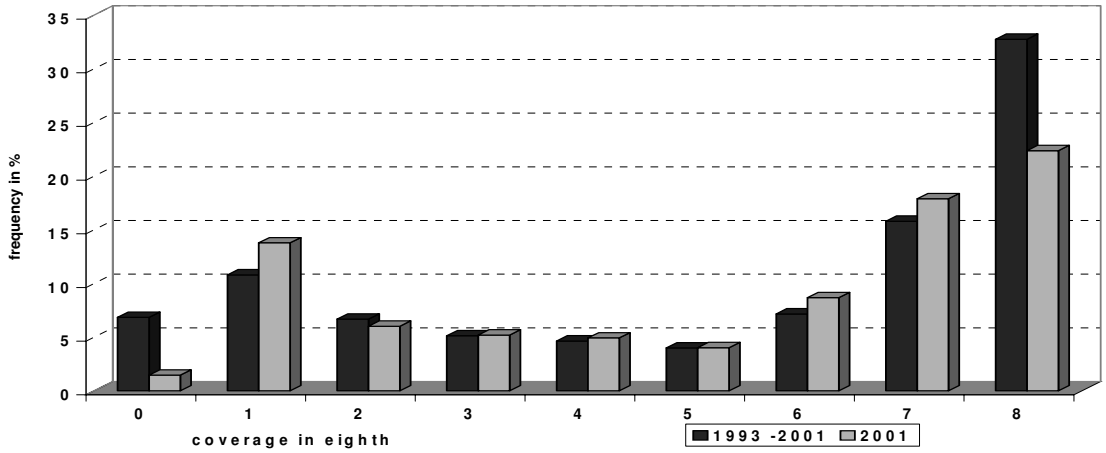

Fig. 4.5: Frequency of the cloud coverage in Ny-Ålesund for 1993 - 2001 and 2001

In the context of the synoptic observations the height (see Fig. 4.6) and type (see Appendix 4.3 Fig. 1) of the clouds can be determined too. Due to the incomplete series of measurements of the first ceilometer LD-WHX, the evaluation of the ceiling was necessary for all heights in the observation period of 1993 to 2001. Further the synoptic observations of the ceiling offer a possibility of comparison with the laser values. The relatively difficult cloud observations during the polar night cannot be compared with those, which were taken during the remaining time of the year (KOENIG-LANGLO 1992). The monthly frequencies for clear sky, low, medium high and high clouds are therefore represented from March to October only in Fig. 4.6. During the year 2001 (see Fig. 4.4), the percentage of low clouds rises over 60 % from April to June. From June to October the percentage of the low clouds exceeds 60 %. The portions for medium high clouds in the synoptic observations between 1993 and 2001 clearly lie over those, which were determined during the year 2001. Their frequency is biggest in March with 29 % and April with 28 %.

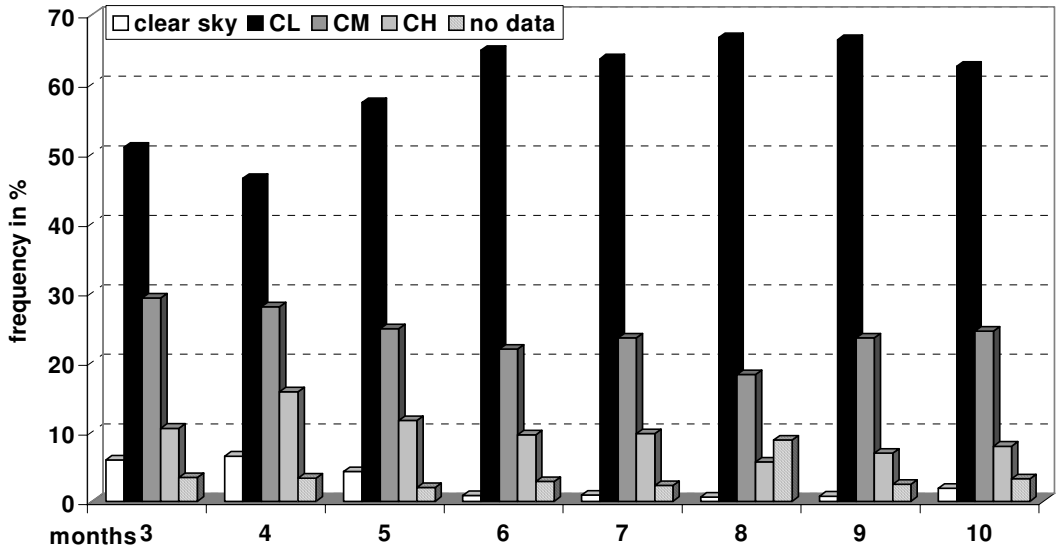

Fig. 4.6: Frequency of low, middle and high clouds at Ny-Ålesund for 1993 – 2001 (C_L - low clouds; C_M – middle clouds; C_H – high clouds)

High clouds arise most in April and May with percentages of approx-imately 16 and 12 %. In the synoptic observations of the Koldewey row the portion of the cloudless sky lies far below that values which were measured with the laser in the year 2001 (see Fig. 4.4).

The cloud types for the 3 cloud floors are represented in Appendix 4.3, Fig.1. In the period 1993 to 2001 the most frequent clouds are of the type Stratus, Stratocumulus and Cumulus (classes 5, 6 and 8) with percentages between 13 and 26 %. Torn cloud layers or bad weather clouds (Stratus fractus) and torn heap clouds (Cumulus fractus) occur with a frequency of 10 % within the floor of the low clouds. Nice weather clouds of the Cumulus species (1-Cu. humilis, Cu. fractus, 2-Cu. mediocris) and rain clouds of the Cumulunimbus species (3-Cb. calvus) occur only very rarely during the observation period.

With the medium high clouds the most typical stable weather form of the Altocumulus (3-Ac. translucidus) can be found most frequently in Ny-Ålesund. The flake and tower formed Altocumulus clouds of the species AC floccus and AC castellanus occur only rarely. The high clouds are the class that appears most rarely. From this layer, the classes 1 and 8 of the Cirrus and Cirrostratus family were observed most frequently. Both ice cloud species Cirrus fibratus and Cirrostratus do not completely cover the sky (DWD 1982, 1987).

The differentiation of cloudless and covered sky is also possible during the polar night, since stars and moon offer good orientation assistance. Fig. 4.7 shows frequency of the days per month for covered and clear sky for the period 1993 - 2001 (see Tab. 4.4). Usually the most days with clear sky can be found in December (9 days) and January (10 days). Between June and September clear sky occurs usually only on 2 to 3 days per month. In these months the sky is covered up to 7 - 8 eighths on 19 and 21 days per month. A similar monthly course of overcast and clear sky was determined in the observations of FØRLAND et al.(1997), see Fig. 4.7 dashed lines). In comparison to the Koldewey data small deviations of 1 or 2 days can be observed.

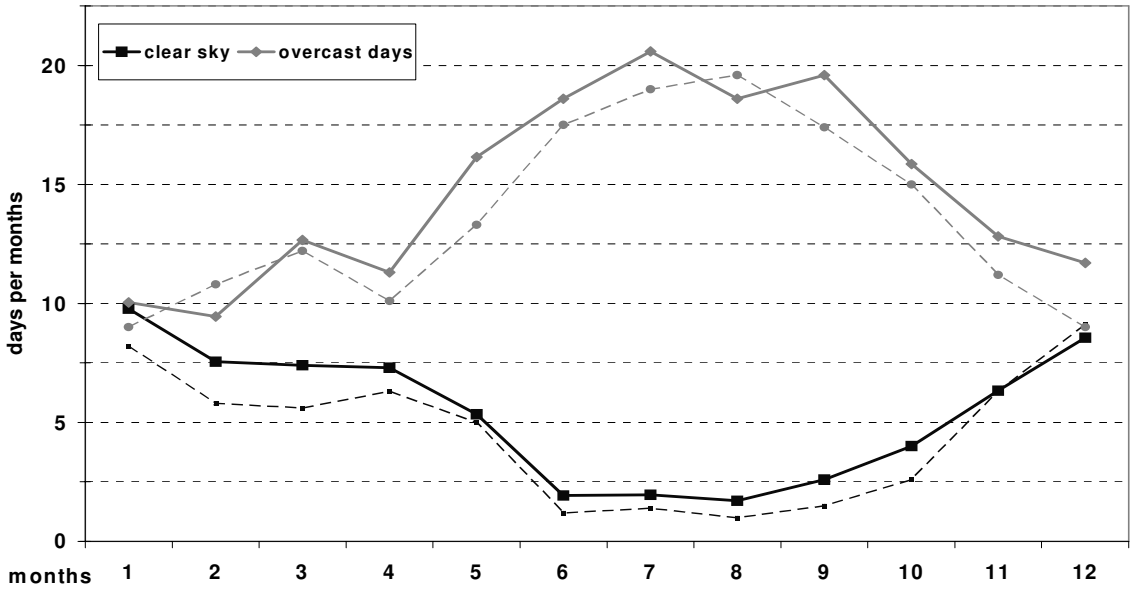

Fig. 4.7: Mean frequency of clear sky and overcast days per months in Ny-Ålesund (solid line: Koldewey data series 1993 - 2001; dashed line: DNMI data series 1975 - 1996)

Tab. 4.4: Mean frequeny of clear sky and overcast days at Ny-Ålesund

	Jan	Feb	Mar	Apr	May	Jun	Jul	Aug	Sep	Oct	Nov	Dec	year
Koldewey – data series (1993 - 2001)													
clear sky (0;1)	9.8	7.6	7.4	7.3	5.3	1.9	2.0	1.7	2.6	4.0	6.3	8.6	64.4
overcast (7;8)	10.0	9.4	12.7	11.3	16.1	18.6	20.6	18.6	19.6	15.9	12.8	11.7	177.3
DNMI – data series (1975 -1996)													
clear sky	8.2	5.8	5.6	6.3	5.0	1.2	1.4	1.0	1.5	2.6	6.3	9.1	54.0
overcast	9.0	10.8	12.2	10.1	13.3	17.5	19.0	19.6	17.4	15.0	11.2	9.0	164.1

Fog is defined to be associated with the vision range in eye level below 1 km (s. Chapter 2). Fog is not a significant weather phenomenon for the inner-fjord-areas of Spitsbergen, a region, where Ny-Ålesund is counted to. During the observation period fog was determined with an average of approximately 10 days per year. In July, the fog frequencies are the highest with 35 %. With a high probability it is advection fog, which develops during the flow of warm, humid sea air onto the cool surface of the fjord. This leads to the cooling of the lowest air layers below the dew point (DWD 1987). Arctic fog is not very thick usually, often only some decameter (HISDAL 1998). Similar fog observations were noticed by FØRLAND, et al. (1997) in the period of 1976 -1996. Compared with the exposed stations Svalbards Bjørnøya, Hopen and Jan Mayen the fog events are very seldom in Ny-Ålesund.

4.4 Radiation

The radiation parameters are recorded on the BSRN station Ny-Ålesund since August 1992. For the evaluation of the radiation values of the BSRN the data series "Koldewey" was choosen (from 1st January 1993 to 31st December 2001), in order to ensure the comparability with other data series. Incomplete data series were presented for the years 1992 and 2002. The validation of the radiation data was done with the meteorological data base "MISAWI" (see Chapter 3.2). For the evaluation only the monthly and annual averages were taken into account for that time, in which the sun was standing above the horizon. The values were calculated without the consideration of the refraction from 21st February to 22nd October from the daily averages. Large daily fluctuations were caused by the diurnal variation of the short-wave radiation. The standard deviations (s_m) were calculated from the monthly mean values (count: n_m; $s_m = s/\sqrt{n_m}$), the used values for radiation and meteorology are represented in the table-appendix.

4.4.1 Direct Solar Radiation

The direct solar radiation is measured with a Normal Incidence Pyrheliometer (NIP) with a field of view of 5 degrees (see Chapter 3.1). During polar night, between end of October to end of February, the NIP is not installed at the solar tracker. Averages and extreme values of the direct and direct-horizontal radiation for the observation period of 1993 - 2001 as well as for the year 2001 are shown in Tab. 4.5.

Tab. 4.5: Means and extreme values of the direct solar radiation and the direct-horizontal radiation in W/m^2

	period	mean and standard dev.	absolute Maximum	absolute Minimum
direct solar radiation	1993 - 2001	110.7 ± 19.5	1142.3 (15.7.1994)	0
	2001	130	963.7 (7.6.2001)	0
direct-horizontal radiation	1993 - 2001	24.4 ± 4.4	534.7 (7.6.2001)	0
	2001	25.7	534.7 (7.6.2001)	0

The mean direct irradiance/year amounts to 110.7 ± 19.5 W/m² for the investigation period. The maximum value of 1142.3 W/m² appeared on 15th July 1994. The values in October are in terms of their amount very small, so that the evaluation of the direct and the direct-horizontal radiation was carried out only for the period between March and September (see Fig. 4.8). Missing values were corrected in the month of polar night (October – March). The maximum average values of the direct solar radiation lie with 182.1 W/m² in April and with 220.6 W/m² in May. They correspond to the observations in which the largest duration of sunshine was determined in both of these months.

In order to get a link to the remaining radiation parameters, that are measured horizontal towards the earth's surface, the direct solar radiation has to be multiplied by the sinus of the solar angle ($\sin h_s$), see Eq. 2.5. The direct solar radiation is thereby related to a horizontal surface and is called direct-horizontal radiation. The monthly average values of the direct radiation and the direct-horizontal radiation are represented in Fig. 4.8. During the observation time an annual average value of the direct-horizontal radiation is calculated with 24.4 ± 4.4 W/m². The biggest direct-horizontal radiation was determined with 534.7 W/m² on 7th June 2001. The maximum monthly average values lie with 77.6 W/m² in May and with 68.0 W/m² in June. Due to a rise of coverage from June until September the

mean direct-horizontal radiation decreases during this time. The maximum radiation is reached in June when the sun rises up to its highest elevation.

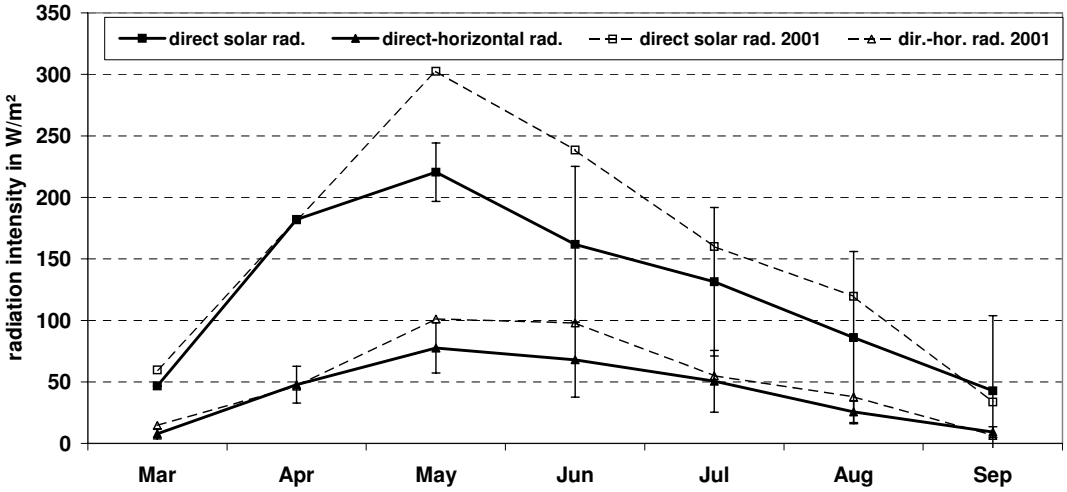

Fig. 4.8: Monthly mean values and maxima of the direct radiation and direct-horizontal radiation for Ny-Ålesund in the period 1993 - 2001

The daily averages of the direct-horizontal radiation, the maxima and minima as well as the seven day running means are shown in Fig. 4.9. The decrease of the direct-horizontal radiation for July in both, in the observation period and in the year 2001 can clearly be recognized in Fig. 4.8 and 4.9. In August 2001 the irradiancy rise again, drops however in September. This dropping can be explained with the absorption and dispersion of the radiation by the high water vapour content of a strong coverage. The shading effect of the surrounding mountains can be recognized in the diagram on the basis of a later rise of the direct radiation in March and the radiation dropping earlier in September. In March and May 2001 the direct radiation will be only slightly reduced by the occurence of clouds. The maximum values are reached during noon time around 11 o'clock UTC.

An overview of the annual average values and the rise of direct, direct-horizontal as well as diffuse sky radiation is given in Tab 4.6 for the period 1993 - 2001.

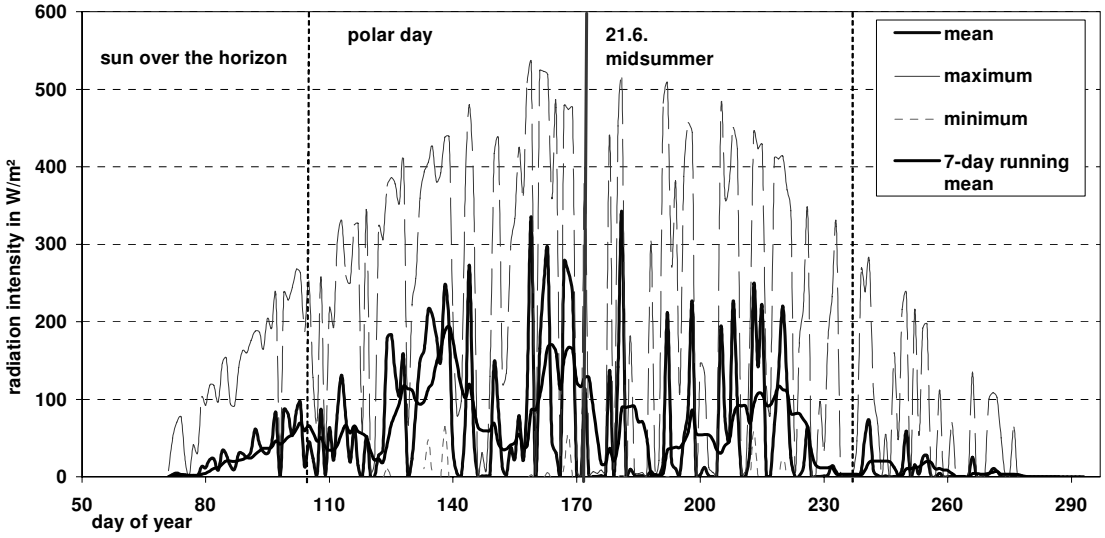

Fig. 4.9: Annual course of the direct-horizontal radiation of the daily means and extreme values in Ny-Ålesund from 21st Februar to 22nd October 2001

Tab. 4.6: Annual means and rise of the direct solar radiation, the direct-horizontal radiation and the diffuse radiation in W/m² for Ny-Ålesund

1993 - 2001	mean	max. mean	year	min. mean	year	initial value	rise/a	abs. rise
Direct	110.7 ± 19.5	117.3	1997	66.4	1994	87.6	4.6	37.0
Direct-horizontal	24.2 ± 4.4	29.5	1997	14.9	1994	20.8	3.6	5.8
Diffuse	70.1 ± 5.7	79.0	1998	63.2	1997	66.8	0.7	5.3

max. mean – biggest average value; min. mean - lowest average value
initial value – initial value of the regression line in the starting year of the referring period
rise/a – rise per year
Absolut rise – rise of the regression line during the observation period

The deviation of the annual averages from the total mean of the investigation period and the tendentious development of the direct-horizontal radiation are shown in Fig. 4.10 and Tab. 4.6. For the exemplary year 2001 the annual average value is about 25.7 W/m² still within the standard deviation of the average annual means of 24.2 ± 4.4 W/m² of the entire observation period. The biggest deviation arises in 1994; here the annual average value only lies at 14.9 W/m². This is the only year where the mean lies outside the standard deviation.

With an initial value of the direct-horizontal radiation of 20.8 W/m² in the year 1993 a rise of the regression line is determined with 5.8 W/m² during the observation period. The rise of the direct radiation amounts from an initial value of 87.6 W/m² (1993) amounts 37 W/m². The increases of the direct radiation and the direct-horizontal radiation lie within the standard deviation.

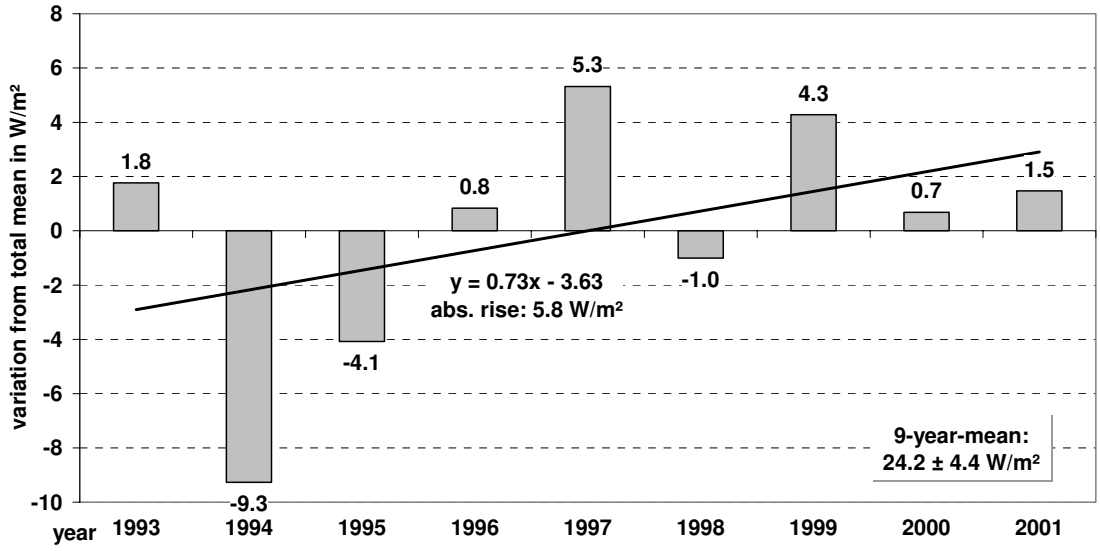

Fig. 4.10: Change of the annual means of the direct-horizontal radiation in relation to the total mean of the Koldewey data series for Ny-Ålesund

The seasonal development of the direct-horizontal radiation from March 1993 until August 2001 is shown in Appendix 4.4.1, Fig. 1. Tab. 4.7 gives an overview of the average values and rises of the direct-horizontal radiation for spring, summer, autumn and for the exemplary month of July during the observation period. The rise of the regression line (Fig. 4.10) is particularly based on the increase of the direct-horizontal radiation around

4.4 W/m² with an initial value of 39.5 W/m² in spring (1993) and around 22.0 W/m² with an initial value of 41.6 W/m² in the summer (1993).

Tab. 4.7: Seasonal means and rise of the direct-horizontal radiation in W/m² for Ny-Ålesund during the period of the Koldewey data series (March 1993 – August 2001)

	mean	Max. mean	year	Min. mean	year	Initial value	rise/a	Abs. rise
spring	45.7 ± 8.3	60.3	1996	34.7	1999	39.5	0.6	4.4
summer	49.4 ± 13.7	63.6	2001	21.1	1994	41.6	2.8	22.0
July	45.4 ± 25.1	93.8	1993	6.3	1994	49.4	0.22	1.8

The July average values and the mean maxima and minima of the direct-horizontal radiation from 1993 to 2001 are represented in Tab. 4.7 and Appendix 4.4.1, see Fig. 2. For the observation period the average direct-horizontal radiation is about 45.4 W/m² in July and thus already 32.2 W/m² lower than the value of May with the highest middle irradiancy of the year. The highest July average values were recorded with 93.8 W/m² in 1993 and with 78.9 W/m² in 1999. The smallest middle radiation amounts about 6.3 W/m² in July 1994. The maximum values which occurred amounted 503.8 W/m² in 1996 and 508.4 W/m² in 2001. The July average values in the total period increased with a small amount of 1.8 W/m² and initial value of 49.4 W/m² (1993).

4.4.2 Diffuse Radiation

The diffuse sky radiation is measured at the Koldewey station with a pyranometer since August 1992, which is shaded from the sun. The average - and extreme values of the diffuse sky radiation are shown in Tab. 4.8 for the period 1993 - 2001 as well as for the year 2001.

Tab. 4.8: Averages, minima and maxima of the diffuse sky radiation in W/m^2

	Period	Mean and standard devation	absolute maximum	absolute minimum
diff. sky radiation	1993 – 2001	70.1 ± 5.7	578.3 (13.6.2001)	0
	2001	66.1	578.3 (13.6.2001)	0

During the observation period the mean value of the diffuse sky radiation is about 70.1 ± 5.7 W/m². The months March till October are represented in the diagram (Fig. 4.11), because during the polar night the diffuse sky radiation is zero.

The maximum value in the observation period for the diffuse sky irradiancy was determined with 578.3 W/m² on 13th June, 2001. The maximum average value during the observaion period was computed with 145.7 W/m² in June. It lies by far over the June value of the direct-horizontal radiation of 68.0 W/m².

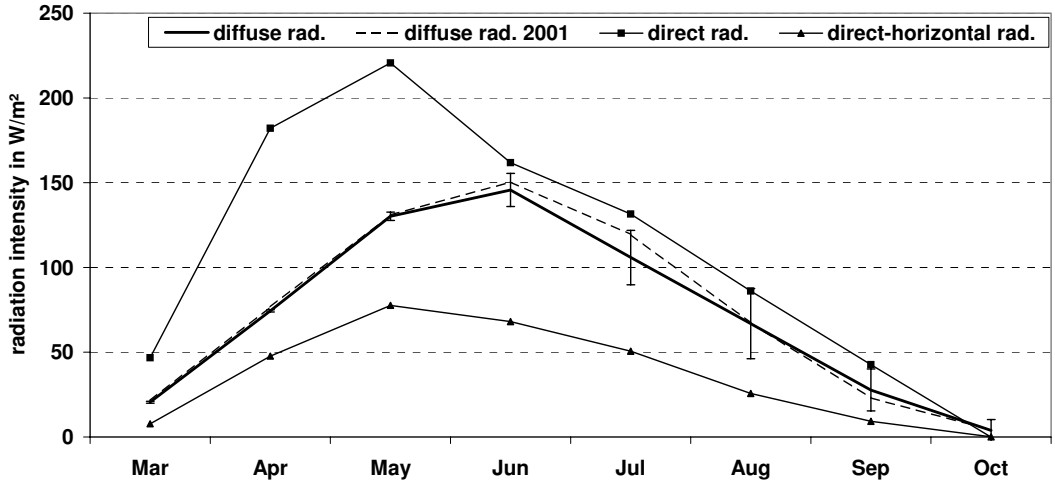

Fig. 4.11: Monthly mean and extreme values and the standard deviation of the direct solar, direct-horizontal and diffuse sky radiation for Ny-Ålesund (1993 – 2001)

The diffuse sky radiation is substantially higher in all months than the direct-horizontal radiation. In the months June until September the average value of the diffuse sky radiation lies only a bit below that of the direct radiation (Fig. 4.11). The averaged June value of the diffuse sky radiation is only 16.1 W/m² smaller than the average value of the direct radiation in June. Still in October the diffuse sky radiation could be registered, while the monthly average values of the direct and direct-horizontal radiation are nearly at zero. The daily averages of the diffuse sky radiation in relation to the sun height for the example year 2001 are represented in Fig. 4.12. Thereby an intensified diffuse sky irradiation could be determined before the summer solstice in relation to the time after the solstice. This can be explained by the high relative humidity and the compression of the deep clouds starting from July. A further cause is the snow cover, which melts by the middle of June. Between the snow cover and the clouds it comes to multiple reflections, with those the diffuse sky radiation is increased.

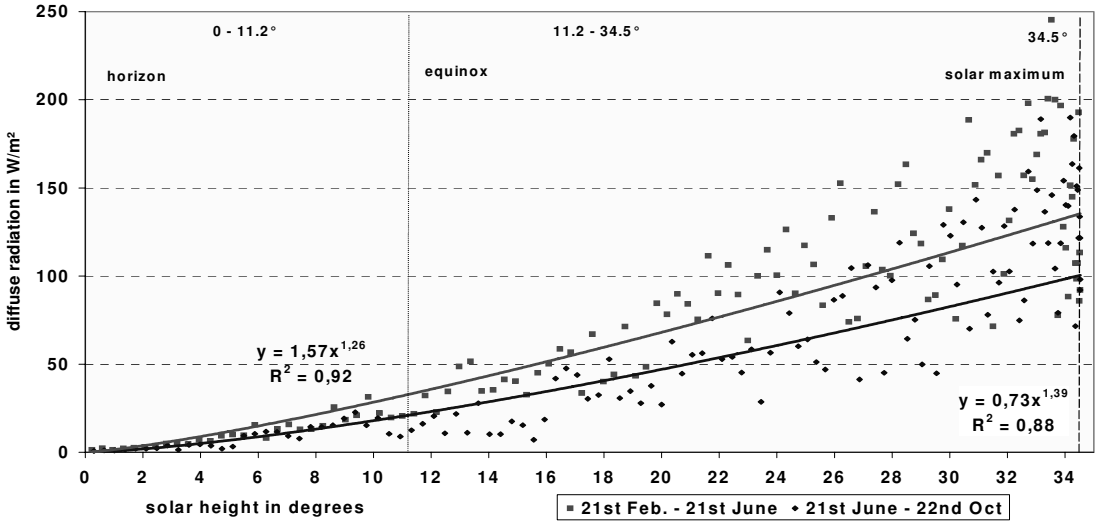

Fig. 4.12: Daily means of the diffuse radiation in relation to the solar elevation Ny-Ålesund for 2001

Another important factor is the relative diffuse radiation. This parameter is expressed by the relationship of the diffuse cloud reflection and the global radiation. The averge value

amounts of 55 ± 30 %. The relative diffuse radiation increases with the density and the thickness of the clouds. The solar altitude plays an important role on thin and water-rich clouds. Thus the albedo rises up to 68 % on thin Stratocumulus clouds with decreasing solar elevation (WMO 1981). Each cloud species has its characteristic mean albedo if the sky is completely covered. The most frequent cloud species occurring in Ny-Ålesund Stratus (St) - 56 %, Stratocumulus (Sc) - 68 %, Cumulus (Cu) and Altocumulus (Ac) – 72% are increasing in density starting from June. A majority of the incident short-wave radiation is reflected back into the universe from the top of the clouds. The global radiation is clearly reduced during this time. Clouds reflect and scatter not only the incident solar radiation, but also the reflex radiation coming from the earth's surface. As previously mentioned, particularly with high albedo of the soil (before the snow melt in June) multiple reflections appear between the earth's surface and cloud down side, which results in an increase of the global radiation. Also with the absorption and reflection of long-wave radiation clouds play an important role. A dense cloud coverage can contribute to the natural greenhouse effect and thus to the heating up of the earth's surface. In comparison to the short-wave radiation the relative diffuse radiation of the clouds is however relatively small for the long-wave spectral regions.

The percentage of the diffuse radiation from the global radiation is represented on the basis the daily averages and the seven day running mean in Fig. 4.13. The diffuse sky radiation reaches the values of the global radiation during low solar elevations at beginning of the first transitional phase and at the end of the second transitional phase. This is to due to the shading effect of the Zeppelinfjellet.

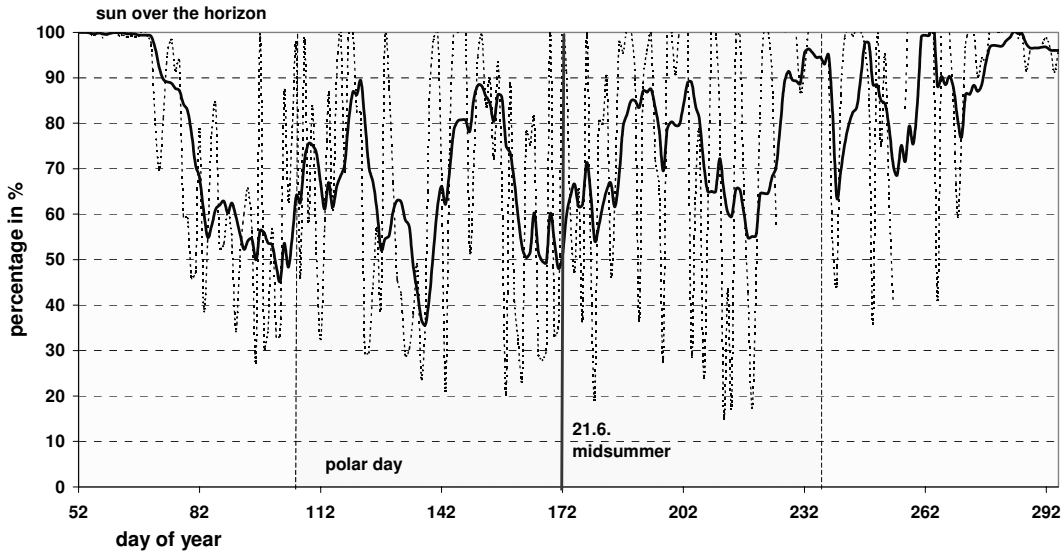

Fig. 4.13: Percentages of the diffuse radiation on the global radiation in Ny-Ålesund for 21.2. - 22.10.2001 (daily means and 7-day running mean)

The fraction of the diffuse radiation on the global radiation can be put into a direct relationship with the cloud coverage as soon as the sun reaches an elevation higher than the Zeppelin mountain. With a high degree of cloud coverage the percentage of the diffuse sky radiation of the global radiation rises too. During the polar day 2001 the percentage of the diffuse sky radiation varied from one day to the others from < 30 % to 100 %. Taken from the diagram the end of March/April, mid of May and June 2001 longer phases with relatively few clouds have been observed. This constant rise started in July and lasted until October. Only in August the diffuse radiation percentage dropped down again to < 20 % for a short time.

The variation of the annual mean diffuse radiation in relation to the total mean for the Koldewey data series is represented in Fig. 4.14. The total annual mean of the observation period amounts 70.1 W/m². The biggest deviations from it appeared in 1997

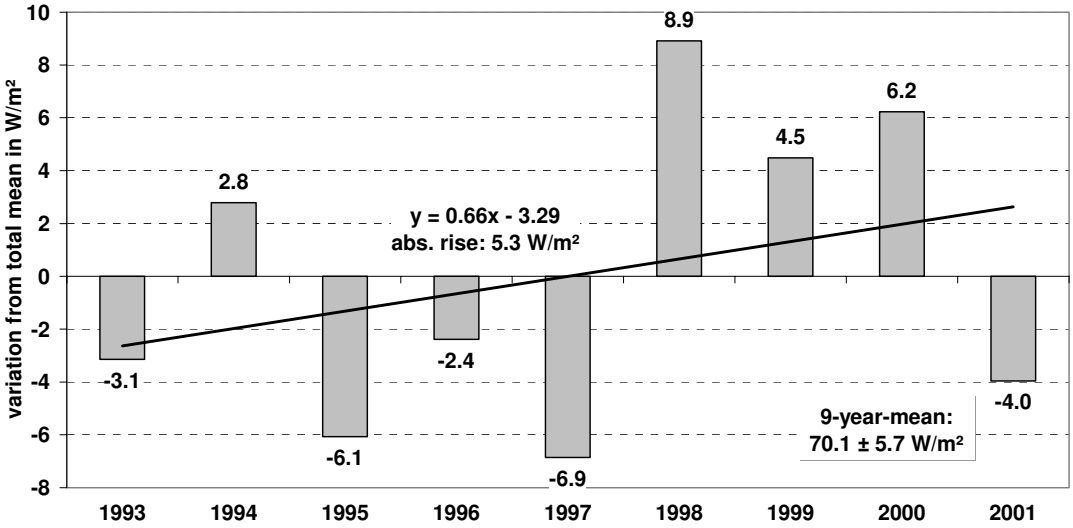

Fig. 4.14: Variations of the annual means of the diffuse radiation in relationship to the total mean for the Koldewey data series

with -6.9 W/m² and in 1998 with 8.9 W/m². With an initial value of 66.8 W/m² in 1993 the regression line of the diffuse radiation rises up with 5.3 W/m² during the observation period. This rise lies within the annual standard deviation of ± 5.7 W/m². The seasonal development of the diffuse radiation is shown for the period March 1993 - August 2001 in Tab. 4.9 and Appendix 4.4.2, Fig. 1. Thereby a rise of the diffuse radiation of 17.9 W/m² can be determined particularly in summer starting with an initial value of 94.9 W/m² (1993). In spring time the rise is substantially lower with 7.7 W/m² and an average value of 74.0 W/m². The autumn could not be evaluated due to the missing diffuse radiation in November.

Starting from July 1993 the direct solar radiation and the diffuse radiation is increased strongly. The rise of the diffuse sky radiation amounts to 3.3 W/m². The July values of the years 1996 and 1998 - 2001 exceed the 100 W/m² mark.

Tab. 4.9: Seasonal means and rise of the diffuse radiation in W/m² for the Koldewey data series (March 1993 – August 2001)

	Mean	max. Meam	year	min. mean	year	initial value	rise/a	abs. rise
spring	74.0 ± 7.8	84.4	1994	63.3	1996	70.2	1.0	7.7
summer	106.1 ± 10.7	124.0	1998	88.2	1997	94.9	2.2	17.9
July	105.9 ± 12.4	119.7	1999	87.9	1997	89.3	3.3	26.4

4.4.3 Global Radiation

The global radiation consists of the direct-horizontal radiation and the diffuse sky radiation (see Eq. 2.5). It is measured in 2 m height with a upward directed pyranometer in Ny-Ålesund since August 1992 (see Chapter 3.1, Fig. 3.3). During the investigation

period an average value was calculated of 113.9 ± 5.7 W/m² (see Tab. 4.10). The largest global radiation was detected with 928 W/m² on 17th June 2000.

Tab. 4.10: Average and extreme values of the global radiation in W/m²

	period	mean and standard deviation	absolute maximum	absolute minimum
global radiation	1993 - 2001	113.9 ± 5.7	928.0 (17.6.2000)	0
	2001	120.7	921.6 (13.6.2001)	0

The monthly global radiation, the standard deviation for the observation period and the average values are represented in Fig. 4.15 for the year 2001. During the investigation period the highest monthly means occur between 221.5 and 231.7 W/m² (see Fig. 4.15) in May and June. Between November and January no global radiation was measured; in February and October only partly. Due to the usual better weather conditions in spring the average monthly global radiation rises strongly towards May/June and drops again with increasing cloud appearance until September.

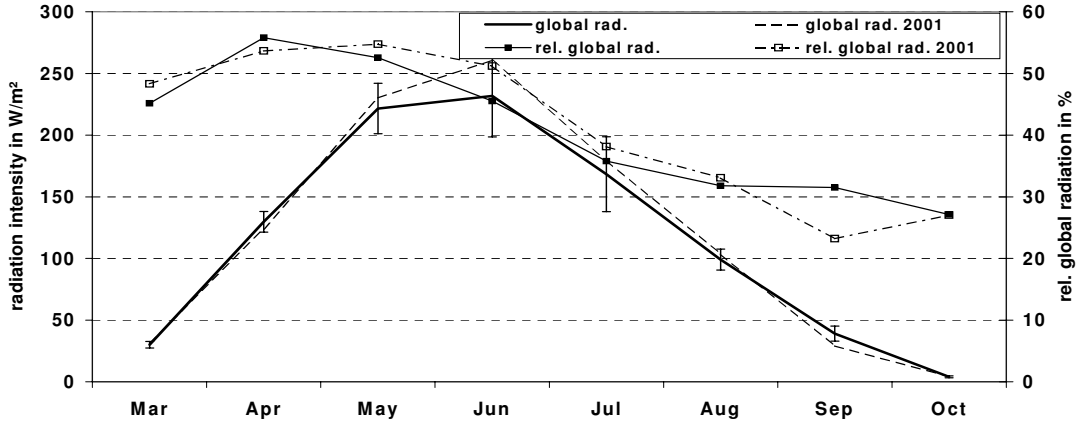

Fig. 4.15: Monthly means of the global radiation in comparison to the diffuse sky radiation, and the direct-horizontal radiation for the period of 1993 – 2001

The diffuse sky radiation is clearly higher than the direct-horizontal radiation in all months where the solar altitude is above the horizon, as mentioned in chapter 4.4.2.

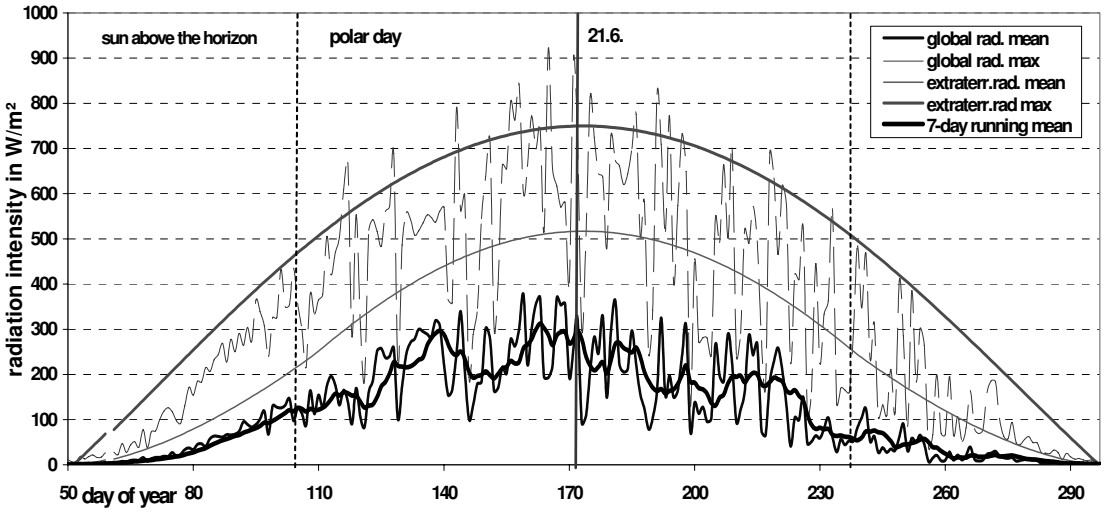

Fig. 4.16: Yearly course of the global radiation and the extraterrestrial radiation in its daily means and maxima for a period of 21.2. - 22.10.2001

From May until August 2001 the global radiation lie over the average values of the Koldewey data series. In June 2001 the mean global radiation reaches its maximum at 260.7 W/m² that surpasses the total average June value of 29 W/m².

Except September the values of the year 2001 stay within the standard deviation of the Koldewey data series. In September 2001 a slightly smaller global radiation was determined, than it was usual during the observation period. The average and maximum global radiation of the year 2001 are shown in Fig. 4.16. for the time in which the sun was standing above the horizon. The annual average 2001 was calculated with 120.7 W/m² that slightly surpasses the average value of the Koldewey-row with 77.4 W/m². The highest value of the year 2001 was measured with 923 W/m²on 13th June.

The global radiation reached its highest average value on 7th June 2001. A seven day running mean was selected, in order to smooth the daily averages of the global radiation 2001 and to minimize short weather fluctuations. It is noticeable that the maximum average values of the global radiation already occur in the time before 21st June 2001. In 2001 it could be also stated that the global radiation rises more rapidly to May/June and afterwards it drops more slowly (see also Fig. 4.17). The transitional phase from polar night to polar day shows a higher global radiation than the transitional phase from polar day to polar night.

The global radiation of the daily and annual course for the year 2001 is shown in Fig. 4.17. A strengthened daily variation of the global radiation is remarkable as a function of the position of the sun above the horizon. The respective maximum of the global radiation usually occurs in the morning between 10 and 11 UTC. The fluctuations of the global radiation in the annual process are more emphasized than the fluctuations in the daily course. As mentioned earlier, the global radiation reached its maximum already before 21st June 2001. From end of September till the beginning of February the global radiation does not rise above 25 W/m², not even at noon. For the night hours this phase persists even till April and begins at the start of August accordingly.

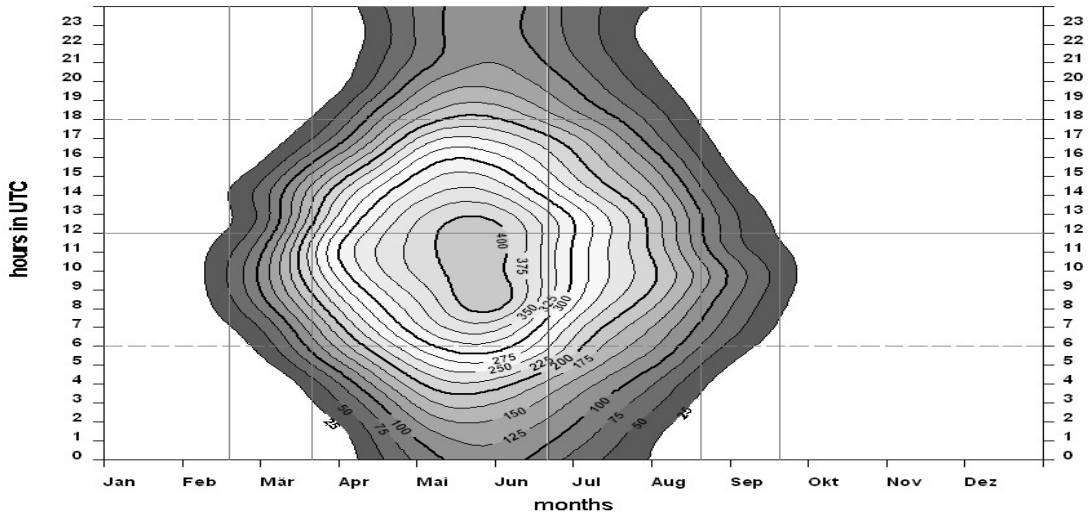

Fig. 4.17: Isopleth-diagram of the global radiation for 2001 (in W/m²), time in UTC

In Fig. 4.16 the global radiation is represented in comparison to the extraterrestrial radiation. The average global radiation lies below the extraterrestrial radiation. The maximum values can exceed the extraterrestrial radiation due to multiple reflections between earth's surface and clouds. This arises particularly during the time, where the ground is covered with snow. This effect is called ice and/or snow blink. The relationship of the global radiation to the extraterrestrial radiation is called relative global radiation *($E_{G\,rel}$)*. It indicates the degrees of the short-wave radiation, which penetrates through the atmosphere:

$$E_{G\,rel} = \frac{E_G}{E_0} \tag{4.2}$$

Radiation losses can result from the absorption of gases, aerosols and water vapour as well as from the reflection at and in clouds. The monthly relative global radiation for 2001 and for the total time is represented in Fig. 4.15. It can be recognized that the relative global radiation is highest in April and May as well as in June 2001 with over 50 %. From July until September it drops again below 40 % due to the strong cloud coverage, in October (and in September 2001) even below 30 %. The daily averages of the relative global radiation as a function of the relative sunshine duration is shown for the year 2001 in Appendix 4.4.3 Fig. 5. It can be concluded that the relative global radiation increases with the relative sunshine duration (HELMET 1989). The average relative global radiation 2001 lies with 44.8 % over the average value of 42.2 %. In 2001 the relative sunshine duration amounts on average 34.5 % and thereby it clearly lies over the average value in the observation period with 28.5 % per year.

The average global radiation during the observation period for July is represented in Appendix 4.4.3, Fig. 1. During this time the maximum values of the global radiation varies between 708 W/m² (1993) and 820 W/m² (2001). The average July values lies between 215.3 W/m² (1993) and 114.3 W/m² (1994). The July average value during the entire investigation period amounts to 168.2 W/m². With an initial value of 165.3 W/m² (1993) a slight rise of the regression line of 0.6 W/m² can be determined until 2001 (see also Tab. 4.11). Using the average July values of the Norwegian Polar Institute between 1974 and 1979 as well as 1981 till 1992 the trend analysis could be followed back until 1974; this is represented in Appendix 4.4.3, Fig. 2. Since 1974 the smallest average value amounts to 114.3 W/m² (1994); the largest average value amounts to 226.0 W/m² (1988). The period 1974 - 2001 shows a decreasing trend of the average global radiation in July of around 0.4 W/m² per year, which is opposite to the rise within the Koldewey data series. This can be explained with the low value at the start of the Koldewey data series (1993 - 2001) in the year 1994.

The seasonal average values and the rise of the global radiation from March 1993 until August 2001 is represented in Tab. 4.11 (see also Appendix 4.4.3, Fig. 3). The seasonal values were calculated by the monthly average values of three consecutive months; starting with the spring from March to May. In the summer the seasonal average value lie between 144.0 W/m² (1994) and 181.3 W/m² (2001). The average value amounts to 166.3 W/m² for the total time. In all summer months (June - August) a rise of the global radiation of around 15.4 W/m² can be determined in the observation period. This rise is even stronger, than in July. The average values of the global radiation in spring lie between 136.2 W/m² (1996) and 117.0 W/m² (1999). A slight reduction of the global radiation in the observation period of 5 W/m² could be recognized.

Tab. 4.11: Seasonal average values and rise of the global radiation in W/m² for March 1993 – August 2001

	mean	max. mean	year	min. mean	year	initial value	rise/a	abs. rise
spring	127.5 ± 6.6	136.2	1996	117.0	1999	130.3	0.6	-5.0
summer	166.3 ± 12.8	181.3	2001	144.0	1994	156.7	1.9	15.4
July	168.2 ± 30.3	215.3	1993	114.3	1994	165.3	0.6	4.7
June (74-01)	175.8 ± 23.2	226.0	1988	114.3	1994	181.4	-0.4	-10.3

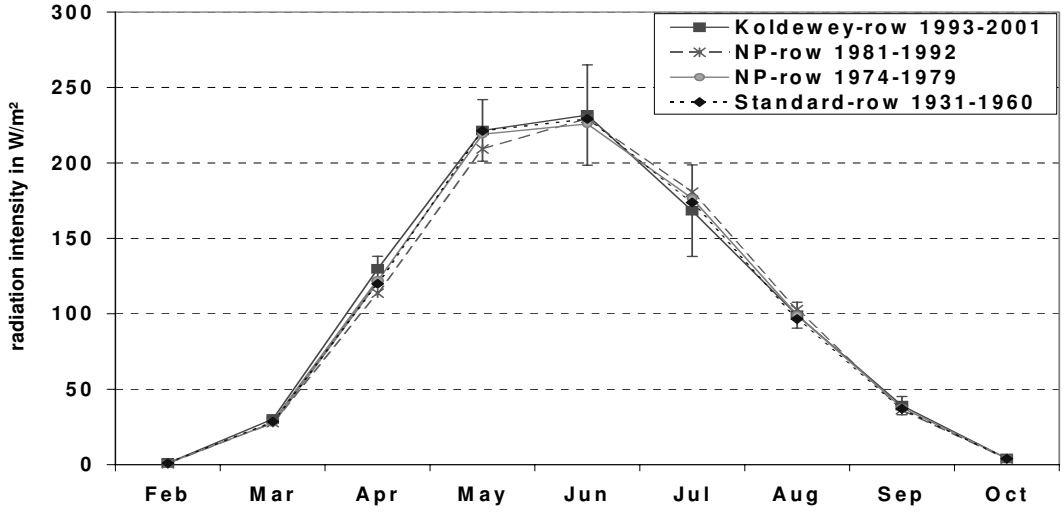

Fig. 4.18: Long-term monthly means of the global radiation in comparison: WMO-standards (1931 – 1960), NP data series (1974 - 1979/1981 - 1992) and Koldewey data series (1993 – 2001)

Because of the strong variability of the global radiation with the change of cloudiness it must be registered constantly, in order to receive representative radiation data (LILJEQUIST und CEHAG 1994[3]). The comparison of the monthly means of the Koldewey data series (1993 - 2001), of the Norwegian Polar Institute (NP) (1974 - 1979 and 1981 - 1992) as well as the WMO standards (1931 - 1960) for Ny-Ålesund is shown in Fig. 4.18. Between February and October an extensive correspondence of all data series could be determined within the ranges of the standard deviations. The average values in these months however do not exceed the 50 W/m² level. Very small differences have been registered in the months of February, March, September and October (see also Appendix 4.4.3, Fig. 4). The largest deviation of the Koldewey data series from the standard row of 1931 - 1960 was determined in April with 9.7 W/m². It should be noted that these standard values only base on irregular measurements. Nevertheless, this period shows the smallest deviations in the comparison to the Koldewey-data series. Only the April value of the standard row lies outside of the standard deviation of the Koldewey data series. The largest average value of all measurement series was calculated in June with 225.9 ± 33.3 W/m² for the Koldewey data series. The NP data series 1981 - 1992 has shown the largest deviations from the Koldewey data series. According to the record of the NP the global radiation for the data series between 1974 and 1992 decreases from April to May and increases again from June to August. This trend is only continued in June with small difference of 3.1 W/m². Both NP data series lies within the standard deviations of the Koldewey data series, except the April value for the period between 1974 and 1979. Additionally, deviations from the NP data series can be based on the hourly mean calculation. Like the direct sun radiation and the diffuse sky radiation the annual averages were only determined for the time in which the solar altitude is above the horizon. The values were calculated without consideration of the refraction from 21 February to 22 October.

Fig. 4.19 represents the deviations of the annual averages from the mean annual average of the Koldewey data series. The annual average values in the period 1993 - 2001 lie up to 7.7 W/m² over and 7.8 W/m² under the total average annual value of 113.9 W/m² (see Tab. 4.12). In the years 1993 and 2001 the average values exceed the standard deviation of 5.7 W/m²; the values of the years 1994 and 1999 fall below it. The annual average values and rises of the global radiation for the periods 1993 - 2001 as well as for 1974 - 2001 are indicated in Tab. 4.12.

Tab. 4.12: Annual means and rises of the global radiation in W/m²

	Mean	Max. mean	year	Min. mean	year	Initial value	rise/a	Abs. rise
1993 - 2001	113.9 ± 5.7	123.1	1993	107.8	1994	111.9	0.4	3.2
1974 - 2001	113.7 ± 6.7	128.7	1979	100.9	1976	111.6	0.14	3.2

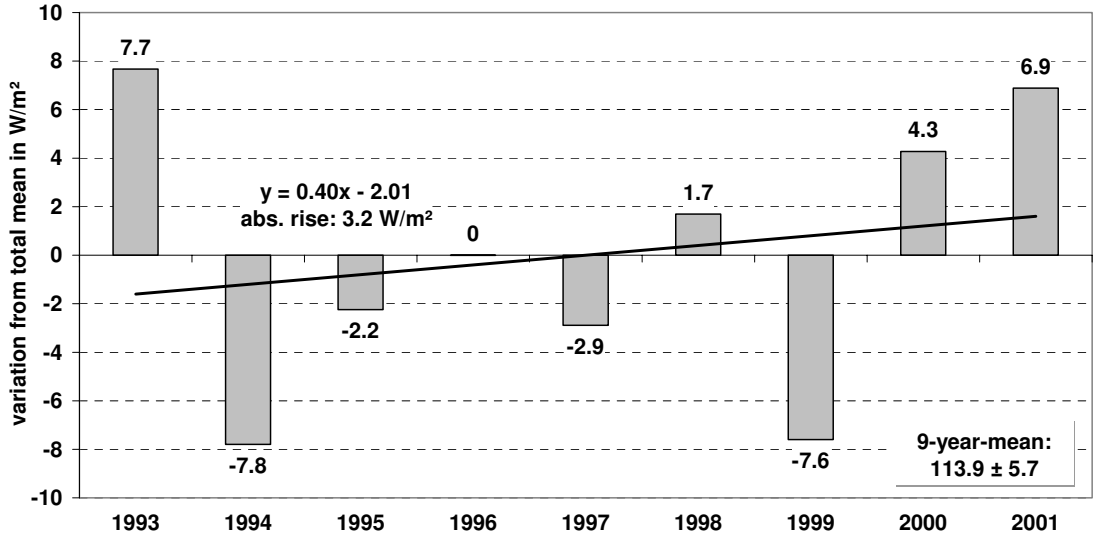

Fig. 4.19: Deviation of the yearly means of the global radiation from its 9-year-total average of the Koldewey data series

With the help of the data of the Norwegian Polar Institute and the Koldewey data series a long-term analysis of the global radiation could be created from 1974 to 2001. Some annual average values could not be determined due to missing datasets. The deviations from the annual average value by the global radiation in this period are represented in Fig. 4.20. The average value for the years 1993 to 2001 exceeds only slightly the means of the entire row 1974 - 2001 with 113.7 ± 6.7 W/m². The analysis results in a small rise of 0.14 W/m²/a up to the year 2001 with an initial value of 111.6 W/m² (1974).

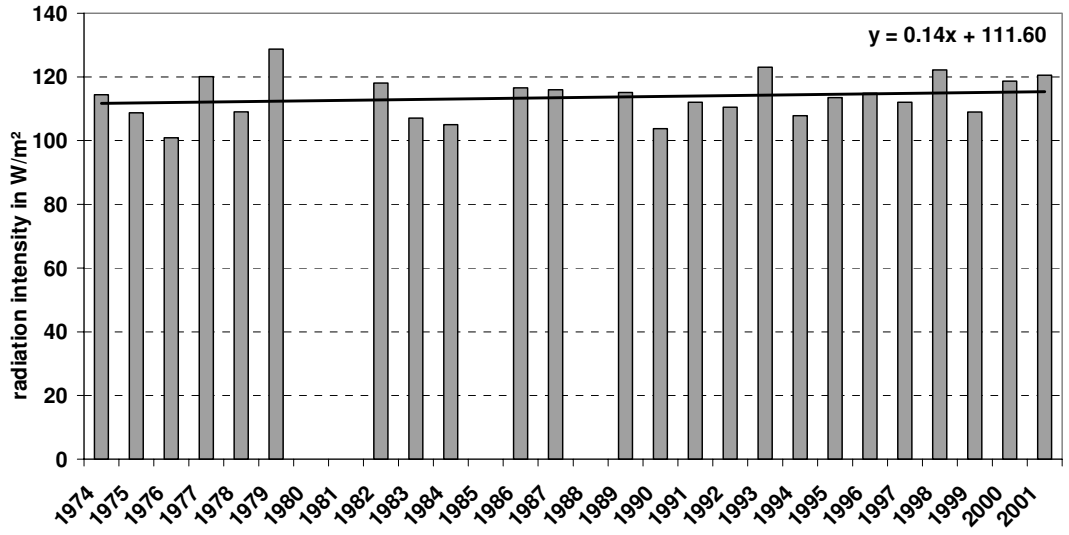

Fig. 4.20: Annual average values of the global radiation in its trend: NP data series (1974 – 1979/1981-2001) and Koldewey data series (1992 - 2001)

In the years 1976 and 1990 the annual averages of the global radiation with 100.9 and 103.8 W/m² fall below the 70 W/m²-level. The highest annual averages were calculated in 1979 with 128.7 W/m² and in 1993 with 123.1 W/m². The regression line of the Koldewey-row shows a 0.4 W/m² higher rise than the total period (1974 - 2001) (see Tab. 4.12). Both rises lie within the standard deviations of the Koldewey-data series and/or of the total data series.

4.4.4 Albedo

A big part of the global radiation is reflected in dependence of the surface structure (reflected radiation). Since August 1992 the reflex radiation is determined in the context of the BSRN with a downward directed pyranometer for the computation of the albedo of the surface (see Chapter 3.1). The albedo is calculated from the relation between the reflected and the global radiation (see Eq. 2.6). Reliable albedo values require a global radiation of more than 50 W/m² (SCHMIDT and KOENIG-LANGLO 1994). In Tab. 4.13 the average and extreme values are indicated for the reflex radiation and the albedo.

Tab. 4.13: Average and extreme values of the reflex radiation in W/m^2 and the albedo in %

	period	mean and standard deviation	absolute maximum	absolute minimum
reflex radiation	1993 - 2001	59.3 ± 8.0	639.4 (4.6.2001)	0
	2001	64.4	639.4 (4.6.2001)	0
albedo	1993 - 2001	51.9 ± 6.2	100	8.2 (25.6.2001)
	2001	53.3	100	8.2 (25.6.2001)

The annual albedo value however does not tell a lot about the change of the reflection ability of the surface in the yearly course. More information contains Tab. 4.14 in which the albedo values of the months from March until October are indicated. A clear downfall of the average values of approximately 80 % in May to approximately 14 % in July can be determined in both time series 2001 and the Koldewey data series. Deviations of both data series occur in the months of June, September and October.

Tab. 4.14: Albedo, relative global radiation and relative sunshine duration for the Koldewey-data series (1993 – 2001) and the examplary year 2001

Period	Mar	Apr	May	Jun	Jul	Aug	Sep	Oct	year
1993 – 2001	77.6	78.7	79.9	52.8	13.9	16.3	32.9	53.4	51.9
2001	78.4	78.9	80.9	59.3	14.0	15.2	25.0	69.9	53.3

The reflex radiation at the Neumayer station (Antarctica / 70°37'S, 8°22'W) varies only with the short-wave radiation and the associated change of the snow surface due to the all-season snow surface (see Appendix. 4.4.4 Fig. 1). In Ny-Ålesund it comes to a very strong decrease of the albedo in June. This is due to a direct connection to the thaw and associated reduction of the reflex radiation. In the example year 2001 the albedo falls down from over 70 % to under 10 % within only one week (from 18th June to 25th June). Due to the missing snow surface in July and the wet soil only a small part of the short-wave radiation is reflected. The reflex radiation decreases from over 200 W/m² to values below 25 W/m² in the same short period.

In August the albedo slightly increases again by 2.4 % in the comparison to the previous month, which can be explained with drying of the soil. The very wet soil in July after the thaw is absorbing the majority of the radiation. Fig. 4.21 describes the

global radiation and the reflex radiation in relation to the albedo during the polar day 2001.

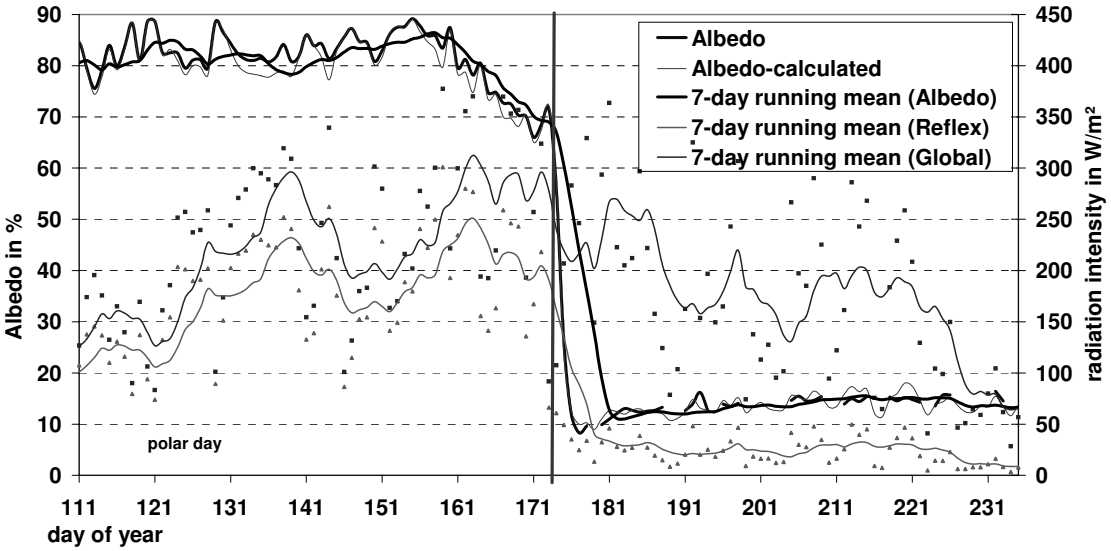

Fig. 4.21: Course of the measured and calculated albedo (daily means), running means of the albedo, global radiation, and reflected radiation during polar day 2001

Daily averages of the albedo (with global radiation: > 50 W/m²) as well as the running means of the global radiation, reflex radiation and the albedo are represented in Fig. 4.21. For the addition of missing albedo values the daily averages from reflex and global radiation (M_R/E_G) were computed without consideration of the 50 W/m² limit of the global radiation. From Fig. 4.21 it can be recognized that global radiation, reflex radiation and albedo strongly drop almost at the same time. The thaw is mainly caused by the radiation and the rise of the air temperature over the 0°C limit. It is probable that around 20/21 June additionally an intensified cloudiness with precipitation occured, which caused a very rapid melting of the snow. From the diagrams (see Appendix. 4.4.4, Fig. 2 and 3) this rapid reduction of the albedo can be found in each year of the investigation period. Thus, it is to be observed that the course of the thaw is always similarly fast. According LILJEQUIST and CEHAG (1994) the albedo for pure snow is between 80 and 90 %, for melting snow between 60 and 70 % and for soil free of snow between 5 and 20 %. The reduction of the albedo from 70 to 60 % lasted from one day to 15 days depending upon the weather conditions. Between 60 % albedo of the snow and the snow-free ground with an albedo of < 20 % it took usually 2 to 4 days (in the years 1994 and 1996 it lasted 6 to 7 days). In 2001 the snow underneath the measuring instrument melted within only two days. The time of the thaw however moved from year to year for 1 to 2 weeks and is to be expected during the entire month of June. The running means of the albedo in Fig. 4.21 represent the time of the thaw somewhat late; but the lines before and after the thaw indicate the mean albedo very well.

The first snowfall in autumn is difficult to determine from the albedo values, due to the 50 W/m² global radiation limits that the albedo values are based on. In this phase (September) the global radiation drops under this limit due to the high cloud coverage. A reliable statement over the time of the rerise of the albedo for the first snowfall cannot be given.

Because of the sharp decrease of the albedo from May to July, a trend analysis was made for these months within the observation period (see Tab. 4.15 and Appendix 4.4.4 Fig. 4). According this, the average values of the albedo vary relatively evenly in May at around 80% and in July at around 14 %. In both months considerable rises can be noted for the observation period. However, in June the albedo values vary between 18 and 65 %; which

can be explained with the fact that the thaw begins at a different time in each June. In the years 1995 and 1999 for example, the thaw already began very early. In the years 1994, 1996, 1998, 2000 and 2001 very high albedo values arose in June; that is why the thaw took place only in the last week of June.

Tab. 4.15: Average values and rises of the albedo (in %) for the months of May, June and July during the Koldewey- data series (1993 – 2001)

	mean	max. mean	year	min. mean	year	initial value	rise/a	abs. rise
May	79.8 ± 4.1	86.4	1998	74.1	1995	79.2	0.13	1.0
June	51.6 ± 15.7	65.1	1994	17.8	1995	46.8	0.96	7.7
July	13.7 ± 1.0	15.3	1993	11.5	1994	13.4	0.06	0.5

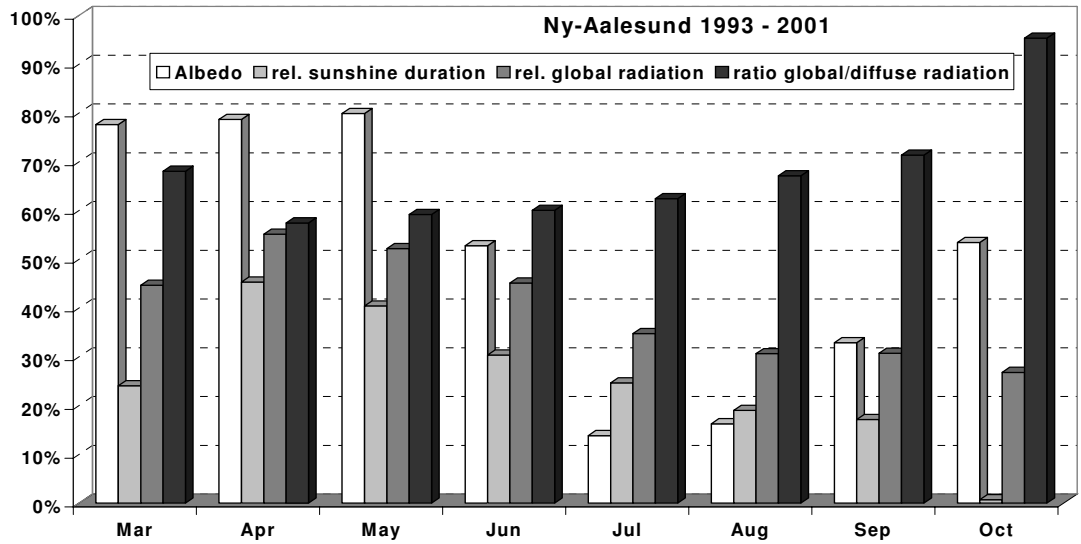

Fig. 4.22: Monthly means of the albedo, relative sunshine duration, relative global radiation and share of the diffuse radiation for the Koldewey data series

The connection between clouds and the albedo of the earth's surface is represented in Tab. 4.16 and in Fig. 4.22.

Tab. 4.16: Monthly means of the albedo, relative sunshine duration, relative global radiation and the fraction of the diffuse radiation for the Koldewey data series (1993 – 2001) and the examplary year 2001 in %

	Mar	Apr	May	Jun	Jul	Aug	Sep	Oct	year
1993 - 2001									
albedo	77.6	78.7	79.9	52.8	13.9	16.3	32.9	53.4	52.0
rel. global radiation	44.7	55.1	52.2	45.1	34.8	30.7	30.7	26.8	42.2
rel. sunshine duration	24.1	45.3	40.4	30.4	24.7	19.0	17.1	0.7	28.5
rel. diffuse radiation	68.1	57.5	59.2	60.0	62.4	67.1	71.3	95.4	61.7
2001									
albedo	78.4	78.9	80.9	59.3	14.0	15.2	25.0	69.9	53.3
rel. global radiation	48.3	53.7	54.8	51.2	38.1	33.1	23.2	27.0	44.8
rel. sunshine duration	34.1	44.6	54.6	44.9	28.1	22.5	12.5	0.7	34.5
rel. diffuse radiation	68.0	62.0	56.9	34.6	62.2	65.0	79.3	98.5	54.8

For this the albedo between March and October is compared with the relative sunshine duration, the relative global radiation and the fraction of the diffuse radiation from the global radiation ("relative" diffuse radiation) (see Chapter 4.2,

4.4.2 and 4.4.3). In the months from May until August the albedo decreases with an increasing density of low clouds (increasing diffuse radiation). Likewise, the relative sunshine duration as well as the relative global radiation decrease in this time. A large part of the incomming solar radiation is reflected back into space from the top side of the clouds. With snow in September and a lower solar altitude the albedo increases again.

At the beginning of October, when the sun disappears behind the mountains of the Brøggerfjellet, the diffuse sky radiation nearly corresponds to the entire global radiation. This parameter can be seen as an indicator for the cloud density, but only in the time of the polar day. Also the albedo varies with the position of the sun. A low solar altitude at a frozen snow cover would lead to an increased reflex radiation. An increase of the albedo occurs when the position of the sun is lower than 10° of height. Therefore, from the data base, no exact date can be given for the first snowfall in autumn.

4.4.5 Long-wave Radiation

The emitted radiation is a long-wave radiation emitted by the earth's surface. It is measured in 2 m height with a downward directed pyrgeometer. The counter radiation is the long-wave radiation emitted from the atmosphere which meets the earth's surface. It gets measurements with an upward directed pyrgeometer which is covered from the direct solar radiation. (see Chapter 3.1). The average values discussed in this section therefore are referred to the whole year. The average and extreme values of the counter radiation and emitted radiation as well as the long-wave radiation budget (LW-radiation budget) for the Koldewey data series from 1st January 1993 until 31st December 2001 as well as for the exemplary year 2001 are represented in Tab. 4.17.

Tab. 4.17: Average – and extreme values of the emitted radiation, counter radiation and LW-radiation budget

	Period	mean and standard deviation	absolute maximum	absolute minimum
emitted radiation	1993 - 2001	286.6 ± 3.0	459.6 (17.7.1999)	134.6 (4.3.1993)
	2001	287.4	430.4 (15.7.2001)	184.8 (2.4.2001)
counter radiation	1993 - 2001	250.8 ± 4.0	388.7 (31.8.1997)	106.0 (13.2.1996)
	2001	251.4	359.6 (13.7.2001)	130.2 (25.12.2001)
LW-budget	1993 -2001	-35.9 ± 3.1	63.5 (31.5.1999)	-168.9 (10.7.2001)
	2001	-36.1	39.4 (12.5.2001)	-168.9 (10.7.2001)

During the investigation period long-term means were calculated for emitted radiation of 286.8 ± 3.0 W/m² and the counter radiation of 250.8 ± 4.0 W/m² (see Tab. 4.17). The monthly means of the emitted - and counter radiation as well as the LW-radiation budget for the Koldewey data series and for 2001 are shown in Fig. 4.23. The largest average emitted radiation with 357.5 W/m² was registered in July. It exceeds the 300 W/m²-level in the months from May to September. The smallest monthly means amount to 247.3 W/m² in January and 244.0 W/m² in February. The average values in December, March and April only lie slightly above them. The maximum value of the emitted radiation was measured with 459.6 W/m² on 17th July 1999. The emitted radiation depends purely on the surface temperature ($LW\uparrow = \sigma T^4$) with $\sigma=5.67\cdot10^{-8}$. This explains the annual cycle shown in Fig. 4.23. The smallest average value of the emitted radiation was registered with 244.0 W/m² in February.

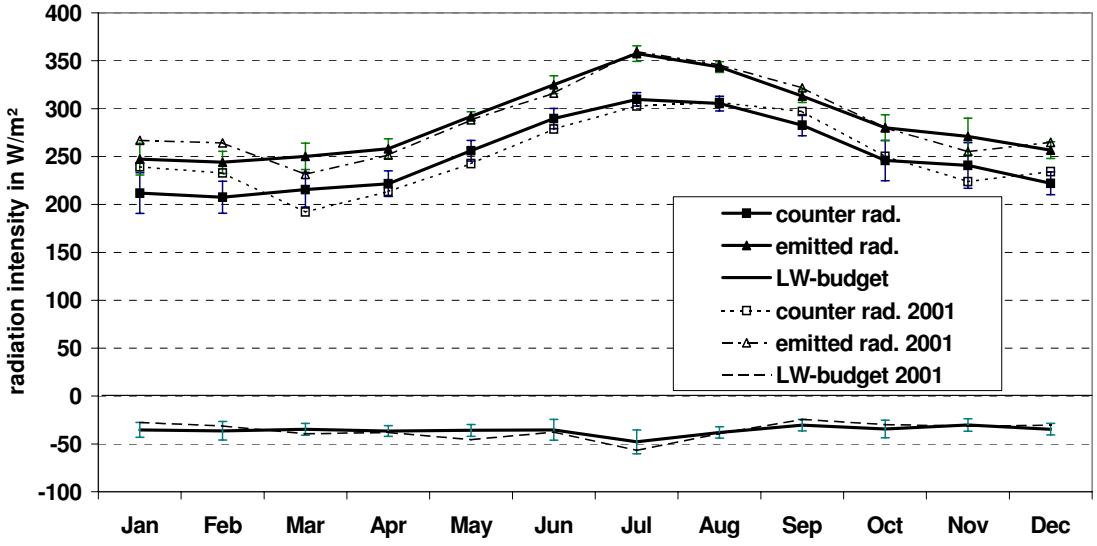

Fig. 4.23: Monthly means of the emitted radiation, counter radiation and LW-radiation budget for the Koldewey data series (1993 – 2001) and 2001

In June the global radiation shows a mean maximum of 231.7 W/m², while the mean maximum of the emitted radiation is with 357.5 W/m² in July. The courses of the monthly means of the emitted radiation and the counter radiation point out nearly constant distances (see Fig. 4.23). The highest average value of 309.8 W/m² lies in July like the emitted radiation. The counter radiation from July to September is clearly higher than in the previous months. This can be explained with the dense cloud ceiling starting from July. The smallest mean of the counter radiation could be determined with 207.7 W/m² in February. The average values of the months January, March, April and December only slightly lie above that value. In Fig. 4.23 it is noticeable that both, the emitted radiation and the counter radiation are higher in December until February 2001 and in November and March clearly lower than the average. In the months from January until March the values of 2001 fall out of the standard deviation for these months for the Koldewey data series.

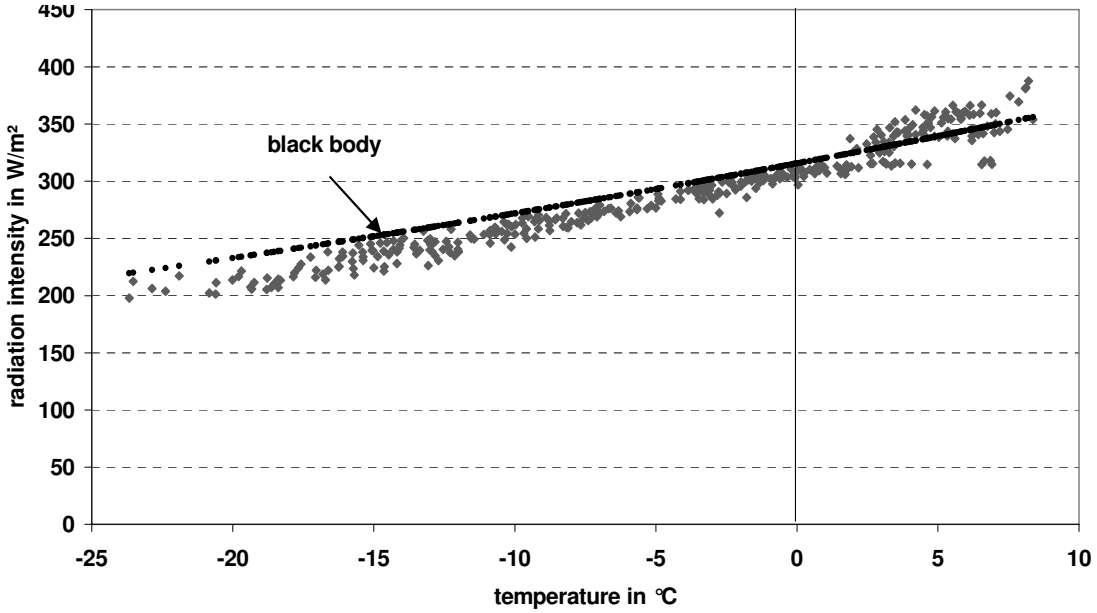

Fig. 4.24: Long-wave emitted radiation versus temperature (in 2 m height) in 2001

The diagram Fig. 4.24 shows the emitted radiation as a function of the temperature in 2 m height for the year 2001. It can be recognized that the emitted radiation increases with rising temperatures. This curve of the measured emitted radiation approaches to the Stefan Boltzmann law for the specific emitted radiation of a black body (black dots), which represents the earth's surface (see Chapter 2.1.1.2). The atmosphere is impermeable for the terrestrial radiation with cloud coverage at the absorption bands for water vapour of 5 – 8 µm and > 18 µm. Clouds absorb and emit this radiation. Additional absorptions for long-wave radiation result from the CO_2-bands at approx. 12 – 17 µm. A high part of the absorbed radiation is converted into heat. This effect is strengthened by the CO_2-entry into the polar atmosphere that means further percentages of the radiation are absorbed within the range of 12 – 17 µm and heat up the atmosphere (HUPFER and KUTTLER 1998[10]). The counter radiation in dependence of the temperature is represented in Fig. 4.25 for the year 2001. The counter radiation increases with the rising temperature. The values lie between the emissivity of a black body (e = 1.0 - black curve) and that of a grey body (e = 0.7 - grey curve).

The monthly means of the emitted radiation (see Fig. 4.23) are relatively evenly distributed between 30 and 38 W/m² above the respective monthly counter radiation. Compared with the curves of rest of the year the counter radiation and the emitted radiation show a greater distance with 47.8 W/m² in July. The emitted radiation from the earth's surface is therefore higher than the counter radiation over the whole year. The long-wave energy loss of the earth's surface results from the difference of emitted radiation and counter radiation and is called LW-radiation budget (Eq. 2.8).

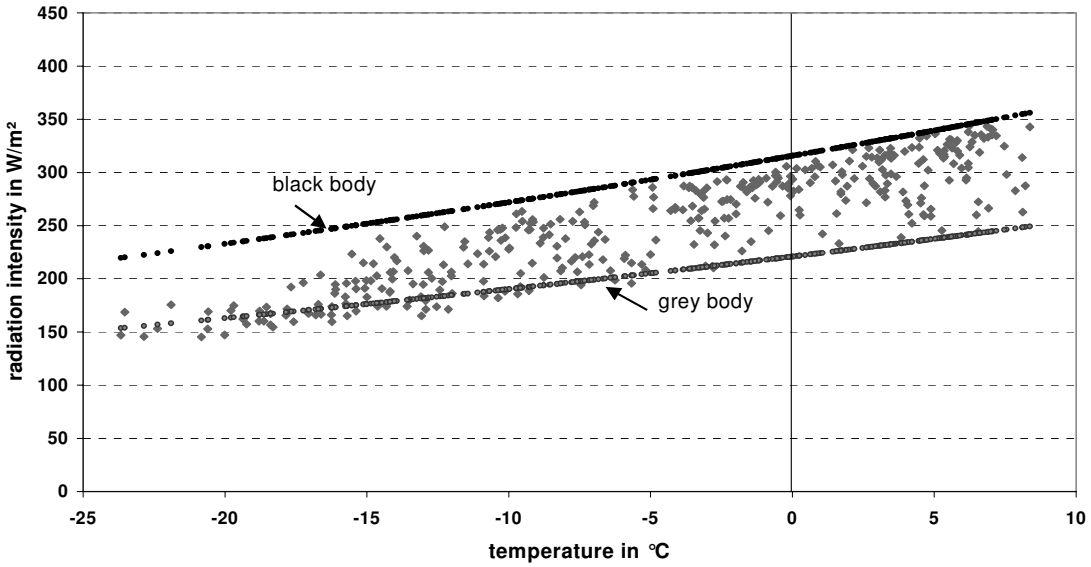

Fig. 4.25: Long-wave counter radiation in dependence of the temperature (in 2 m height) for 2001

In July the LW-radiation budget falls with 47.8 W/m² clearly under the value of the global radiation with 168.2 W/m². The global radiation however only affects the energy budget during that time, where the solar altitude is above the horizon, while the long-wave radiation is effective in the whole year

In order to represent the energy loss of the earth's surface, the LW-radiation budget is set into the negative range. With the long-wave energy budget the cloud coverage can also be described. The LW-radiation budget at the earth's surface under a low, dense cloud cover indicates values from approximately -20 to -30 W/m². In single cases to the values reach ≥ 0 W/m² in the middle of June (Fig. 4.26). In this case the values of the

counter radiation exceed those of the emitted radiation. For polar night this description is one of the methods for the determination of the cloud cover.

The yearly variation of the emitted radiation and the counter radiation and the LW-radiation budget for the year 2001 is represented in Fig. 4.26. The annual average and extreme values are indicated in Tab. 4.17.

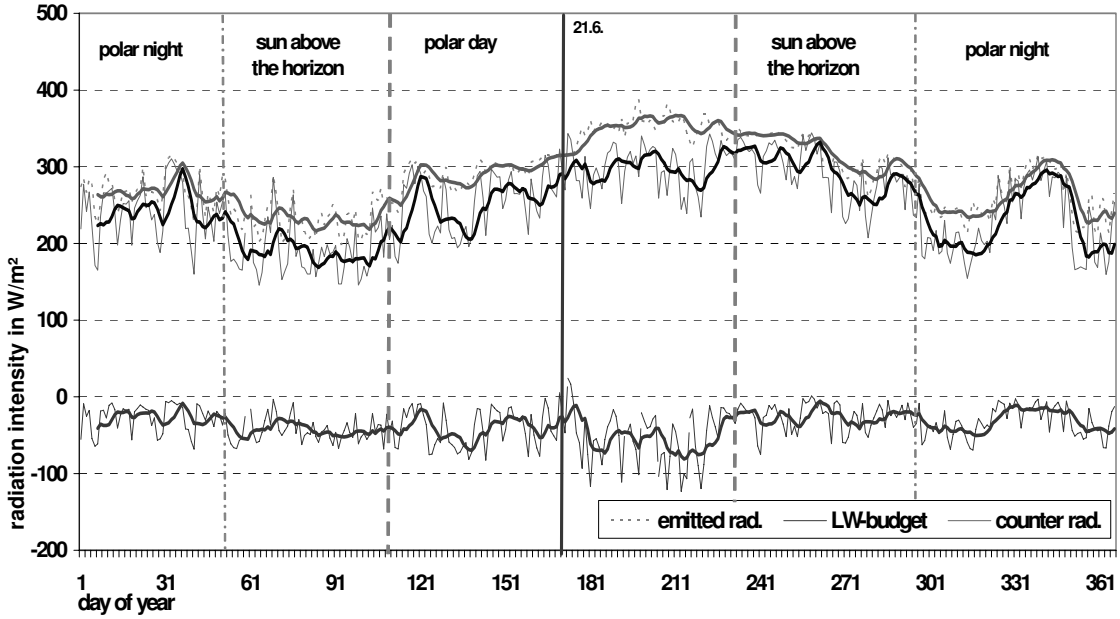

Fig. 4.26: Daily means of the emitted radiation, counter radiation and LW-radiation budget for 2001

In the yearly course of the LW-radiation budget a few emphasized minima show up between May and July (Fig. 4.27). A relatively steep decrease of the LW-radiation budget from -45 to -75 W/m² could be determined. This can be explained with the snow-free and wet soil in July, which is strongly warmed up that more long-wave radiation can be emitted into the atmosphere. The strongest daily fluctuations of the LW-radiation budget between -40 W/m² during the night hours and -75 W/m² at noontime could also be determined in July. In the spring it comes to variations of the LW-radiation budget in the daily course due to the changing positions of the sun. The biggest value of the LW-radiation budget arises before the beginning the polar night in August and/or September between 15 and 21 o'clock. According to Fig. 4.27 it can be noticed, that the emitted radiation in this period drops relatively evenly, the counter radiation however reaches its maximum average values.

For the months of January and July as well as for the season trend analyses were made for the investigation period; they are represented in Tab. 4.18 to 4.20. Additional analyses are shown in Appendix 4.4.5, Fig. 1 to 3. According to that the counter radiation rose from 192.5 W/m² in January 1993 for 31 W/m² in January 2001. The emitted radiation increased for around 22.6 W/m² starting with 233.2 W/m². Therefore a rise could be registered for the LW-radiation budget too (see Tab. 4.20). This is however smaller with 8.4 W/m² than the rise of the emitted radiation and the counter radiation, since the latter increases more strongly than the emitted radiation. The difference between the values of the two parameters becomes smaller. Also in the remaining winter months a decrease of the LW-radiation budget could be registered.

In July a slight increase of the emitted radiation of around 0.9 W/m² and a decrease of the counter radiation of around 11.1 W/m² could be observed in the investigation period.

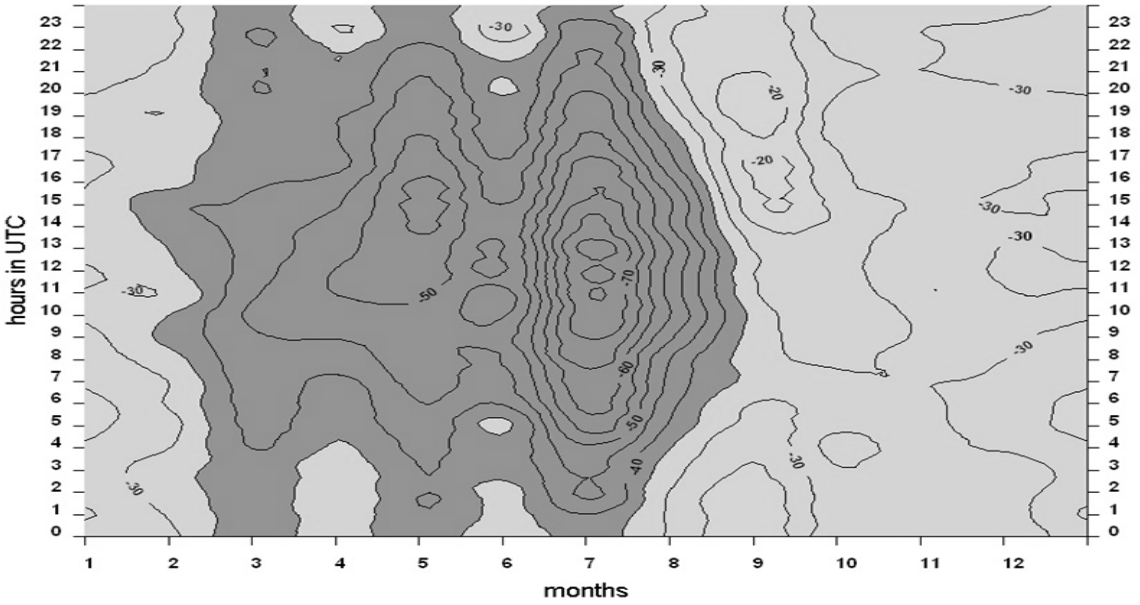

Fig. 4.27: Isopleth-diagramm of the LW-radiation budget in W/m² for 2001

The difference of both values increases and thus also the decrease of the LW-radiation budget by 12 W/m² with an initial value of -40.3 W/m² in July 1993. This decrease in July varies with 9.5 W/m² only slightly from the decrease of the LW-radiation budget of the entire summer. In the autumn both emitted radiation and counter radiation in the observation period increase. The counter radiation exhibits again a higher rise than the emitted radiation. The LW-radiation budget rises with a value of 8 W/m² from -36.7 W/m² in autumn 1993. Since the LW-radiation budget represents the energy loss of the earth's surface, it means a reduction of these losses for the autumn in the investigation period. In the winter, spring and summer the energy losses increase in the observation period.

With the help of the data of the Norwegian Polar Institute it was possible to retrace the trend for the months January and July for the emitted radiation and LW-radiation budget until 1982 and for the counter radiation even until 1974. According to that the counter radiation decreased slightly by 0.12 W/m² /a in January between 1982 and 2001 and stronger by 0.46 W/m² /a in the period of 1974 - 2001. This decrease was not observed in the period of the Koldewey data series (1993 - 2001). Also the values of the emitted radiation fall with 0.48 W/m² in January during the period 1982 - 2001. The strong rise with 2.8 W/m²/a of the emitted radiation in January between 1993 and 2001 let assume that between 1982 and 1992 an even stronger decrease of the emitted radiation took place.

Tab. 4.18: Seasonal means and rise of the emitted radiation in W/m² (seasons: 12/1992 - 11/2001; January/July: 1982 - 2001, 1993 - 2001)

	mean	max. mean	year	min. mean	year	initial value	rise/a	abs. rise
winter	248.9 ± 9.2	262.7	2001	234.7	1998	240.5	1.7	13.5
spring	266.8 ± 6.9	277.6	1994	257.1	2001	273.0	-1.24	-9.9
summer	342.0 ± 6.4	349.1	1993	332.1	1994	343.6	-0.3	-2.5
autumn	288.1 ± 8.8	303.7	2000	273.7	1994	280.2	1.6	12.7
January	247.3 ± 16.5	267.0	2001	219.3	1998	233.2	2.8	22.6
July	357.5 ± 8.0	369.7	1993	344.3	1994	357.0	0.1	0.9
January (82-01)	254.3 ± 17.2	292.7	1990	219.3	1998	259.4	0.48	-9.1
July (82 –01)	357.4 ± 13.0	384.4	1986	325.4	1984	353.8	0.34	6.5

Tab. 4.19: Seasonal means and rise of the counter radiation in W/m² (seasons: 12/1992 - 11/2001; January/July: 1974 - 2001, 1982 - 2001, 1993 - 2001)

	mean	max. mean	year	min. mean	year	initial value	rise/a	abs. rise
winter	213.1 ± 9.6	228.1	2001	198.3	1998	206.6	1.3	10.5
spring	231.1 ± 9.9	249.0	1994	216.1	2001	241.8	-2.15	-17.2
summer	301.6 ± 5.4	307.5	1993	262.2	2000	309.2	-1.5	-12.1
autumn	256.4 ± 13.3	283.7	2000	238.3	1995	243.5	2.6	20.8
January	211.9 ± 21.1	243.3	1996	183.8	1998	192.5	3.9	31.0
July	309.8 ± 7.0	322.0	1994	298.6	1999	316.7	-1.4	-11.1
January (82-01)	217.2 ± 19.1	247.4	1990	183.8	1998	218.5	-0.12	-2.3
July (82 –01)	313.9 ± 12.0	335.2	1986	293.0	1988	323.0	-0.87	-16.5
January (74-01)	219.0 ± 19.6	252.4	1974	183.8	1998	225.9	-0.46	-12.4
July (74 –01)	319.4 ± 15.1	352.8	1978	293.0	1988	339.0	-1.3	-35.1

Tab. 4.20: Seasonal means and rises of the LW-radiation budget in W/m² (seasons: 12/1992 - 11/2001; January/July: 1982 - 2001, 1993 - 2001)

	mean	max. mean	year	min. mean	year	initial value	rise/a	abs. rise
winter	-35.8 ± 4.2	-27.7	1996	-43.0	2000	-33.9	-0.38	-3.0
spring	-35.7 ± 3.8	-28.6	1994	-41.0	2001	-31.2	-0.93	-7.4
summer	-40.4 ± 7.4	-24.9	1994	-47.6	1995	-34.4	-1.2	-9.5
autumn	-31.7 ± 5.6	-20.0	2000	-39.8	1995	-36.7	1.0	8.0
January	-35.5 ± 7.7	-21.8	1996	-46.3	1995	-40.7	1.05	8.4
July	-47.8 ± 12.4	-22.3	1994	-63.8	1999	-40.3	-1.5	-12.0
January (82-01)	-37.1 ± 7.5	-21.8	1996	-48.4	1983	-40.9	0.35	6.7
July (82 –01)	-43.5 ± 14.2	-19.1	1983	-67.2	1988	-30.8	-1.21	-23.0

In January 1982 - 2001 the emitted radiation drops more strongly than the counter radiation, thus, the rise of the LW-radiation budget is smaller than in the period of 1993 - 2001. In July an acceptance of the counter radiation and the LW-radiation budget can be observed as well as an increase of the emitted radiation for all periods. The rises of the emitted radiation (0.1 - 0.34 W/m² /a) and the decreases of the counter radiation (0.87 - 1.4 W/m² /a) show small deviations for all time series. Except the counter radiation in July 1974 – 2001 which decreases slightly under the standard deviation of ± 15.1 W/m² all trends lie within the respective standard deviations.

The deviation of the annual LW-radiation budget from the 9-yearly average value of the Koldewey data series is shown in Fig. 4.28. With an average value of -35.9 ± 3.1 W/m² the highest deviations have been registered with 6.2 W/m² in 1994, with 4.4 W/m² in 1995 and with 3.2 W/m² in 1996. These annual averages fall out of the mean standard deviation of the LW-radiation budget of 3.1 W/m². The rises of emitted radiation and counter radiation during the observation period are represented in Tab. 4.21 and in Appendix 4.4.5 Fig. 3; 4. With the emitted radiation a higher rise of 4.3 W/m² (initial value 284.2 W/m² in the year 1993) could be recognized than at the counter radiation with 0.8 W/m² (initial value 250.3 W/m² in the year 1993). The increased emitted radiation causes an energy loss of the earth's surface and explains the decrease of the LW-radiation budget.

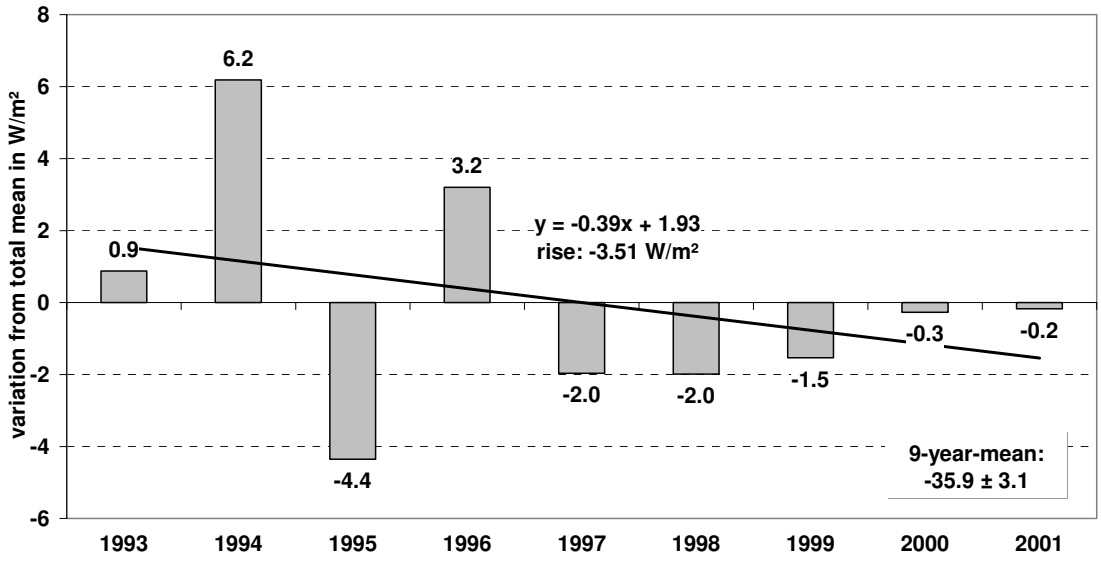

Fig. 4.28: Variation of the yearly average LW-radiation budget over the 9-yearly mean for the Koldewey data series (1993 – 2001)

With the help of the Norwegian data series an extension of the time series could also be accomplished back until 1982 with emitted radiation and the LW-radiation budget as well with the counter radiation until 1974. The Tab. 4.21, Fig. 4.29 and Appendix 4.4.5, Fig. 5 show the trend analyses for the emitted radiation and counter radiation show the as well as the LW-radiation budget for the respective periods. Compared with the observation period 1993 - 2001 reversals can be recognized in the courses of emitted radiation and the counter radiation. While a rise of both parameters can be noticed for the Koldewey data series, there is a decrease over the long period of 1982 to 2001. The annual average values of the counter radiation in the period drop stronger those of the the emitted radiation in the 1982 - 2001 period. In consequence, a decrease of the LW-radiation budget of 0.51 W/m² could be registered. In relation to the observation period (0.44 W/m² /a) the LW-radiation budget decreases stronger in the total period from 1982 to 2001, which means the energy loss of the surfacewas higher in the lengthened period than during the time of the Koldeway data series. All trends are within the standard deviations.

Tab. 4.21: Yearly means and rises of the long-wave radiation in W/m²

	period	mean	max. mean	year	min. mean	year	initial value	rise/a	abs. rise
emitted rad.	93 - 01	286.6 ± 3.0	290.2	2000	282.6	1998	284.2	0.54	4.3
	82 - 01	287.7 ± 3.6	294.9	1983	282.6	1998	289.2	-0.31	-2.5
counter rad.	93 - 01	250.8 ± 4.0	254.8	1996	244.4	1998	250.3	0.1	0.8
	82 - 01	253.8 ± 6.5	261.3	1990	244.4	1998	261.2	-0.64	-12.2
	74 - 01	257.4 ± 9.5	279.6	1974	244.4	1998	269.8	-0.81	-21.9
LW-budget	93 - 01	-35.9 ± 3.1	-29.7	1994	-40.2	1995	-33.9	-0.44	-3.5
	82 - 01	-33.9 ± 4.1	-28.8	1986	-40.2	1995	-28.0	-0.51	-9.7

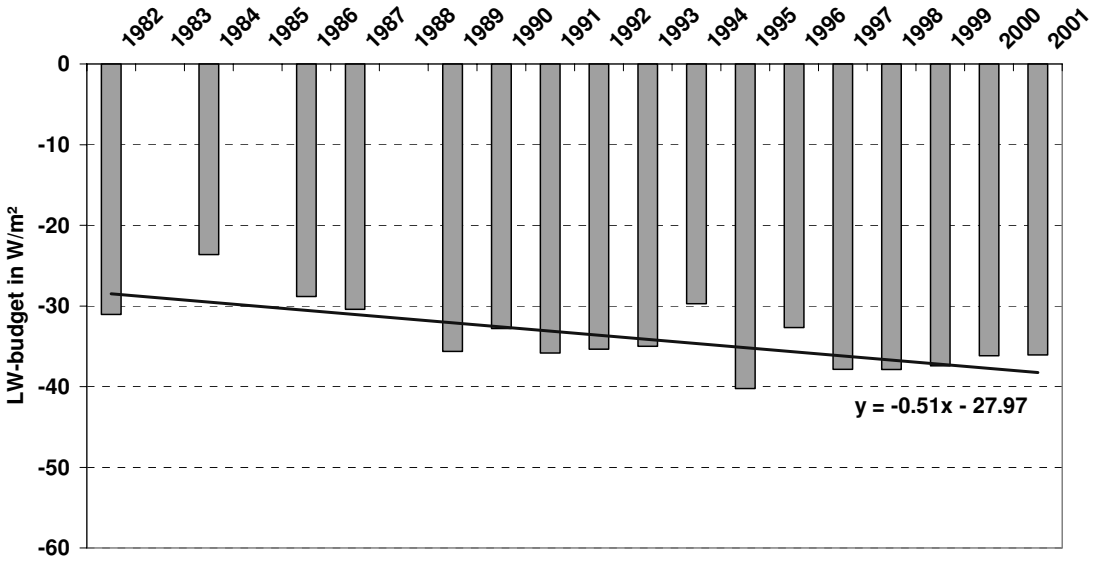

Fig. 4.29: Yearly means of the LW-radiation budget (1982 - 2001)

4.4.6 Radiation Budget

The surface radiation budget is the short- and long-wave energy exchange between the earth and the atmosphere. It is consisting of the short-wave and the long-wave radiation budget (Eq. 2.9). Since this energy exchange takes place during the whole year, the radiation budget was referred to 365 days.

Tab.4.22: Average and extreme values of the radiation budget in W/m²

	period	mean and standard deviation	absolute maximum	absolute minimum
Radiation budget	1993 - 2001	1.4 ± 3.2	658.8 (23.6.2001)	-103.2 (20.7.1998)
	2001	1.7	658.8 (23.6.2001)	-91.5 (22.5.2001)

During the investigation period a small positive average annual radiation budget of 1.4 ± 3.2 W/m² could be determined (see Tab. 4.22). The monthly average values of the radiation budget are represented in Fig. 4.30. From September till April the monthly average values drop down to the negative range. With a negative radiation budget the earth's surface looses energy and cools down. The largest energy losses occur in the coldest months of the year: with -35.5 W/m² in January and with -35.9 W/m² in February. This negative budget becomes balanced again in the months of the polar day by an increased short-wave radiation. The highest average value of the radiation budget appears in July at about 97.2 W/m². The radiation budget lies in a positive range, when the earth's surface absorbs more radiation energy than it emitts or reflects and warms up (LILJEQUIST und CEHAG 1994). It can be noted that the radiation budget has its maximum in July, while the maximum of the global radiation already appears in May - June. This is directly connected with the decreased albedo by the thaw. The reflected radiation clearly decreases starting from June, due to the bigger absorption of energy by the surface.

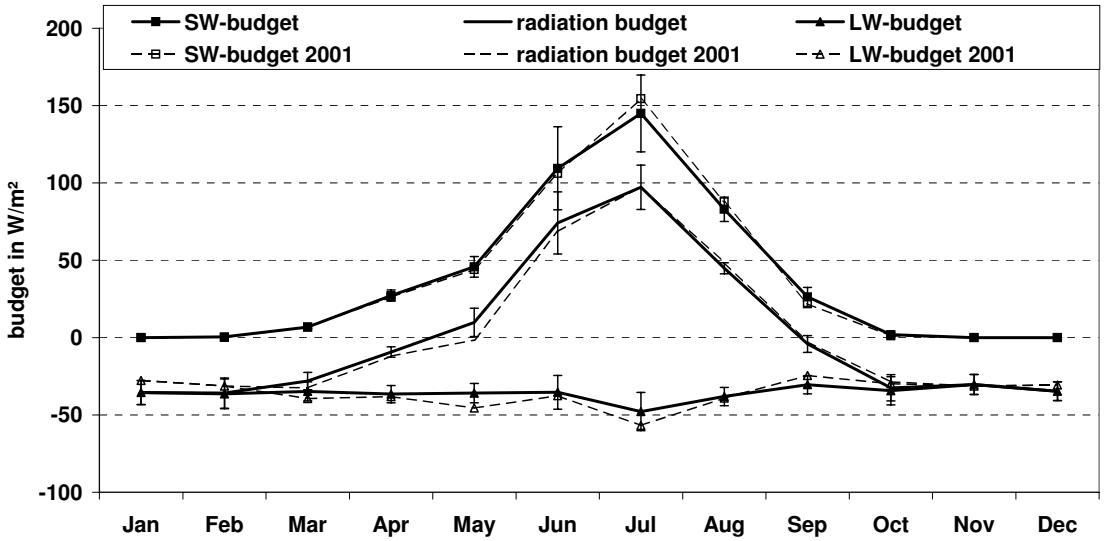

Fig. 4.30: Monthly means of the radiation budget for the Koldewey data series (1993 – 2001)

The long-wave budget reaches its minimum in July (see Fig. 4.30). From the representation of the daily averages in Fig. 4.31 it becomes evident that the radiation budget rises intensely with the thaw in the year 2001. Since there is not any short-wave radiation existant during the polar night, the radiation budget equals the values of the long-wave radiation budget during this time; the earth's surface is loosing energy.

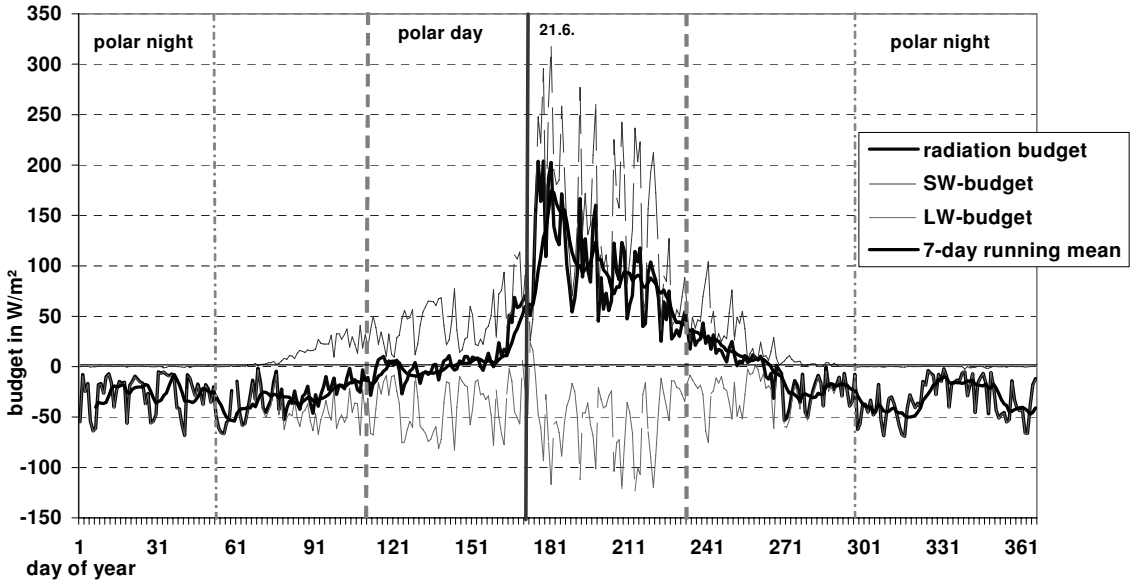

Fig. 4.31: Annual course of the radiation budget (daily means) for 2001

The short-wave energy gain due to the high sunshine duration in April and May becomes balanced again by long-wave energy losses of the same rate. The daily values of the total balance vary around the zero point. Only in June the radiation budget rises slightly over the 50 W/m² limit. For Ny-Ålesund, the most important energy gain of the year only took place after the thaw. Within somewhat more than three months the surface absorbs more energy, than emitted during the remaining months.

The daily and yearly course of the radiation budget is represented in the isopleth-diagramm of Fig. 4.32. The maximum of the average radiation budget of > 175 W/m² was reached between middle of June and middle of July in 2001, at noon, when the sun

reaches its zenith. In the months of June and July the radiation budget reaches its minimum in the night hours, but does not fall under zero.

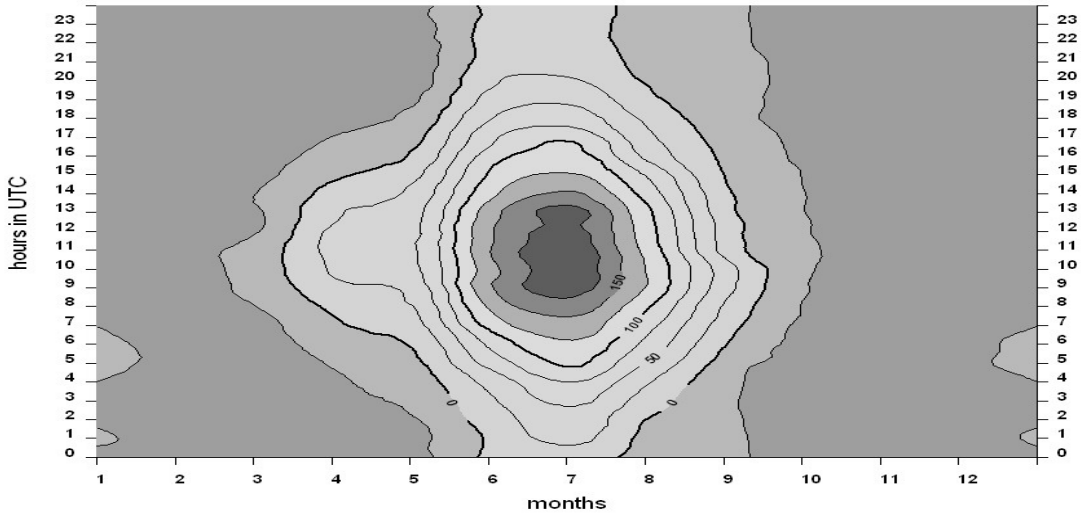

Fig. 4.32: Isopleth-diagramm of the radiation budget for 2001 (in W/m²), time in UTC

The radiation budget in the Arctic is strongly variable. In order to represent this variability, trend analyses were accomplished for January and July as well as for the entire seasons. The average values and the rises of the regression lines are shown in Tab. 4.23 as well as in Appendix 4.4.6 Fig. 1 to Fig. 3.

Tab. 4.23: Seasonal means and rises of the radiation budget in W/m² (Mar. 1993 – Nov. 2001)

	mean	max. mean	year	min. mean	year	initial value	rise/a	abs. rise
winter	-35.7 ± 4.3	-27.4	1996	-43.0	2000	-33.6	-0.41	-3.3
spring	-9.2 ± 6.4	-3.2	1995	-15.4	1997	-3.5	-1.14	-9.1
summer	72.1 ± 22.7	89.6	1995	60.1	1994	76.4	0.88	-7.0
autumn	-22.3 ± 7.7	-13.1	2001	-28.0	1998	-24.9	0.53	4.2
January	-35.5 ± 7.7	-21.8	1996	-46.3	1995	-40.7	1.05	8.4
July	97.2 ± 14.3	122.0	1993	76.3	1997	102.1	-0.99	-7.9
January (1974-2001)	-37.2 ± 7.8	-21.8	1996	-48.4	1983	-32.6	-0.18	-4.9
July (1974-2001)	110.7 ± 16.6	139.1	1985	76.3	1997	129.0	-1.22	-32.9

The short-wave radiation budget is missing in January; thus the radiation budget is corresponding with the long-wave radiation budget. For the observation period a rise of the radiation budget could be registered in January; which explains the temperature rise at that time (see Chapter 4.5). During the remaining winter months a slight rise of the radiation budget could be determined within the standard deviation. Large fluctuations of the radiation budget arise in summer due to differences of the solar exposure. This leads to the observation of a slight decrease of the radiation budget. A similar trend is determined in July. In autumn the slight rise of the radiation budget is also reflecting in the gradient of the temperature.

Like already discussed for some radiation parameters, the time series for the radiation budget could also be extended for the months of January and July until 1974. The average values and trend are represented in Tab. 4.23 as well as in Appendix 4.4.6 Fig. 4.5. In January a course was determined that was tending in an opposite direction in the period of 1974 - 2001. The rise of the radiation budget by 1.05 W/m² during the Koldewey data series 1993 - 2001 conflicts with a slight decrease of 0.18 W/m² for the

lengthened period of 1974 - 2001. In the selected month July of the total period of 1974 - 2001 the radiation budget decreases with 1.22 W/m² substantially more strongly than in the selected month July 1993 - 2001 with 0.99 W/m². None of the trends for the radiation budget in January, July and the seasons drop-out of the respective ranges of the standard deviations. The radiation budget 2001 lies with 1.7 W/m² only slightly above the total mean of 1.4 W/m². The change of the annual radiation budget to the annual average for the observation period 1993 - 2001 is shown in Fig. 4.33. According that, a variation of the radiation budget between 6.2 W/m² (1995) und –2.9 W/m² (1997) could be observed. In the years 1997, 1998 and 2000 a slightly negative annual budget from -3.4 to -0.7 W/m² could be established. The largest deviations of the total means were registered with 4.8 W/m² in 1995 and with 4.3 W/m² in 1997. Based on an initial value of 2.2 W/m² the trend slightly falls with 3.6 W/m² in the observation period.

The annual average values and rises of the radiation budget for the Koldewey data series (1993 - 2001) and for the period of 1974 - 2001 are represented in Tab. 4.24. In the total period of 1974 - 2001 the average annual average lies with 5.7 ± 6.1 W/m² clearly above that of the Koldewey data series, but still within the standard deviation. The average values vary between 15.9 W/m² and -2.9 W/m². A decrease of the radiation budget can be also observed in the lengthened period. This decrease of 0.45 W/m² per year is identical to the decrease that was determined in the Koldewey-data series. When looking the average annual radiation budget of the period 1974 - 2001, which are represented in Fig. 4.34, it is noticeable that the radiation budget only drops under zero in the latest years. Altogether, the radiation budget only lies in a slightly negative range in the years of 1990, 1997, 1998 and 2000.

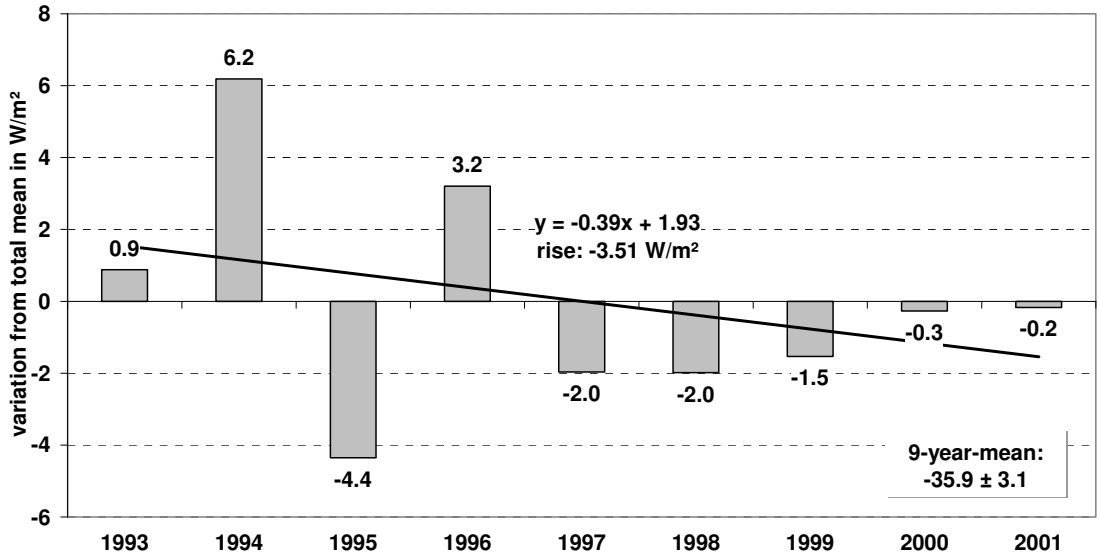

Fig.4.33: Divergence of the yearly means of the radiation budget from the 9-yearly mean (1993 - 2001)

Tab. 4.24: Yearly means and rises of the radiation budget in W/m²

	mean	max. mean	year	min. mean	year	initial value	rise/a	abs. rise
1993 - 2001	1.4 ± 3.2	6.2	1995	-2.9	1997	2.23	-0.45	-3.6
1974 - 2001	5.7 ± 6.1	15.9	1976	-2.9	1997	11.2	-0.45	-12.2

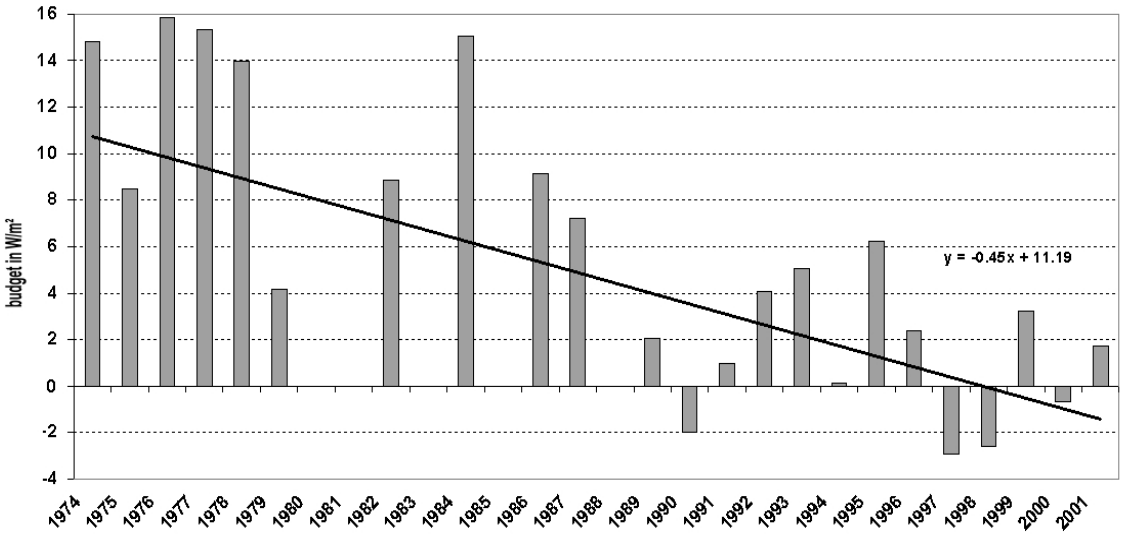

Fig. 4.34: Yearly means of the radiation budget in trend of the years 1974 – 2001: according the data by the NP (Norsk Polarinstitutt: 1974 - 1979/1981 - 1992) and the Koldewey data series (1993 - 2001)

4.5 Meteorology

4.5.1 Air Temperature

The air temperature in 2m standard height is to be evaluated for the Koldewey station in the period from 1st January 1994 to 31st December 2001. Table 4.25 shows the means, standard devations and extrema for the observation period as well as for the year 2001. For the latest mentioned period a yearly mean was determined of –5.1 ± 6.8°C, which like all meteorologic parameters was weighted because of the change in the rhythm of the measurements (13./14. Juli 1998), see Chapter 3.2.

Tab. 4.25: Means and extreme values of the temperature for 1994-2001 as well as for the year 2001

period	mean ± standard dev.	abs. maximum	abs. minimum
1994 - 2001	-5.1 ± 6.8°C.	18.2°C (18.7.1999)	-35.4°C (13.2.1996)
2001	-4.7 ± 6.9°C	15.0°C (9.8.2001)	-28.9°C (2.4.2001)

According FØRLAND, et al. (1997) in Ny-Ålesund already temperatures were measured below of –40°C (-42.2°C in March 1986). The monthly means, standard devations as well as the absolute maxima, and minima for the Koldewey data series are shown in Fig. 4.35. The coldest month with a mean of -13.1 ± 6.3°C is February. The minimal values of this month lie around -35.4°C, and the maximal temperatures do not exeed 5°C. The warmest month is July with a mean of 5.3°C (Minimum: -1.3°C; Maximum: 18.2°C) on an average standard deviation of ± 2.3°C. The maximal values rise up over 15°C during the warmest months July and August, but do not reach 20°C (see Fig. 4.34). But even in these months it is not rare that the temperatures fall below the freezing point (HANSSEN-BAUER et al.1990).

In Ny-Ålesund the maximal temperatures of July fluctuate between 9.5°C (1996) and 18.2°C (1999); the minimal values lie between 2.8°C (2002) and -1.3°C (2000).

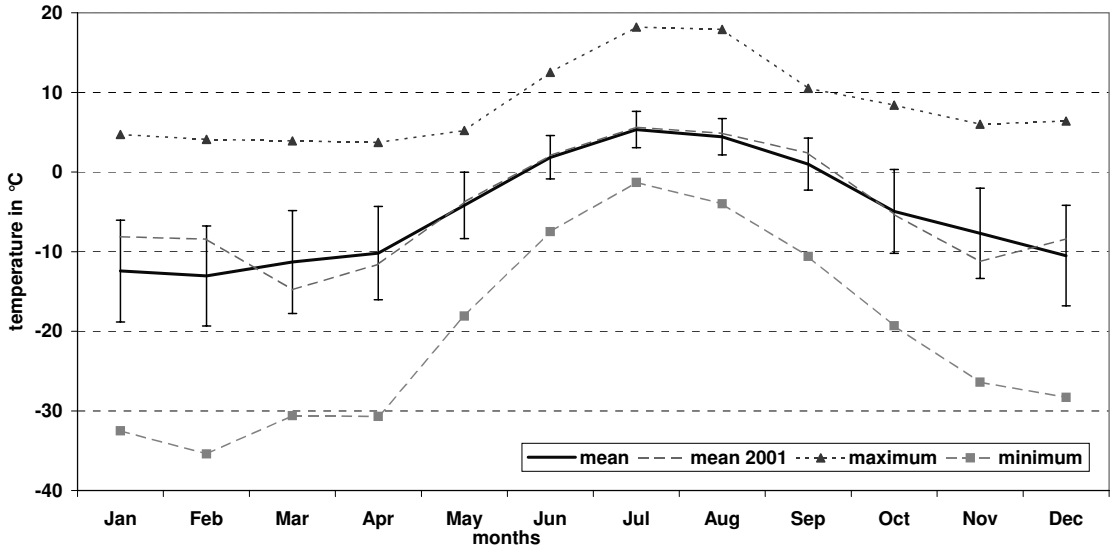

Fig. 4.35: Mean and extreme values of the temperature for 1994 – 2001

The annual variation of the temperature in 2001 based on daily averages is represented in Fig. 4.36. Since the temperature is affected by the position of the sun, the diagram contains the following phases: the twilight phases of the polar night, the transitional phases from the polar night to the polar day and from the polar day to the polar night, the polar day as well as the zenit of the sun on 21 June.

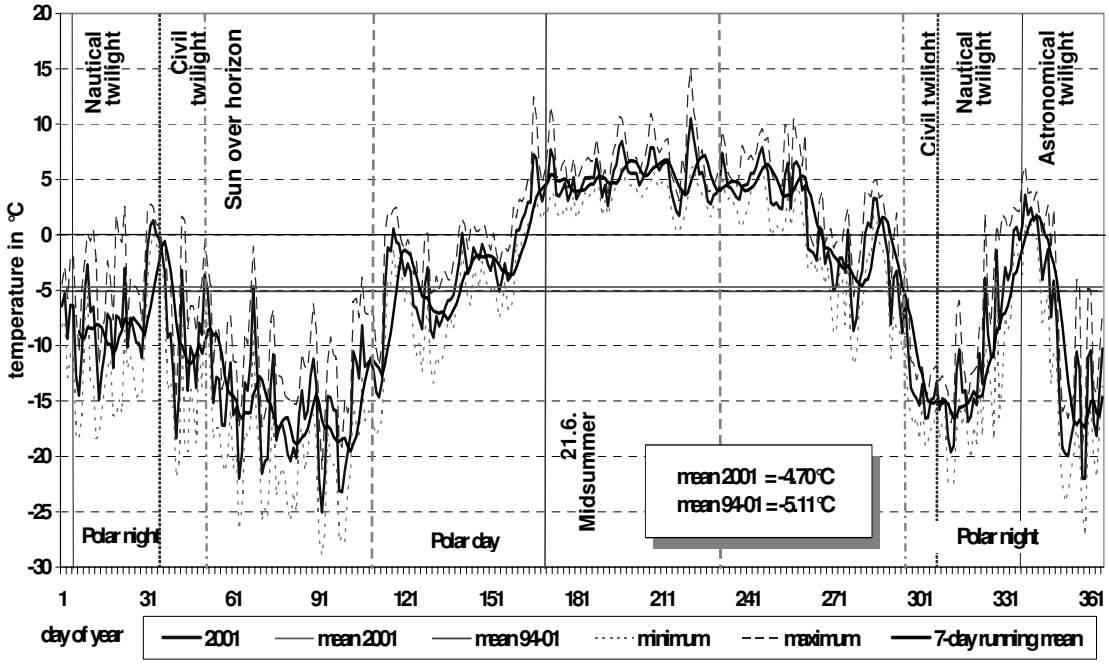

Fig. 4.36: Yearly course of the temperature for 2001

For the year 2001 the largest temperature variations arise in March/April as well as in December. In these months very high temperature fluctuations up to 17°C could be determined within only a few hours. These extreme variations of the temperatures can be explained with the high zonal temperature gradients. (see Chapter 2.2), see HISDAL (1998). In order to eliminate extreme weather situations a seven day running mean was used. The annual average temperature of 2001 lies with -4.7°C above the average temperature

value (5.1°C) of in the entire observation period. In comparison with other years it is noticeable that the winter temperatures were relatively mild in the period from 1999 to 2001.

The yearly and the diurnal variations of the mean temperature in Ny-Ålesund during the year 2001 are represented in Fig. 4.37. The typical yearly course of the thermoisopleths in polar regions can be observed. From the diagram it can be noticed that throughout the whole year the lowest temperature fluctuations appear in the daily courses.

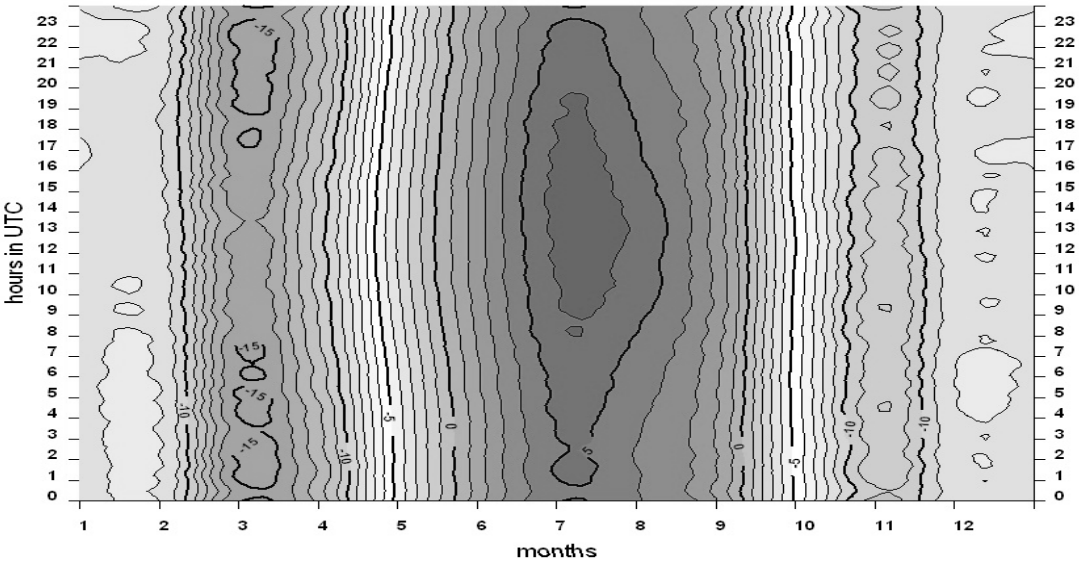

Fig. 4.37: Thermoisopleth-diagram for 2001 (temperature in °C)

This can be explained with the following processes: The winter days are usually clear by the influence of cold air flows from northeast; the earth's surface emits heat (upward longwave radiation). Warm air masses come from the south cause the cloud formation and reduce the loss of heat. In the summer the conditions nearly converted: With a higher sun position the surface gets heated under clear sky; sea-wind conditions are developing, which cause the formation of clouds likewise. The cloud coverage reduces the surface's emittance (upward longwave radiation), in the night hours see HISDAL (1998). Short effective irradiation (see Chapter 2.2) as well as turbulent mixing of larger air layers by high wind velocities cause heat exchanges and decrease daily temperature fluctuations (DWD 1987).

The biggest temperature changes do not arise during the course of the day, except from extreme weather situations, but in the yearly course. Essentially this is due to the yearly rhythm of the sun in the polar latitudes. The coldest mean temperatures 2001 were noted about one month before the beginning of the polar day. From this it can be concluded that the yearly variation of the air temperature is following the solar altitude and thus the global radiation. During the polar day the course of the air temperature shows the form of a simple wave (see Fig. 4.35). The maximum temperature arises about half a month after the sun's highest level. The mean temperature minima usually decreases about two months after the sun's lowest position and later than in the moderate latitudes (DWD 1987).

The seasonal average temperatures and the temperature rise from December 1993 until August 2002 are shown in Tab. 4.26 and in the diagram (Appendix 4.5.1 Fig. 3). The seasonal values were calculated respectively from the monthly means of three consecutive months; beginning with the winter from December to February (see Chapter 3.2.3).

Tab. 4.26: seasonal means and rises of the temperature in °C for Dec. 1993 – Aug. 2002; comparison of the January and July values with the DNMI data series 1935 – 2000

	mean	max. Mean	year	min. mean	year	initial value	rise/a	abs. rise
winter	-12.0 ± 2.3	-9.0	2000/01	-15.3	1998	-14.4	0.5	3.9
spring	-8.6 ± 1.1	-7.1	1994-99	-10.1	2001	-7.4	-0.2	-1.9
summer	4.0 ± 0.6	4.5	1998	3.1	2000	3.5	0.1	0.8
autumn	-3.9 ± 2.1	-0.6	2000	-7.1	1994	-6.3	0.5	3.7
January	-12.5 ± 6.4	-8.4	2001	-18.4	1998	-16.25	0.8	5.9
July	5.3 ± 2.3	6.9	1998	4.6	1996	5.0	0.1	0.6
Jan (1935-00)	-12.7 ± 4.3	-3.4	1947	-22.4	1981	-	-	-
July (1935-00)	4.9 ± 0.8	6.2	1960/85	3.2	1947	-	-	-

max. mean – maximum average value; min. mean - minimum average value
initial value – initial value of the regression curve in 1994
rise – rise of the regression curve during the investigation period

In autumn and winter high rises of the temperature appear between 3.7 and 3.9°C for the observation period. The variations between the smallest and the largest average value amount to 6.5°C in autumn and 6.3°C in winter. In contrast to that there is a temperature drop of 1.9°C in spring with a deviation of the average values of 3°C. In summer the temperature during the observation period mainly remains constant; a smaller rise can be registered around 0.8°C.

The average values, standard deviations, maxima and minima of the temperature in the month of January are shown in Appendix 4.5.1 Fig. 1. For the investigation periods 12/1994 - 8/2002 (1935 -2000) the average January temperatures amount to –12.5°C (-12.6°C) with an average standard deviation of ±6.4°C (±4.2°C). Both values vary only slightly from each other (see Tab. 4.26).

The coldest temperature, which was measured in January, was -32.5°C in the years of 1997/98, while on 19th January 1996 a temperature maximum of 4.7°C had been registered. The trend analysis using the linear regression for the month January of the investigation period results in a temperature rise of approximately 5°C with an initial value of -16.3°C in 1994.

However, all mean value fluctuations in the month January lie far over this rise, thus it can not be indicated as a significant temperature trend. The January values of the years 1996 and 1998 show particularly high standard deviations of ±8.9°C and ±9.2°C. Generally large variations in temperature can be determined during the winter months until into April in all years (see Fig. 4.35).

Average values, standard deviations, maxima and minima of the month July are shown in Appendix 4.5.1 Fig. 2 and Tab. 4.26. The mean standard deviation in July of the years 1994 - 2001 lies between ± 1.5°C (2001) and ± 2.8°C (1999); far under the fluctuations from January. In July a less clear rise of the temperatures than in January is recognizable. The evaluation results in a tendentious rise of 1°C with an initial value of 5.0°C (1994). Still, this rise lies below the smallest standard deviation of ± 1.5°C (2001).

The temperature change of the annual average values in relation to the total mean of the Koldewey data series (1994 – 2001) is shown in Fig. 4.38. In 2001 the annual average temperature lies 0.4°C above the total mean of -5.1°C of the Koldewey data series (1994 – 2001). In this period a temperature rise of 1.8°C occurred, with an initial value of -1.0°C in 1994. However, this value cannot be called significant, since high temperature variations arise in the relatively short observation period (lowest average

value: -0.8°C; highest average value: 1.2°C). The annual average temperature even decreased in the years between 1999 and 2001.

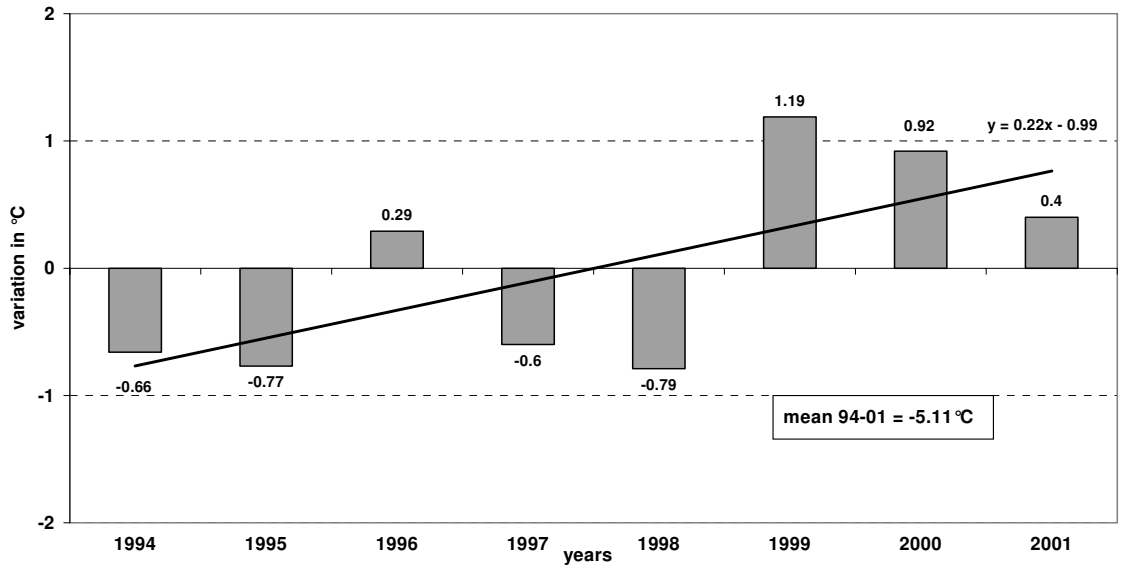

Fig. 4.38: Variation of the yearly means of the temperature over the total mean (1994 – 2001)

Tab. 4.27: Yearly means and rises of the temperature in °C

	mean	max. mean	year	min. mean	year	initial value	rise/a	abs. rise
1993 - 2001	-5.1 ± 6.8	-3.9	1999	-5.9	1998	-6.1	0.22	1.54

According to the WMO, climatological standards (normals) are based on average values for continious measurements of 30-year periods: 1901 - 1930, 1931 - 1960, 1961 - 1990 (FØRLAND et al. 1997). In order to estimate the determined temperatures in Ny-Ålesund correctly, the computed monthly average temperatures of the years 1994 – 2001 and the WMO normals of 1931 - 1960 and 1961 - 1990 were put into comparison. The normals of 1961 - 1990 and their standard deviations are shown in Fig. 4.39. The values of the row 1931 - 1960 lie within the range of these standard deviations. The monthly means of the 8-yearly Koldewey data series lie above the WMO standard row 1961 – 1990, except the May values, but do not fall out of the standard deviation.

The deviations of the monthly average temperatures of the Koldewey data series and the normal data series 1931 - 1960 towards the WMO normals of 1961 - 1990 are represented in Appendix 4.5.1, Fig. 4. In some parts the measurements in Ny-Ålesund deviate strongly from the normals of 1961 – 1990 in winter and at the beginning of spring. The values of February lie 1.8°C, of March 2.9°C and of November 2.3°C higher than the normals (see also Fig. 4.39). The coldest month is February in all the rows, whereby the WMO normal of 1961 - 1990 sinks under the 8-yearly February mean of the Koldewey data series. With exception from June the series of measurements exhibit rises in temperature in all months. In the months of September and November until March the temperatures rose for more than 1°C in comparison with the normals of 1961 - 1990. The measured values compared with the normals of 1931 - 1960 show smaller deviations than compared with the normals of 1961 - 1990. The best correspondence of all three series of measurements can be observed in the months May until August. In comparison with the normals of 1961 - 1990 the Koldewey data series shows deviations from 0.2 to 0.5°C in these months. In all these rows the warmest month is July.

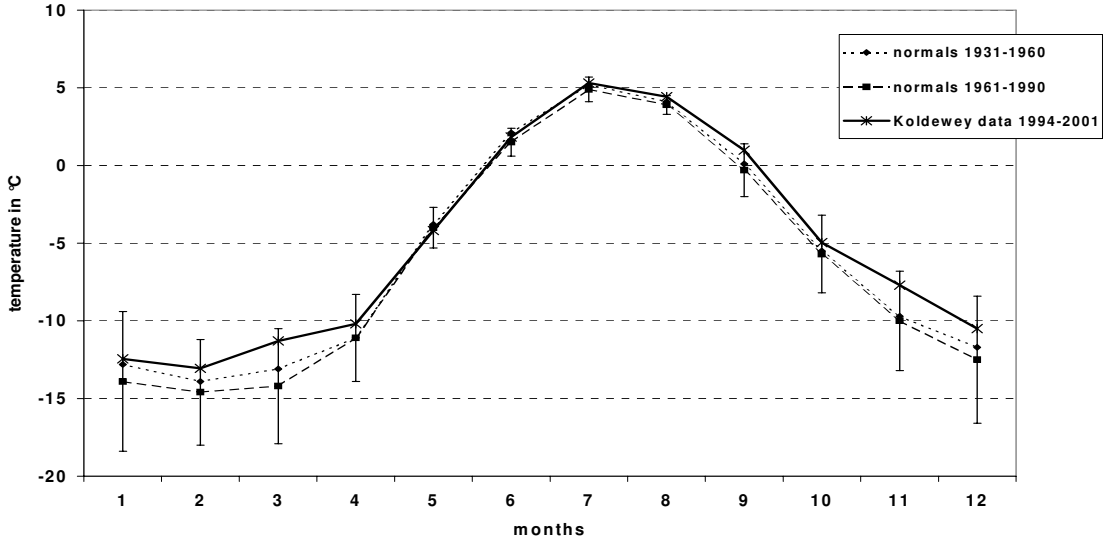

Fig.4.39: Long-term monthly means of the temperature in comparison: WMO-normals of 1931 - 1960, 1961 - 1990 (DNMI) and the Koldewey data series (1994 - 2001)

The temperature course of the normals of 1931 - 1960 lies over this one that was determined for the normals of 1961 - 1990. From this it can be concluded that particularly during the winter months and in the transitional phases a cooling trend could be registered, which however is not continued in the Koldewey data series during the 90'ies. In these periods the Koldewey data series clearly show a heating up in comparison with the normals of 1961 -1990. The normals of 1961 - 1990 show a cooling from –5.8°C to -6.3°C in comparison with the normals of 1931 - 1960. The annual average temperature of the Koldewey data series (1994-2001) amounts to -5.1°C and lies thereby around 0.7°C higher than the reference value of the normals of 1931 - 1960 and around 1.2°C higher than the refering value of the row 1961 - 1990.

Trend Analysis for 1935 – 2000

Thanks to the support of the DNMI a trend analysis for the annual average temperature for the period of 1935 - 2000 was possible. Since no continuous measurements were present for the time before 1969, the period between 1935 and 1968 of Isfjord Radio (78° 04' N; 13° 38' E) was homogenized and referred for Ny-Ålesund according to NØRDLI in HANSSEN-BAUER et al. (1997). The temperature values of Isfjord Radio, the data of the ESRO station (78° 55' N; 11° 53' E) from 1969 to 1974 and the data of the Norwegian Polar Institute (78° 55' N; 11° 56' E) from 1974 to 2000 for Ny-Ålesund were composed to a continuous data series.

The annual average values vary between a minimum value of -9.4°C in the year 1968 and a maximum value of -3.3°C in the year 1984. The average value of this period of -5.8 ± 1.3°C is about 0.7°C lower than the average annual temperature of the Koldewey data series. The rise of the annual average temperatures of the Koldewey data series, however, is not significant in the comparison to the DNMI data series (1935 – 2000). Starting at an initial value of -5.6°C (see Fig. 4.40) the linear trend shows a decrease of 0.6°C from 1935 to 2000. This straight regression line however does not show the fluctuations that arise during these long periods. The trend of the entire time series (global) is estimated by a regression function with an approximation of the measuring points. In order to approximate the nearly periodically changing dispersions of the measured values in shorter periods and to represent a mean course of the curve, different smoothing procedures

were used. FØRLAND et al. (1997) used similar calculations at comparable long time series for Spitsbergen.

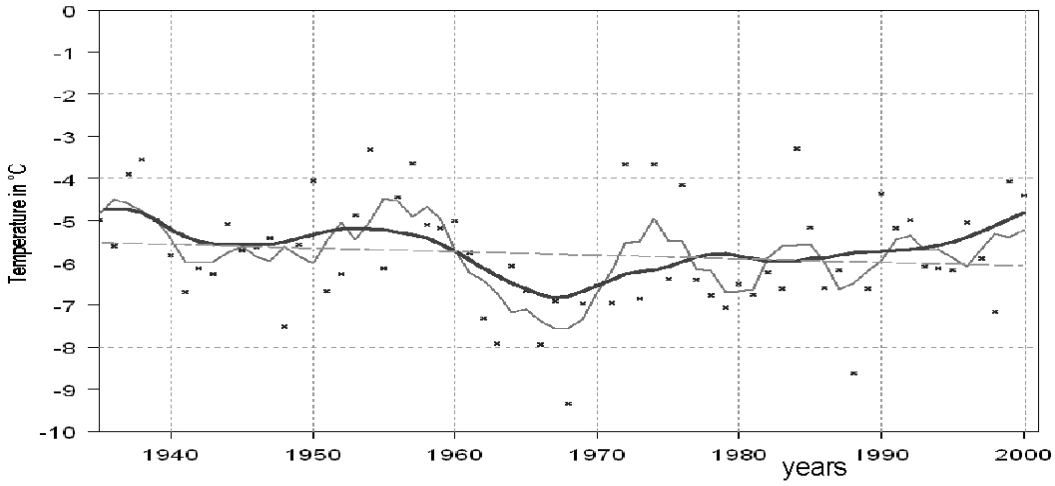

Fig. 4.40: Annual means for 1935 – 2000 for Ny-Ålesund (dashed line: linear trend, bold line: Friedmanns Super smoothing, thin line: Kernel-smoothing filter: 5)

A smoothing of the period can be realized with a low-pass filter, which suppresses brief peak values and emphasizes medium-term tendencies better than the linear regression (SCHÖNWIESE 2000). The thin line approximates well the fluctuations of the temperatures in relatively short periods (5-years) see Fig. 4.40. Thereby it is to be noticed, that in the middle of the 30'ies 50'ies and 70'ies local maxima, and in the 40'ies, 60'ies and 80'ies local minima could be found. A particularly strong decrease of the trend was obvious in the middle of the 60'ies; in this period also the smallest annual average value of -9.4°C was determined.

Also the bold curve exhibits periodic oscillations in a nearly decadic rhythm. Beginning with -4.8°C in the year 1935 the temperatures drop down in the 40ies and rise again in the 50'ies up to a similar level of the 30'ies. After the decrease of the trend to a minimum in the 60'ies a continuous rise of the temperatures could be determined up to the year 2000 interrupted by slight temperature drops at the beginning of the 80's. The temperatures of the 90'ies lie within the range of the values between 1935 and 1960 and clearly over the values between 1961 and 1990, like it was already pointed out in sec. 4.5.1.2. HISDAL (1985) already referred to these not unusual decadic changes of the temperature trend since 1915.

These periodic temperature variations may be based on the different extend of the Arctic oscillation (AO). There is a zyclonal stream around the northern polar cap in about >2 km height. In winter this stream is strengthened by the cold temperatures in the hight between 17 and 40 km. This leads to the formation of a polar vortex. At a strong development it causes a rise of the wind velocity close to the earth's surface. Through that, warm, humid air can be brought to Svalbard from the south (positive phase). During a warming of the stratosphere over the northpole it may occur that this stream breaks down and cold air anticyclonally flows down to Svalbard from the polar basin (negative phase). These phases alternate in unregular intervals reaching from a few days to some months. But when the phenomenon is watched over years and decades, there is always one of the states dominating, which may explain the decadic fluctuations of the temperature (HISDAL 1985, LIPPSETT 2002, DORN 2002).

4.5.2 Relative Humidity

The relative humidity is measured in a standard height of 2 m at the meteorological tower (position 1, see Chapter 3.1). Trend and variation of the relative humidity are evaluated together with the temperature for the period from 1st January 1994 to 31st December 2001 (VDI 3786/4). Following average values, standard deviations and extreme values were determined for the Koldewey data series (1994-2001) as well as for the year 2001 (see Tab. 4.28).

Tab. 4.28: Means and extreme values of the relative humidity for 1994-2001 as well as for the year 2001

Period	mean/year temperature	mean ± st. dev. /year relative humidity	maximum	minimum
1994 – 2001	-5.1°C	73.5 ± 5.5 % r.H.	100 % r.H.	25.1 % r.H. (29.3.2000)
2001	-4.7°C	73.6 ± 6.0 % r.H.	99.9 % r.H.	28.2 % r.H. (29.12.2001)

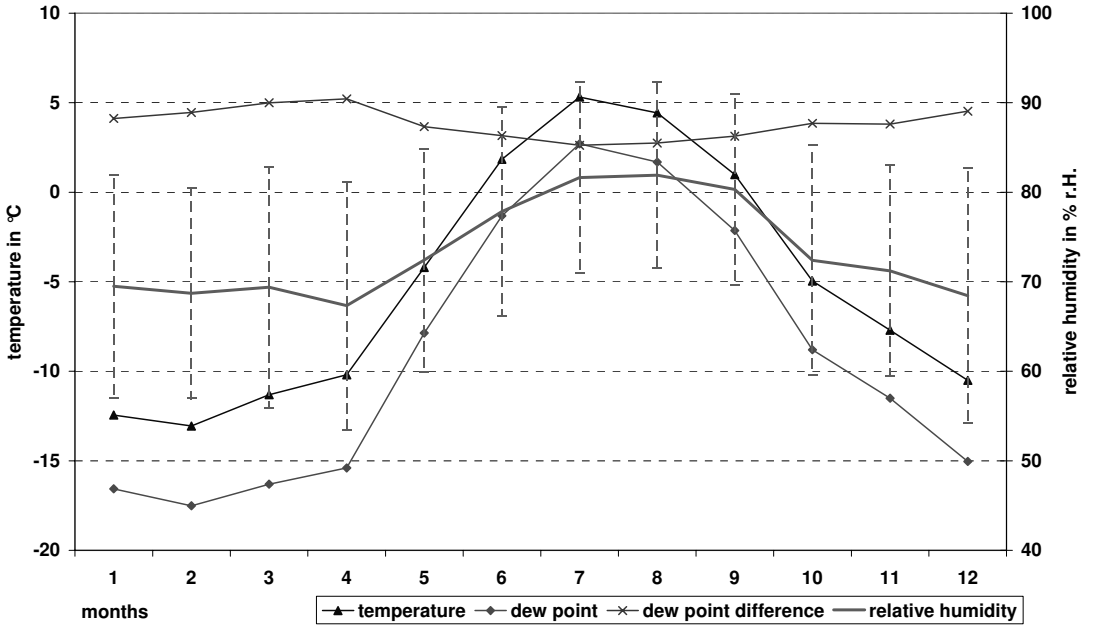

Fig. 4.41: Monthly mean – and extreme values of the relative humidity with standard deviations 2001

Monthly average values of the relative humidity, the temperature and the dew point temperature are shown in Fig. 4.41. The smallest monthly average values of the relative humidity are determined with < 70 % r.H. at temperatures below –10°C from December to April. The smallest monthly mean occurs with 67.3 % r.H at a mean temperature of -10.2°C in April. The small values of the humidity in the winter can be result by the ice coverage of the sea associated with the continentality and by the low absorption of water vapour of the cold air. The polar sea ice achieved its largest expansion in April. The highest monthly average values > 77 % r.H. lie at temperatures above 1°C in the months June until September.

The highest monthly average value of the relative humidity occurs with 81.9 % r.H. at 4.4°C in August. There is only a small difference to the maximum temperature means with 5.3°C and 81.7 % r.H in July..The monthly average values of the relative humidity show, alike the temperature, a simple wave over the year and lie between 67 and 82 % r.H. in the yearly course. On the other hand the fluctuations of the mean temperature vary between -13.1 and 5.3°C. Compared with the yearly course of the monthly average temperature, which already drops again in August, the humidity shows a relatively constant maximum until September. This can be explained by the high evaporation rate of an ice-free sea,

which has its largest expansion to the north in September (see Chapter 2). In Fig. 4.41 it becomes clear that the temperature and the dew point temperature show similar courses. The dew point difference (difference between the actual temperature and dew point temperature) indicates the saturation of air with water vapour. From November to April this difference is relatively high at a small humidity. In the months from June to August the dew point temperature lies in the range of 0 and 2.7°C.

In this range the formation of dew begins, if the temperature of the earth's surface is under the dew point temperature of the direct environment. The standard deviations of the average monthly relative humidity shows a nearly constant range during the yearly course of ± 10.4 % r.H. (± 2.3°C) in August to ± 14.3 % r.H. (± 6.4°C) in December. Standard deviations of the monthly average temperature are smallest in July/August with 2.3°C and highest in March with 6.5°C. The high humidity in June can be caused by the thaw of the snow cover and in July by the high water content of the soil as well as by the high degree of cloud coverage (Stratus) , see Fig. 4.41.

The daily averages of the relative humidity in the yearly course are shown in Fig. 4.42 for 2001. In the diagram the most important sun phases are represented for the relative humidity similarly as in Fig. 4.36 (temperature variation for the year 2001). The smallest value of 28.2 % r.H. was measured on 29th December of the exemplary year. The daily averages vary between 41.8 and 100 % r.H. The maximum values of the mean relative humidity could be observed with > 85 % r.H in July and August 2001 and the lowest daily means occurred with < 65 % r.H in March and April. (see Fig. 4.42 ; 4.43).

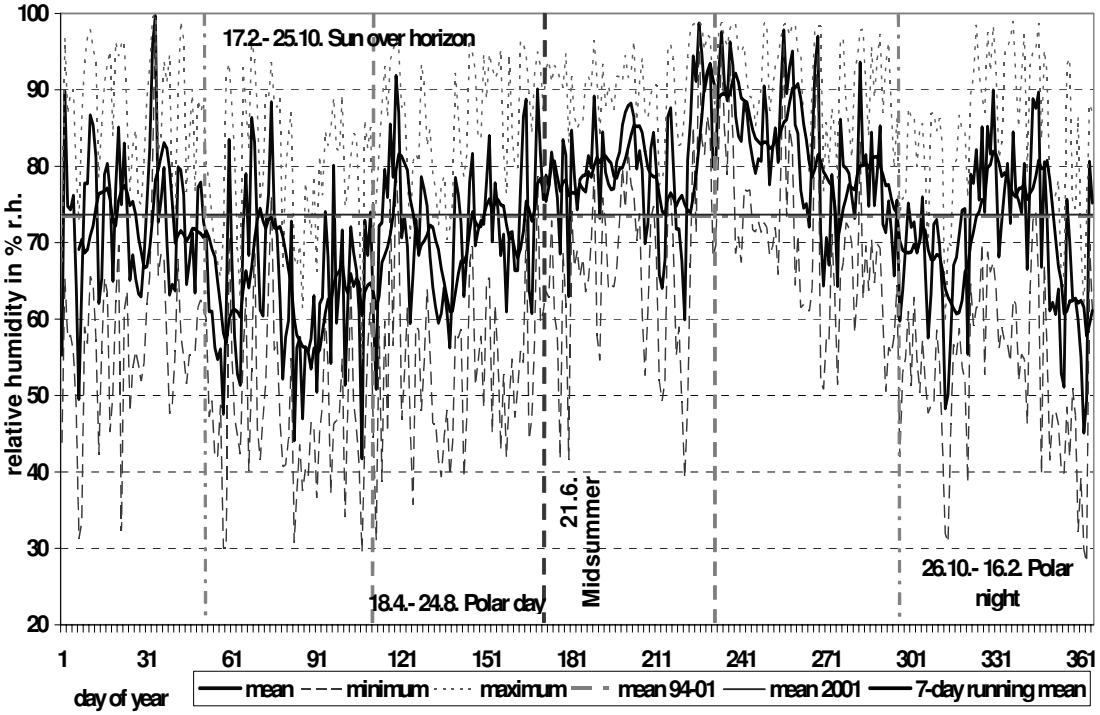

Fig. 4.42: Yearly course of the relative humidity for 2001

The Isopleth-diagram shows the relative humidity in dependence of the monthly and hourly means (see Fig. 4.43). Similarly to the air temperature (see Fig. 4.37) the biggest changes of the relative humidity occur in the yearly course. Daily fluctuations are particularly remarkable in April with the lowest relative humidity during the night hours and in the late summer with the smallest values at noontime[2]. During the mornings in

[2)] Measuring errors can occur at hair hygrometers without ventilation. The rel. humidity appears at these ones too low especially at higher temperatures resulting from strong solar radiation.

summer the steam content of the deeper air layers increases. Radiation, turbulence or convection can decrease the humidity at noontime. With less radiation, turbulence and convection in the evening the humidity rises again. The daily fluctuations are stronger emphasized in summer than in winter. In March the smallest humidity values arise at noontime.

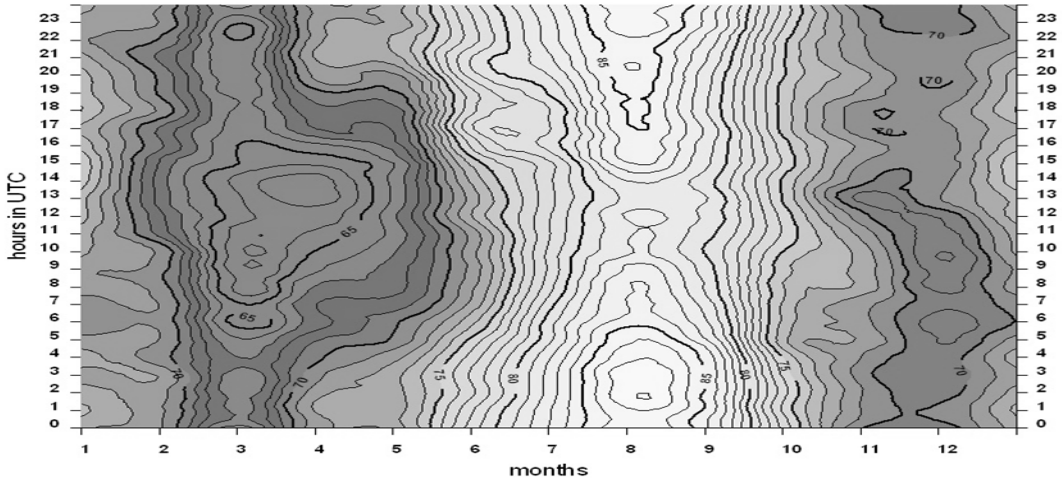

Fig. 4.43: Isopleth-diagram of the relative humidity for 2001

In this month the sea is mainly covered with ice and the evaporation rate is very small. Since in the noontime strengthened turbulences can occur, a bigger transport of water vapour takes place into the higher layers of the atmosphere than it is evaporated at the earth's surface. Under cloudy weather conditions a distinct diurnal variation cannot develop in the second transitional phase from the polar day to polar night (LILJEQUIST and CEHAG 1994). The yearly fluctuations result mainly from the transport of warm humid air from the south and cold dry air from the arctic basin or from Greenland.

The average values, maxima and minima of January of the years 1994 – 2001 are shown in Appendix 4.5.2 Fig. 1. The January average values vary between 61.2 % r.H. (1994) and 72.5 % r.H. (2001). With exception of 1996 in all of the years some values occur < 44% r.H.. The smallest relative humidity in January amounts to 31.3 % r.H. (7th January 2001). In the years 1995 - 2001 maximum values of the relative humidity reached and surpassed 94 % r.H.. A slight increase of the January average values of the relative humidity of 5.8 % r.H. could be registered in the Koldewey data series. This however is a substantially smaller increase than the observed variation range of this month.

In July the rise of the Koldewey data series is negligible with 1.2 % r.H.. (It lies within the range of the indicated measuring deviation of the equipment (see Appendix 4.5.2 Fig. 2).) A relative stability could also be noticed at the temperature in July (see Appendix 4.5.1 Fig. 2). The July average values of the relative humidity vary from 78 % (1997) to 86 % r.H. (1998). In the years 1998 - 2000 minimum values of humidity occur < 42 % r.H.. The smallest July value was registered with 37.8 % r.H.on 22nd July 2000. In all years maximum July values could be measured at > 96 % r.H..

Seasonal average values and the rise of the relative humidity from December 1993 until August 2002 are shown in Tab. 4.29 (see Appendix 4.5.2 Fig. 3). In the observation period small decreases of the relative humidity were determined from 72.4 to 67 % r.H. in winter as well as from 71.5 % to 68.9 % r.H. in the spring. In the winter season the rise in January is exceeded by the decrease of the values in the months of December and February. In this time the average humidity varies between 63.3 % and 79.2 % r.H. In summer and autumn the relative humidity increases by 4.6 and 6.1 % r.H., respectively. The differences between

the smallest and highest average values amount to 10 % r.H. in summer and 14.6 % r.H. in autumn.

Tab. 4.29: Seasonal mean and rises of the relative humidity in % r.H. for Dec. 1993 – Aug. 2002

	mean	max. mean	year	min. mean	year	initial value	rise/a	abs. rise
winter	68.6 ± 4.7	79.2	1996	64.4	2000	72.4	-0.7	-5.4
spring	70.1 ± 3.8	75.5	1994	63.3	1997	71.5	-0.3	-2.6
summer	81.0 ±3.3	85.2	1999	75.2	1997	78.4	0.5	4.6
autumn	74.7 ±4.1	81.8	2000	67.2	1997	71.2	0.8	6.1
January	69.5 ± 12.5	84.0	1996	61.2	1994	66.2	0.7	5.1
July	81.7 ± 10.7	86.0	1998	78.0	1997	81.0	0.2	1.2

The annual average of 2001 lies only very slightly (0.2 % r.H.) over the total mean at 73.5% r.H of the Koldewey data series (1994 - 2001) see Fig. 4.44 and Tab. 4.30. During this 8-year period the humidity rises for 0.2 % r.H., which is still within the range of the measuring deviation. With exception of the year 1997 in which a 4.9 % r.H. lower value arises, the relative humidity lies in all the years over 2 % r.H. over the total mean of 73.5 %r.H..

It can be established that both, the temperature and the humidity exhibit a relative stability during the investigation period (see Fig. 4.38; 4.44).

For the comparison of the Koldewey data series (1994 – 2001) the monthly means of the standard- row 1931 - 1960 and their standard deviations as well as a data-row of the DNMI of 1975 -1990 (FØRLAND et al. 1997) was consulted (see Fig. 4.45).

Tab. 4.30: Yearly means and rises of the relative humidity in % r.H.

	mean	max. mean	year	min.mean	year	initial value	rise
1993 - 2001	73.5 ± 2.1	75.4	1999	68.6	1997	-0.11	0.21

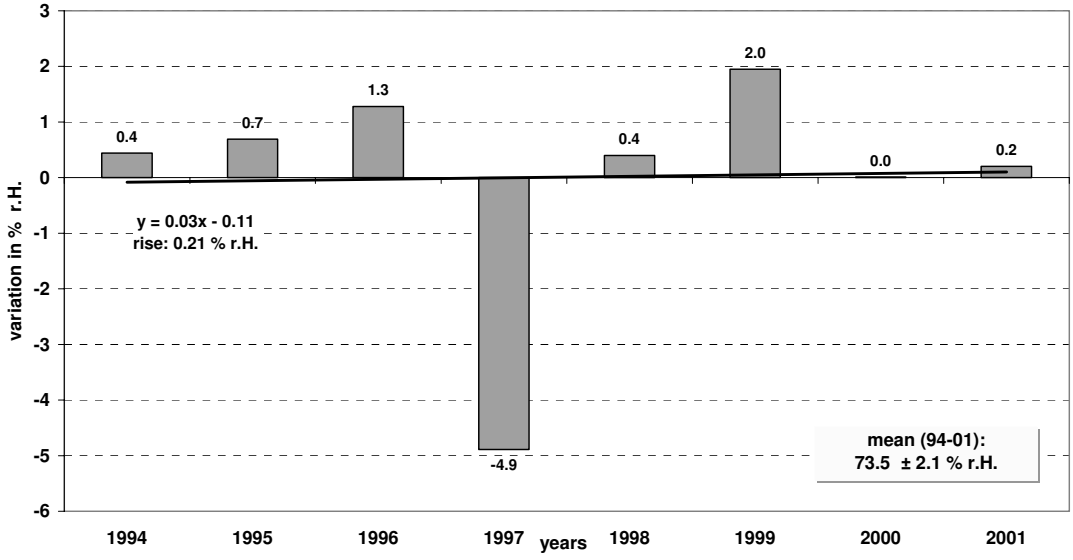

Fig. 4.38: Variation of the yearly means of the relative humidity over the total mean (1994 – 2001)

The average value of the normal row 1931 - 1960 is indicated with 79 % r.H.. The highest monthly average values of 85 and 87 % r.H. arise between June and September. From January to May the average values of the normals vary within the range of 77 and 81 % r.H.. The months from Octobers to December are clearly drier with humidity values between 68 and 71 % r.H.. The standard deviation lies between 4 % (August) and 7 % r.H. (December to February, April). The highest standard deviations arise during the winter months.

At the comparison of the DNMI data series with the normals of 1931 - 1960 a decrease of the relative humidity could be observed in the months from January to September with up to 4.3 % r.H. (in January). The values of the DNMI data series lie within the standard deviations of the normal-row of 1931 -1960.

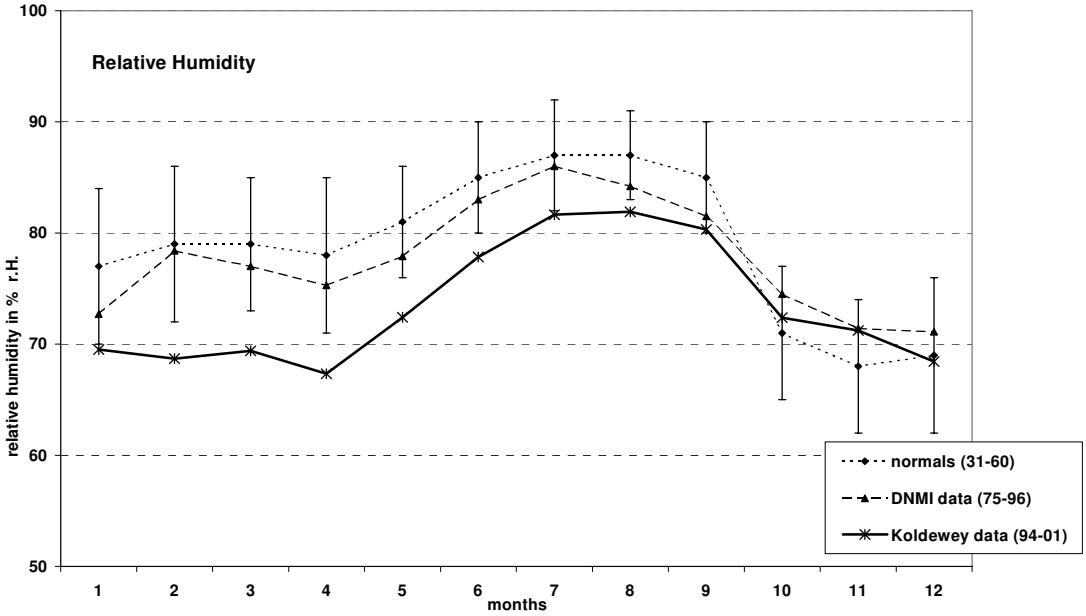

Fig. 4.45: Long-term monthly means of the relative humidity of the Koldewey data series (1994 - 2001) in comparison with the WMO normals 1931 - 1960 and the DNMI data series 1975 - 1990 (FØRLAND et al. 1997)

In this time the Koldewey data series lies between 1.2 and 9.7 % r.H. (80.3 % r.H. in September; 68.7 % r.H. in February) below the DNMI data series and between 4.7 and 10.7 % r.H. (80.3 % r.H. in September; 67.3 % r.H. in April) and below the normals of 1931 - 1960 (see Appendix 4.5.2 Fig. 4).

From January to August the monthly values of the Koldewey data series drop out of the ranges of the standard deviations of the normals of 1931 - 1960. A direct comparison of these values is however difficult, since within the time technical and climatic changes appeared. Moreover local conditions and measuring rates are not well-known and the standard deviations of the DNMI data series were not available. Both compared data series lie within the standard deviations of the Koldewey data series. In the months of October to December higher humidity values were determined using the DNMI data series up to 3.5 % r.H. (74.5 % r.H in October) and using the Koldewey data series up to 3.2 % r.H. (71.2 % r.H. in November) compared with the normals of 1931 - 1960. The comparison of the long-time annual average values of the DNMI data series in relation to the normals of 1931 – 1960 shows a decrease of the relative humidity from 79 % r.H. to 77.8 % r.H.. The average value of the Koldewey data series lies with 73.5 % r.H. clearly under both reference values.
In the Appendix 4.5.2 Fig. 5 the measuring deviations and standard deviations are recorded for the period 1994 – 2001, that resulted during the comparison of the measuring

values of the humidity sensors at the position 1(NE) and 2(SE) (see Chapter 3.1). Measured values and standard deviations show good correlations. For the monthly average values of the position 1 and 2 an average deviation of 0.9 % r.H. was determined for the Koldewey data series. For comparison the standard deviation of the normals of 1931 – 1960 was used.

4.5.3 Air Pressure

The air pressure at the Koldewey station is measured in the Blue House in 11 m above the sea level (P). These values go directly into the data base and are evaluated for the Koldewey data series (1994 – 2001) and the examplary year 2001. In comparison with other measurement series the air pressure values are reduced to the sea level (P_0).

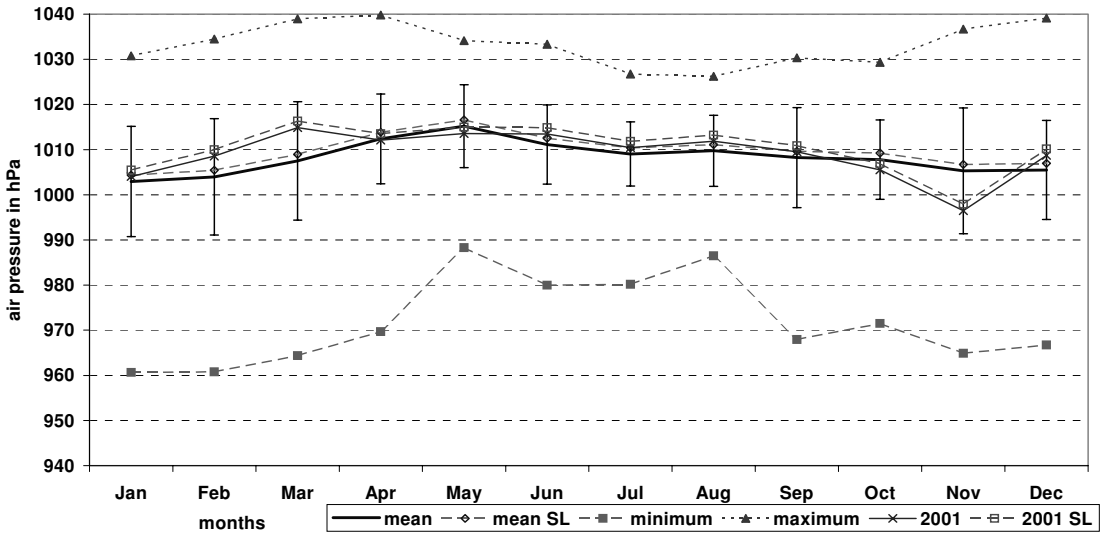

Fig. 4.46: Monthly mean - and extreme values of air pressure in 11m height above sea level and at sea level (SL) for 1994 – 2001 and for the year 2001

Tab. 4.31: Means and extreme values of the air pressure in 11m above sea level for 1994 – 2001 and 2001

period	mean sea level	mean ± st. deviation 11 m above sea level	maximum	Minimum
1994 - 2001	1009.7	1008.3 ± 3.6	1039.8 (9.4.1996)	956.4 (8.3.1997)
2001	1010.5	1009.1 ± 5.1	1037.6 (25.3.2001)	966.6 (25.11.2001)

The central and extreme values of the air pressure for these periods are represented in Tab. 4.31; an annual average air pressure of 1008.31 ± 3.6 hPa could be determined. On 9th April 1996 a maximum air pressure value of 1039.8 hPa and on 8th March 1997 a minimum value of 956.4 hPa was recorded for the station height. On 6th January 2002 a new minimum value was measured of 945.36 hPa.

The monthly air pressure average values and extrema in 11 m height and on sea level (NN) for the Koldewey data series (1994 – 2001) and for 2001 are shown in Fig. 4.46. For the Koldewey data series the highest average air pressure values were determined for the months from April to June; they lie above the mean annual average value. The highest monthly average lies in May with 1015.18 hPa. In these months also the longest sunshine duration was recorded (see Chapter 4.2). The lowest average air pressure values were observed with 1002.9 hPa and 1004.0 hPa in January and February. The smallest measured values vary between 960.7 hPa and 960.8 hPa in January and February as well as between 988.3 hPa and 986.5 hPa in May and August, respectively.

The maximum values lie between 1039.8 hPa in April and 1026.2 hPa in August. During the evaluation of the monthly means it is noticeable that the extreme values between May and August lie closer to the average values than in the remaining months. Something similar can be observed in the year 2001 (see also Fig. 4.46). An earlier rise of the air pressure from January to March and an earlier decrease of the air pressure can be recognized in October/November. The values deviate strongest by 7.3 hPa and -8.8 hPa in March and November from the respective monthly means of the Koldewey data series. The air pressure is very variable in each month and in each year, therefore the daily averages and extrema are to be examined for the year 2001 (see Fig. 4.47). The largest deviations occur with a minimum of 12.8 hPa in 12th January below of the daily average and with a maximum of 14.3 hPa in 14th December above the daily average.

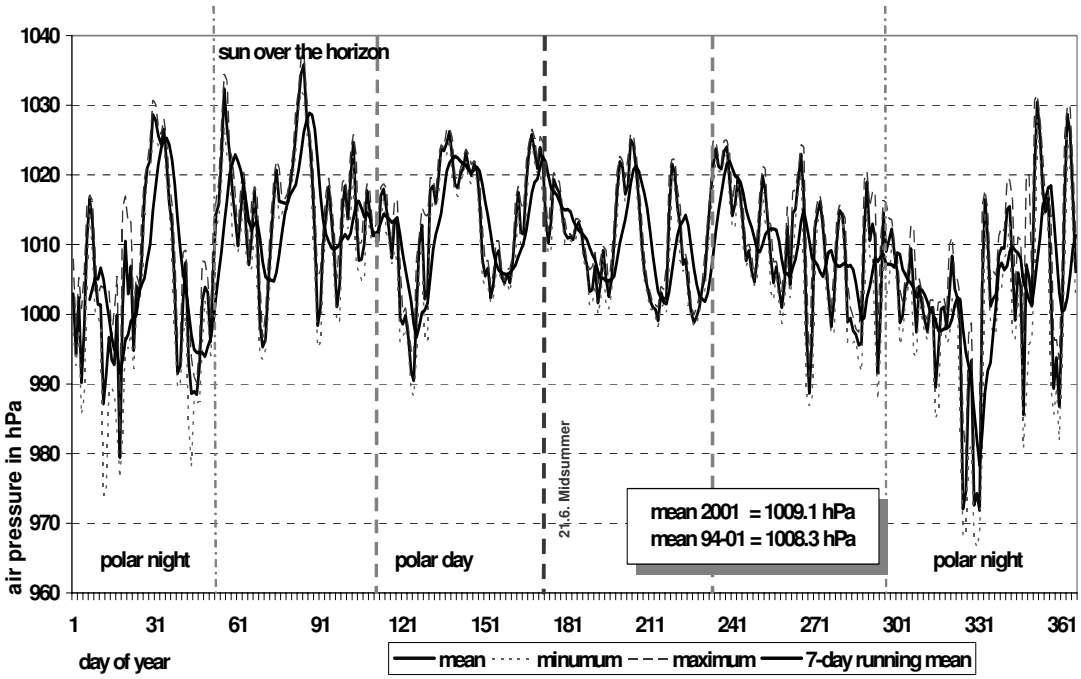

Fig. 4.47: Yearly course of the air pressure for 2001 (11 m above sea level)

Pressure variations result from the shift of high- and low pressure areas in irregular periods. Regular changes can be observed in the daily variation of the air pressure. In the polar regions these daily variations are substantially smaller in comparison with the equatorial regions. For Ny-Ålesund the pressure changes are important, that result from the shift of cyclones and anticyclones (DWD 1987).

The Isopleth-diagramm (isobar diagram) in Fig. 4.48 represents the daily and the yearly variation of the air pressure of the year 2001. Here it can be recognized that the biggest differences of pressure occur in the course of the year, similar to the temperature. Daily fluctuations have been observed only rarely in 2001. In the diagram a similarity with the temperature gradient in Fig. 4.37 could be established.

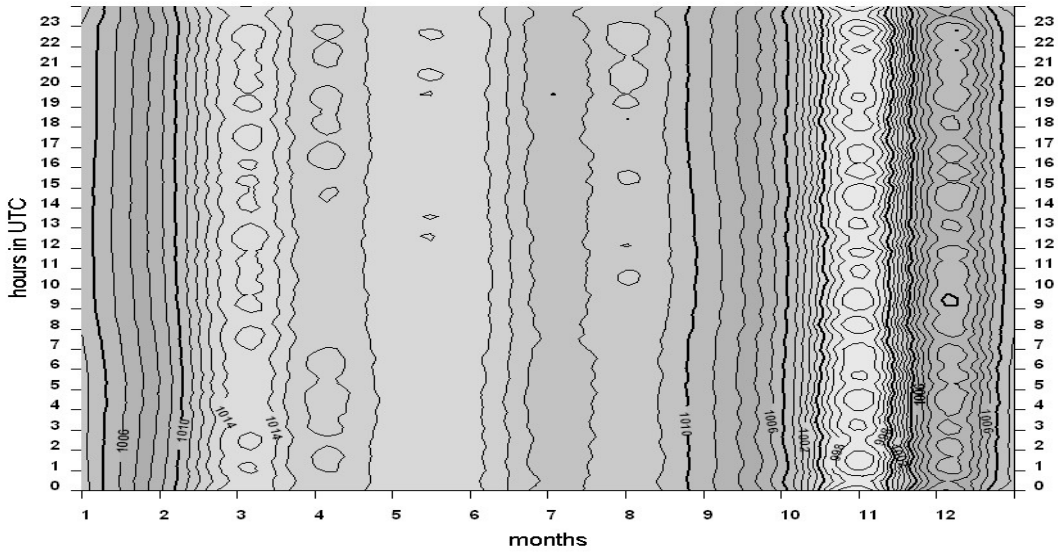

Fig. 4.48.: Isopleth-diagram of the air pressure [hPa] in station height (11 above sea level) for 2001

According the study of the related isobar maps (http://www.wetteronline.de) and Fig. 4.47; 4.48 the following conclusions can be drawn: The high air pressure of February/March leads to a temperature and humidity minima of ≤ -15°C and ≤ 65 % r.H. in the year 2001. This can be explained with the transport of cold air masses from the arctic basin. An isobar map which represents this typical situation for 1979 is shown in Appendix 4.5.3, Fig. 4. This dry cool air is transported at the back of a cyclone and called polar air out break. At the end of October / at the beginning of November a cyclone expanded over the North Atlantic, which reached to Spitsbergen. It transported dry and cold air masses from Greenland to Spitsbergen (see Fig. 4.49).

In the period of the thaw from mid to end of June the influence of warm maritime air is recognizable (Appendix 4.5.3 Fig. 5). In this time the humidity rises to 80 % r.H.. Also in winter such warm air mass transportations towards Spitsbergen can be observed quite frequently. They are possibly the reason of the winter temperature rise in the latest years (see also HISDAL 1998; HUPFER and KUTTLER 1998).

With exception of the years 1997 and 2000 the medium monthly air pressure rose above 1000 hPa in each month January of the Koldewey data series (see Appendix 4.5.3 Fig. 1). In January 1998 the average value lie even about 1012.3 hPa. The lowest January values were measured with 996.4 hPa in 1995 and with 960.7 hPa in 1997. The highest January maximum values were registered in with 1029.2 hPa 1996 and with 1030.8 hPa in 2001. The average air pressure in January drops with 3.8hPa with an initial value of 1005.1hPa for the Koldewey data series (1994 - 2001). The average air pressure amounts to 1002.9 hPa for the month January during the entired period.

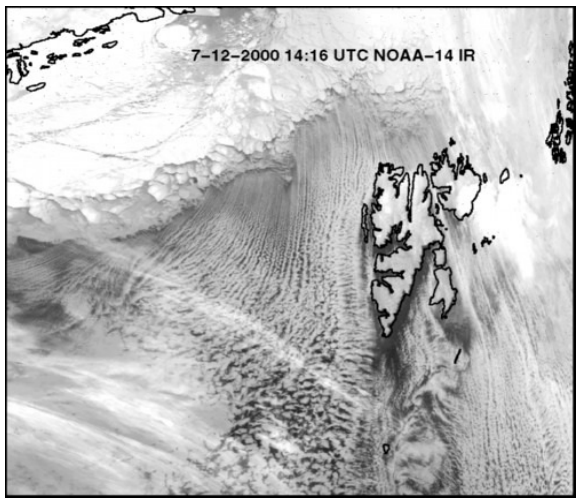

Fig. 4.49: Typical polar air out break over the northern polar sea (Infrared- satellite picture by NOAA-14 on Dec/7/2000)

In July a rise of the average air pressure values is determined with 6.7 hPa which is based on an initial value of 1005.2 hPa (1994) (see Appeendix 4.5.3, Fig. 2). The average air pressure amounts to 1009 hPa in July. In the years 1997, 1998, 2000 and 2001 the mean July values of the air pressure lie with 1.4 to 5.5 hPa above this value. The highest maximum value was measured with 1029.7 hPa in July 1997. The absolute July minimum could be determined with 980.2 hPa in 1995.

The seasonal evaluations (see Tab. 4.32 and Appendix 4.5.3, Fig. 3) resulted in slight rises in winter, spring and summer between 1 and 3 hPa and a decrease of 4.2 hPa in autumn in the observation time. All trends (rises) for the seasons as well as for the months of January and July lie within the respective standard deviations.

Tab. 4.32: Seasonal means and rises of the air pressure in hPa from Dec.1993 – Aug.2002 (11 m above sea level)

	mean	max. mean	year	min. mean	year	initial value	rise/a	abs. rise
winter	1002.7 ± 4.5	1007.9	1998	996.4	1995	1002.0	0.1	1.0
spring	1011.8 ± 3.1	1014.9	1996	1006.9	1994	1009.9	0.4	3.0
summer	1010.6 ± 2.7	1015.2	1998	1007.2	1995	1009.5	0.2	1.6
autumn	1007.2 ± 3.7	1012.7	2000	1003.6	1999	1009.8	-0.5	-4.2
January	1002.9 ± 12.2	1030.8	2001	996.4	1997	1005.1	-0.5	-3.8
July	1009.0 ± 7.1	1014.5	1997	1003.7	1994	1005.2	1.0	6.7

The changes of the annual averages for the air pressure in station height are represented in Fig. 4.50 and Tab. 4.32. The largest deviation with 3.8 hPa from the total mean could be determined in the year 1998. This value was the only annual average value of the Koldewey data series that was outside of the standard deviation of ±3.6 hPa. In the Koldewey data series a slighter rise of 1.5 hPa could be observed. This rise also lies within the standard deviation.

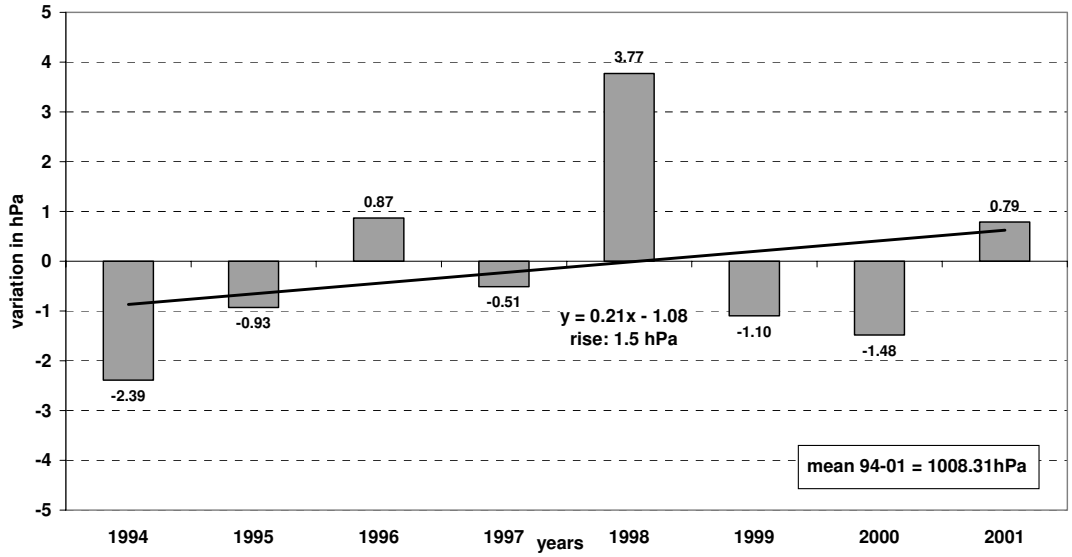

Fig. 4.50: Variation of the yearly means of the air pressure over the total mean (1994 – 2001)

Tab. 4.33: Yearly means and rises of the air pressure in hPa for Ny-Ålesund (11 above sea level)

	mean	max. mean	year	min. mean	year	initial value	rise
1994 - 2001	1008.3 ± 1.9	1012.1	1998	1005.9	1994	1007.7	1.5

In order to compare data series with each other, the station values of the air pressure in 11 m above sea level have been reduced to the sea level using the barometric height equation (Eq. 2.13):

$$p_0 = p \cdot e^{\frac{g}{R \cdot T} \cdot z} \tag{4.3}$$

p - pressure, $p_{0\_}$ pressure at sea level, z – height above sea level [m], g – 9.81 m/s², T - temperature [K], R = 287,05 J kg^{-1} K^{-1} (constant for dry air)

By the small height of the station over the sea level the mean temperature of the station can be included into the equation. The mean monthly air pressure values related to sea level are represented in Fig. 4.46 (dashed line). According to that, the air pressure in station height is approximately 1.5 hPa lower than the air pressure on sea level. The mean annual air pressure value increases from 1008.3 hPa to 1009.7 hPa with the reduction to the sea level. Thus is it only slightly higher than the mean annual air pressure of the DNMI data series (1975 - 1996) with 1009.2 ± 2.2 hPa and the normals (1931 - 1960) with 1009.6 ± 4.1 hPa. A significant deviation could not be recognized.

Fig. 4.51 shows the mean monthly values of the Koldewey data series for the air pressure on sea level in comparison to the DNMI data series of 1975 - 1996 and to the WMO normals of 1931 - 1960. For the estimation of the data the standard deviations of the DNMI data series were used, since these were determined during a longer period than those of the Koldewey data series. Bigger deviations from the standard row are particularly noticeable in December and January. The pressure of the Koldewey data series is around 6 hPa higher in December than the comparable value of the normals for December (1000.9 hPa). This December value of the Koldewey data series however lies within the standard deviations of the DNMI data series as well as the normals.

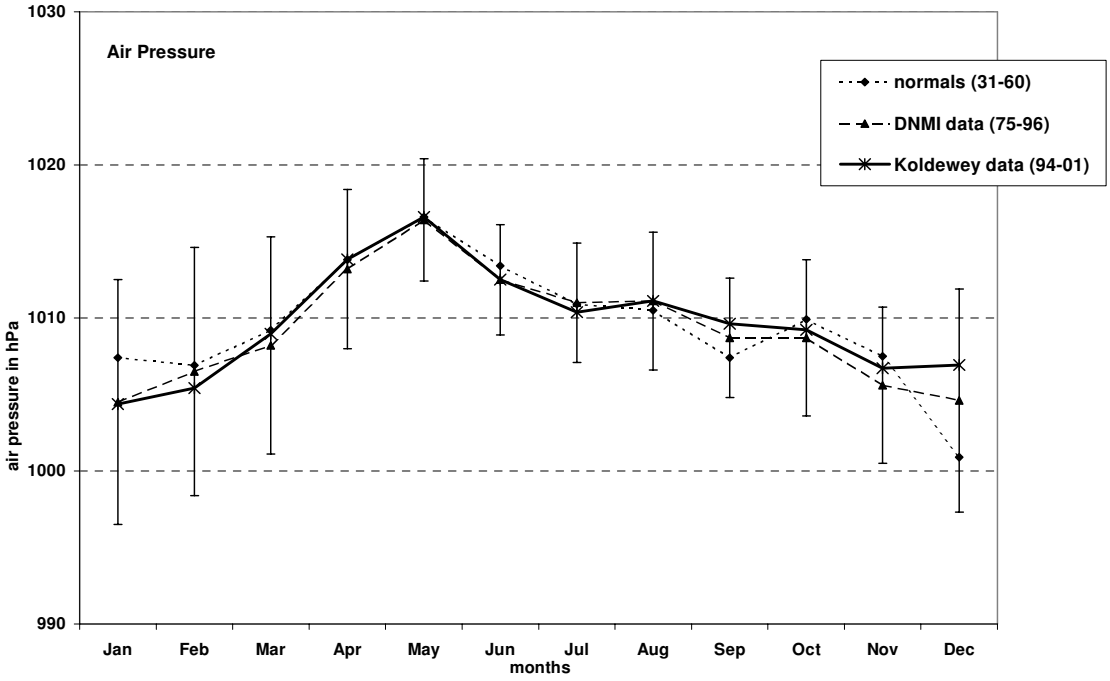

Fig. 4.51: Long-term monthly means of the air pressure (sea level) the Koldewey data series (1994-2001) in comparison to the WMO normals of 1931 – 1960 and the DNMI data series 1975 – 1996 (FØRLAND et al. 1997)

4.5.4 Wind

The wind measurements are accomplished in the context of the BSRN since August 1993 at the meteorological tower in heights of 2 and 10 m. Since both, wind velocity and wind direction at ground level are affected by friction and an uneven snow surface, wind conditions in the standard height of 10 m are regarded in this work. The polar-coordinates diagram in Fig. 4.52 and Tab. 4.34 show the shares of the wind direction, the mean and the maximum wind velocity in Ny-Ålesund of the period 1994 - 2001 (wind velocity see also Fig. 4.53). Since the measurements only started in the late summer 1993, and thus no complete annual cycle is given, the analysis starts in 1st January 1994. The prevailing wind direction in Spitsbergen is northeast to southeast. The near-surface winds are affected by the regional relief conditions. These winds appear especially along the valleys and/or fjords from the inland to the coast. According HANSSEN-BAUER et al. (1990) this is caused by the channel effect and by cold catabatic winds that blow towards the warmer sea.

In Ny-Ålesund the preveiling winds come from east to southeast direction. Due to the location of the Kongsfjorden in NW-SE-direction and the Kongsbreen in east direction it cannot be exactly differentiated from the representation in Fig. 4.52 whether these winds originate of supraregional pressure differences, catabatic glacier winds from the Kongsbreen or from both.

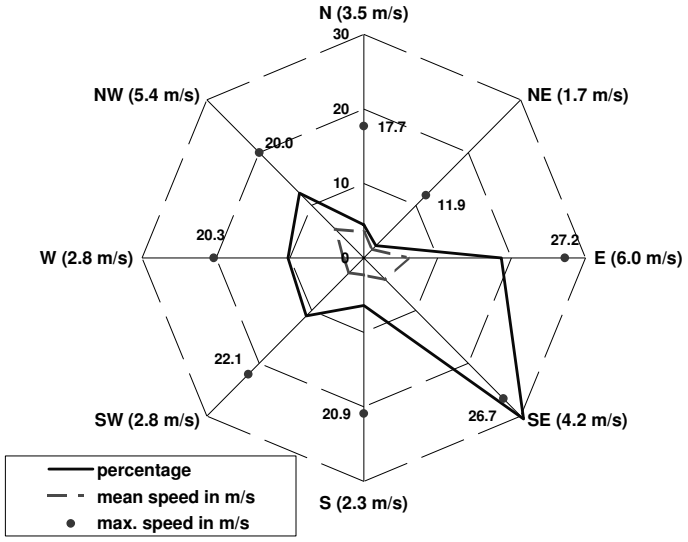

Abb. 4.52: Wind conditions in 10 m height for 1994 - 2001

Tab. 4.34: Wind conditions in 10 m height

	N	NE	E	SE	S	SW	W	NW	calmness	no data
percentage	4.4	2.3	18.6	30.6	6.4	11.0	10.3	12.3	1.8	2.3
avg. speed [m/s]	3.5	1.7	6.0	4.2	2.3	2.8	2.8	5.4	0	--
max. speed [m/s]	17.7	11.9	27.2	26.7	20.9	22.1	20.3	20.0	0	--

East and southeast winds usually have their origin as catabatic winds and develop the highest velocities. This winds result from regional temperature differences between glaciers and sea where air masses over the glacier are cooled down. Cold and heavy air increases in velocity and it is transported towards the warmer sea. This effect is even strengthened by the chanalizing effect of the fjord. The east winds achieve the biggest average velocity of 6 m/s (4 Beaufort) and the highest maximal speed with 27.2 m/s between 1994 and 2001, measured on 21st November 1998 (10 Beaufort).

The earlier discribed observations of the influence of the Kongsbreen to Ny-Ålesund can be supported with the evaluation of the Koldewey data series (see Chapter 2.3). Southeast winds dominate in Ny-Ålesund mostly during the year. Only in the summer months the east wind component of the Kongsbreen dominates (see Tab. 4.35). The two main wind directions of the seasons are represented with their percentages and speeds in Tab. 4.35. In the winter months November until March the winds from east-southeast

are very strong. Warm water is transported along the west coast of Spitzbergen towards the north and a high temperature gradient of the cold air masses can be registered in the northeast.

The climate of Ny-Ålesund is affected by winds from northwest during the summer months. The percentage of the northwest winds clearly increases in April and reaches its maximum in June. The position of the sunstands all days in April is above the horizon and warms up the land surface. Now from the cold sea the winds flow in direction inland. This wind system is called land-sea-wind. Cool, humid sea-air ascends and condenses over the warmer land surface. Actually deep clouds and rain are not rare during the summer months. The average velocities of these sea winds amount to 4.7 m/s (3 Beaufort) and clearly lie below those of the east winds with 8.9 m/s in winter. Also during northwest-wind-conditions the velocity (rose) rises up to 20 m/s (8 Beaufort).

In Ny-Ålesund a constant wind direction can be usually observed only at speeds over 5 m/s (4 m/s in 2 m height). If the speed falls below this level, light winds from all directions will appear. Among these winds are westerly to southerly winds from the mountains Schetlig, Brøggerfjellet and Zeppelin, which barely have an effect on the climate conditions in Ny-Ålesund with speeds between 2 and 3 m/s (2 Beaufort). Nevertheless, a top speed was determined with 22.1 m/s (9 Beaufort) at winds from southwest direction.

These winds arise relatively constant during the whole year. During the transitional phases between polar night and polar day their rate is slightly strengthened. In these times the mountain-valley-winds may occur during the daily course.

Tab. 4.35: Seasonal wind conditions in 10 m height (in m/s) for the Koldewey data series (1994 – 2001)

94-01	winter		spring		summer		Autumn		January		July		year	
prevail.direction	SE	E	SE	E	E	NW	SE	E	SE	E	SE	E	SE	E
percentage	39	20	36	16	23	19	32	16	40	25	44	25	31	19
mean speed	5.0	8.9	3.8	6.0	2.6	4.7	4.2	7.4	5.3	9.1	4.9	8.8	4.2	6.0
max. speed	23.5	25.4	21.8	22.5	18.5	16.2	26.7	27.2	23.5	25.4	22.9	24.3	26.7	27.2

Calmness only occurs in 1.8 % of the cases. Data losses with a percantage of 2.3 % are not considered in Fig.4.52. In Fig. 4.53 the monthly means of the average and maximum wind velocity are in the height of 10 m and the average wind velocity in the height of 2 m. Thereby, the average wind velocities in 2 m height are 0.4 to 0.8 m/s less than in 10 m height due to the friction of the ground. The average speed amounts to 4.0 m/s in 10 m height in the period 1994 - 2001. During the summer months a clear decrease of wind velocity has been determined. The main wind velocities lie between 2.9 and 3.3 m/s (2 Beaufort) in this height from May to August. The average values of the months April and September slightly lie above that with 3.5 and 3.4 m/s; however, they are already assigned to the strength 3 in the Beaufort's scale. Likewise the medium speeds of the the months October until March correspond to the strength 3. These months with average values between 4.4 and 5.3 m/s already belong to the upper range of this Beaufort stage, which covers speeds of 3.4 to 5.4 m/s. The top speed in the summer lies with 7 - 8 Beaufort clearly below the winter values (9 -10 Beaufort). Due to large fluctuations in winter the values of the standard deviations are accordingly high; they reach values between 3 and 4.2 m/s from September to April. From May to July the standard deviation continuously drops down to 2 m/s and then rises again until September.

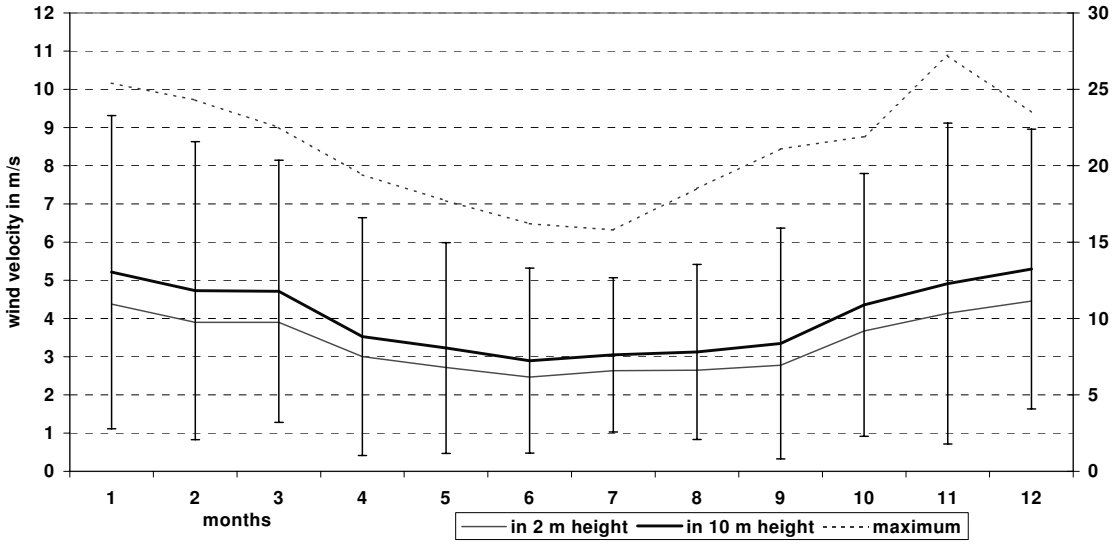

Fig. 4.53: Maximum and mean wind speed and standard deviation in 10 m height, mean windspeed in 2 m height for the Koldewey data series (1994 –2001)

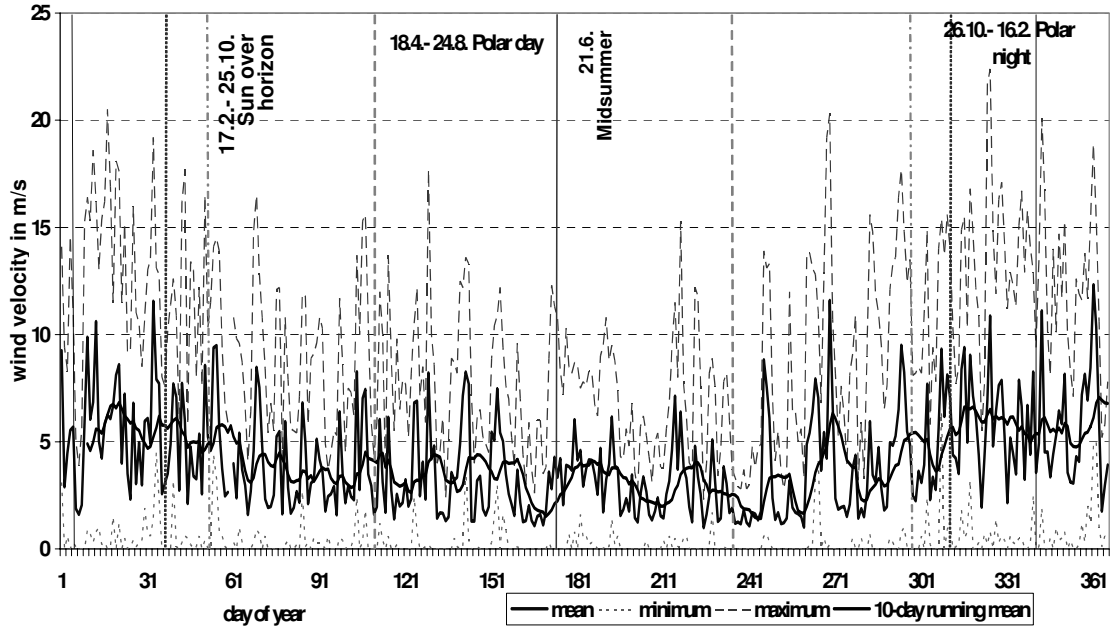

Fig. 4.54: Yearly course of the wind speed in 10 m height for 2001 (daily means)

As it is represented in Fig. 4.54 by the example of the year 2001, there are large fluctuations of the wind velocity during the annual course. In 2001 the average wind velocity amounts to 4.1 m/s and lies only 0.1 m/s over the 8-yearly-mean from 1994 to 2001. It varies between 1 and 12 m/s. A fast rise or decrease of the wind velocity occurs very frequently. These increases not rarely happen even within a few hours. Particularly during polar night and the transitional phases between polar day and polar night it comes to strengthened fluctuations of the wind velocity, which arises the mean during these times for about 1-2 m/s. Likewise, the top speeds occur more frequently in these phases. In the year 2001 the highest wind velocity was determined with 22.4 m/s on 21st November.

Tab. 4.36: Monthly wind conditions in 10 m height for 2001 (in m/s)

2001	Jan	Feb	Mar	Apr	May	Jun	Jul	Aug	Sep	Oct	Nov	Dec	year
prev.direction	SE	SE	SE	SE	SE	NW	E	E	SE	SE	SE	SE	SE
percentage	34	35	49	45	29	25	38	34	23	30	34	40	31
mean speed	5.2	4.7	3.8	3.3	4.0	4.8	2.2	2.4	3.5	3.3	5.4	5.3	3.9
max. speed.	17.9	15.1	14.3	14.4	13.0	12.2	8.7	12.2	13.8	14.3	16.9	19.4	19.4
temperature[°C]	-8.4	-9.9	-15.2	-13.7	-3.8	1.4	6.2	5.0	2.4	-3.9	-11.6	-8.6	-4.8
rel. humidity [% r.H.]	70.2	66.1	62.3	65.7	68.1	78.6	79.2	84.4	78.5	74.4	64.7	68.6	71.2

The monthly wind -, temperature- and humidity conditions for the prevailing wind direction are presented in Tab.4.36. It is to be recognized that with exception of the summer months also in the year 2001 the SE- winds determine the weather conditions in Ny-Ålesund.

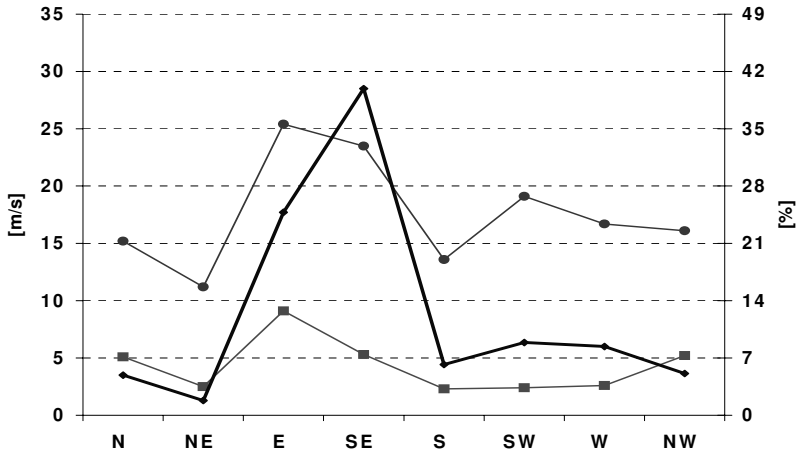

Fig. 4.55a: Monthly wind conditions in 10 m height in January for 1994 – 2001

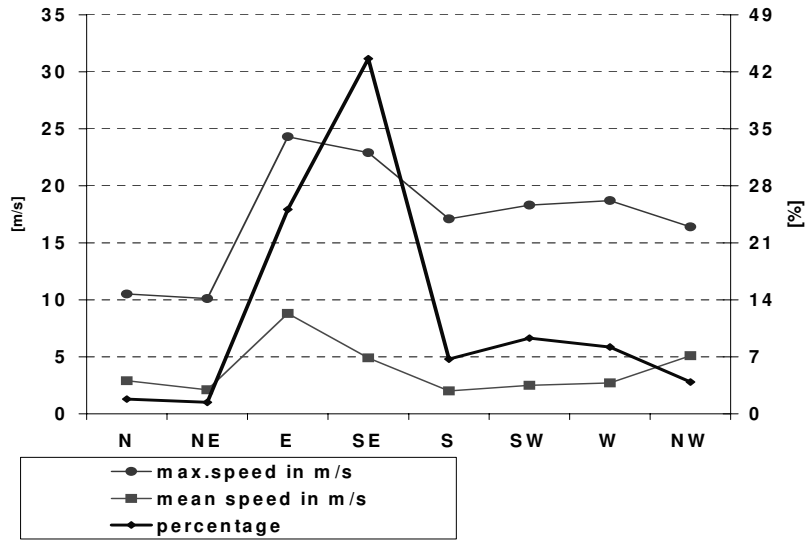

Fig. 4.55b: Monthly wind conditions in 10 m height in July for 1994 – 2001

Wind conditions in July 2001 differ from those in the observation period. The wind velocities and wind direction for the months January and July 1994 - 2001 are represented in Fig. 4.55. While in July 2001 the east component is dominating, the wind in July 1994 - 2001 mainly originates in southeast. The conditions in July 1994 - 2001 are quite similar to the conditions in January.

4.5.5 Snow Drift

Snow drift frequently occurs in the polar regions; it depends on the wind direction and strongly on the wind velocity. At velocities from 5-7 m/s the precipitation or snow and ice particles from the ground (from 7 m/s) get blown up and carried away by the wind. With increasing wind velocity, the size of the snow drift and their density rises as well. The range of vision can drop to 5 - 10 m. The highest speeds are reached by southeast and easterly winds. Snowstorms have a strongly erosive effect and often they persist for some days. The snow that hasn't been blown away by these strong winds becomes hard like stone (STONEHOUSE 1989, LILJEQUIST und CEHAG 1994[3]).

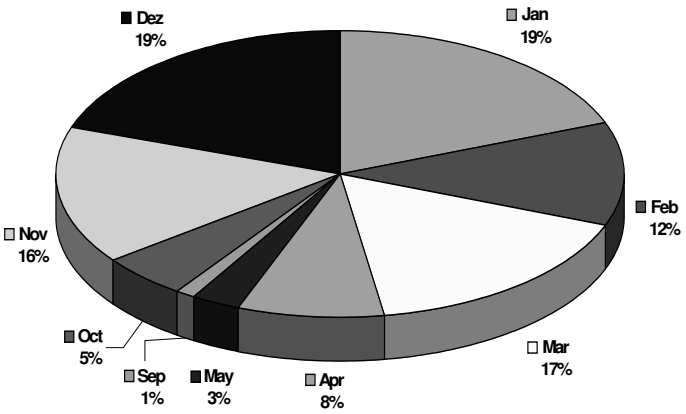

Fig. 4.56: Appearance of snow drift related on the number of observations between 1994 and 2001

In Fig. 4.56 the proportional distribution of the snow drift is shown for the months September until May. The data are based on the synoptic observations accomplished by the Norwegian Polarinstitut. Most frequently snow drift arises with a percentage of altogether 83 % in the months November until March. In December and January their rate is with 20 and 19 % particularly high. The drift is usually slight and occurs below the eye level in 70 to 80 % of the cases. In the months November until January in which the average wind velocities increase in both, in 2 m and in 10 m height, the rate of the snow drift above the eye level rises too. The frequency of a strong snow drift is biggest in January.

4.6 The Daily Courses of the Radiation - and Meteorological Parameters

The daily courses of the radiation - and meteorological parameters were already outlined on the basis of the isopleth-diagrams. By the example of two days in May 2002 the parameters and their connections should now be analyzed exactly. This concerns the 25th May, a clear day and 29th May, a cloudy day. Both days lie in the time of the polar day, when the sun does not sink under the horizon. On 25th May the solar altitude lies between 10° and 32° and on 29th May approximately one degree higher.

There is no influence on the direct radiation by the mountains of the Brøggerfjellet in the evening hours. The sun reaches its highest point at 11:03 UTC and its lowest point about one hour before midnight (UTC). The most important radiation - and meteorology values are shown in Tab. 4.37. On both days the albedo lies between 75 and 83 % which means the snow layer is still present. The values in this section originate from both, the measured data of the Koldewey station and the synoptic observations by the Norwegian Polar Institute.

A documentation with photographs by the webcamera of the Zeppelin station for the two daily courses (in 3-hourly-rythm) is attached to Appendix 4.6 Fig. 5 - 20.

Tab. 4.37: Average - and extreme values as well as the differences of the average values for the days of 25th May and 29th May 2002

	25th May 2002			**29th May 2002**			difference
	mean	max	min	mean	max	min	
temperature [°C]	-0.6 ± 0.7	0.9	-4.0	2.2 ± 0.7	4.9	0.8	2.8
relative humidity [% r.H.]	55.7 ± 5.5	70.4	42.8	95.4 ± 2.3	100.0	83.6	39.7
wind speed [m/s]	1.0 ± 0.4	2.9	0.0	1.5 ± 0.7	7.4	0.0	0.5
pressure in station height [hPa]	1027.5 ± 0.9	1029.8	1026.3	1021.7 ± 1.3	1023.1	1018.5	-5.8
diffuse radiation [W/m²]	59.8 ± 12.3	89.7	39.8	119.3 ± 64.8	258.1	26.5	59.5
direkt-horizontal radiation [W/m²]	292.7 ± 134.6	490.8	61.4	0.0 ± 0.9	2.3	0.0	292.7
global radiation [W/m²]	353.4 ± 154.2	575.9	140.7	120.6 ± 65.8	260.4	26.8	-232.8
reflex radiation [W/m²]	274.1 ± 88.5	395.1	147.1	94.2 ± 51.1	201.5	21.9	-179.9
albedo [%]	82.7 ± 12.1	100.0	67.3	78.2 ± 1.1	80.9	74.8	-4.5
SW-budget [W/m²]	79.3 ± 67.0	188.1	-6.6	26.4 ± 14.8	60.1	4.9	-52.9
emitted radiation [W/m²]	297.1 ± 7.6	307.7	284.5	315.2 ± 0.6	317.2	314.0	18.1
counter radiation [W/m²]	230.3 ± 2.4	236.0	225.0	324.7 ± 1.9	330.2	320.2	94.4
LW-budget [W/m²]	-66.8 ± 9.2	-52.9	-79.1	9.5 ± 1.6	13.5	5.0	-76.3
net radiation budget [W/m²]	12.5 ± 58.6	109.6	-61.9	35.9 ± 14.3	68.7	13.2	23.5

4.6.1 Clear Day: 25th May 2002

The 25th May is a day without any cloud coverage. The horizontal view was estimated with over 50 km by the synoptic observations. The pressure in the height of the station amounted to 1027.5 ± 0.9 hPa; it decreased during the day from 1029.8 to 1026.3 hPa (from 1031.2 to 1028.0 hPa on sea level). SE-winds and westerlies reached their mean speeds 1 m/s and their maximal speed at 2.9 m/s. The dew point temperature lies between - 7.7 and - 10.7°C. On a clear day in the early summer, as it is shown by the example of 25th May the sun heats the surface. Still the air temperature in 2 m height lies only on an average of –0.6 ± 0.7°C. The global radiation on this day was with 353.4 ± 154.2 W/m² clearly higher than on 29th May (see Appendix 4.6 Fig. 1). It varied however with the position of the sun; which is shown by the daily variation of the global radiation and the relatively high standard deviation. The relative global radiation was at an average of 74 % and the diffuse sky radiation amounted about 19 % of the global radiation.

Further on this day a big part of the incident solar radiation is reflected due to the high albedo, which lies at approximately 80% in the end of May. This can be due to the change of the upper snow layer that is melting during the day by the increased solar radiation. The mean short-wave radiation budget lay at 79.3 ± 67.0 W/m² on 25th May clearly above the value of the 29th May. The courses of the air temperature and the radiation budgets are represented in Fig. 4.57. The the net radiation budget can raise the temperature in the daily course; however, on this day it was about 2.8°C colder than on the overcast day of 29th May despite the higher solar radiation. The cooler temperature is also caused by an energy input into the snow melt. The long-wave energy balance is more important for this day. With the supply of short-wave energy also the value of the emitted radiation increased up to 307.7 W/m², while the counter radiation only varied

slightly around the average value of 230.3 W/m² (see Appendix 4.6 Fig. 2). The counter radiation was clearly smaller than the emitted radiation due to the clear sky. The long-wave energy loss corresponded to an average of 66.8 ± 9.2 W/m². While the short-wave energy gain of >50 W/m² lasted only between 5 and 18 UTC, the long-wave energy loss also continued at the "night" with values > for 50 W/m² at lower sun positions.

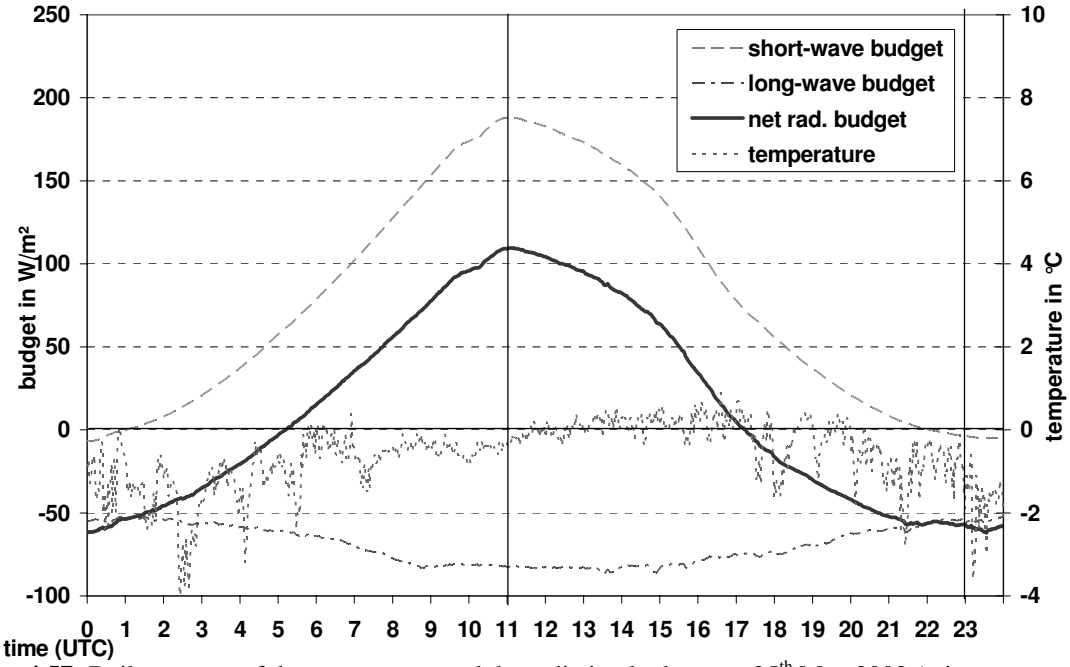

Fig. 4.57: Daily courses of the temperature and the radiation budgets on 25th May 2002 (minute means)

The effective energy gain (net radiation budget) of this day was with 12.5 W/m² clearly smaller than on 29th May, which was expressed in the lower temperature (see also HISDAL 1998).

4.6.2 Overcast day: 29th May 2002

On 29th May 2002 all three synoptic observations exhibited 8 eighths of coverage on the day. A closed cloud cover of the Stratus- und Stratocumulus family in 2 to 4 km height indicated humid air masses. The relative humidity is about 95.4 ± 2.3 % r.H in 2 m height. In the early morning hours a slight rain was determined. The horizontal view was estimated at 20 km. The temperature lay at 2.2 ± 0.7°C on 29th May which is 2.8°C above the value of the 25th May. The pressure in station height decreases from 1023.1 to 1018.5 hPa (1024.5 - 1021.0 hPa on sea level) on this day. The prevailing winds in 10 m height came from NE to SE with average speeds of 1.5 m/s and reach maximum speeds of 7.4 m/s. The courses of temperature and the radiation budgets are represented in Fig. 4.58.

On this day it could not be registered any direct solar radiation. The diffuse sky radiation corresponded to 99 % with the global radiation (see Appendix 4.6 Fig. 3). Small deviations could have been caused by measuring errors. The average value of the diffuse sky radiation was at 119.3 W/m² and thus clearly above the value from 25th May. The global radiation intensity amounted to an average of 23.5 % from the extraterrestrial radiation. Between 9 and 16 UTC the global radiation rose over the 200 W/m² limit. This can be explained with the higher sun position and the stronger irradiation. The reflex radiation exhibits a similar course as the global radiation and lay in average about 26 W/m² below the curve of the global radiation. The albedo values varied between 75 and 81 %. During the night hours the

global radiation dropped below 50 W/m², and therefore no more albedo values could be determined.

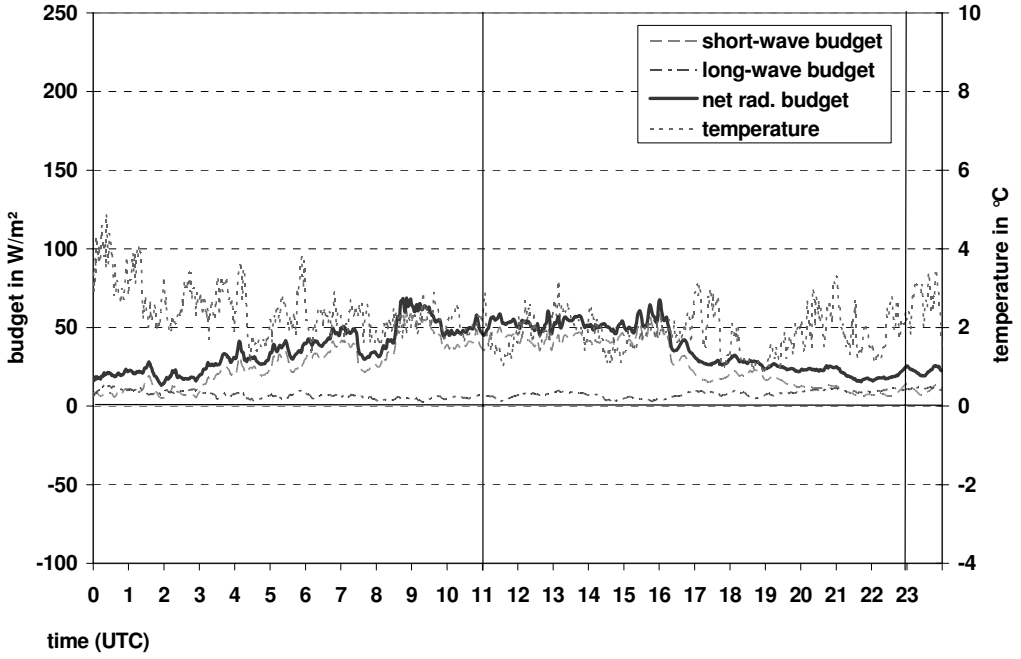

Fig. 4.58: Daily courses of the tenperature and the radiation budgets on 29th May 2002

Due to the overcast on 29th May the counter radiation increased by 94.4 W/m² in relation to 25th May. The emitted radiation on 29th May was approximately 18 W/m² higher than on 25th May. The values of the counter radiation were bigger on this day than the values of the emitted radiation, so that the long-wave radiation budget lay in a slightly positive range (see Appendix 4.6 Fig. 4). Therefore the net radiation budget and the temperature increased on 29th May. In this case an advection of warm air could be the reason for the raise of the temperature. The increase of the temperature at the night cannot be explained with the available data of radiation, wind and humidity.

5 Summary

The thinning of the ozone layer, a possible melting of polar icecaps, the polluted atmosphere due to anthropogenic aerosols and greenhouse gases are only few actual questions that are to be solved only within international cooperations. One of these worldwide networks for the detection of climate change is the Baseline Surface Radiation Network (BSRN). The German-French AWIPEV Arctic Research Base in Ny-Ålesund, Spitsbergen (78°55'N, 11°53'E), formerly called Koldewey Station belongs to the BSRN network since 1992. It contains the mea-surements of radiation and meteorologic parameters by the Koldewey-Station and the sy-noptical observations by the Sverdrup-Stationen of the Norwegian Polarinstitute.

This work is the first extensive analysis of radiation and meteorologic data of the BSRN station in Ny-Ålesund for the time period from 1993 to 2002.

Spatial and temporal changes of meteorologic parameters such as air pressure, humidity, temperature, wind and precipitation as well as solar and terrestric radiation are important for climatologic questions and weather forecasts. The nessesary data are recorded by measurements and observations at the ground level and up to the middle stratosphere by launching of rawin- and ozone sondes. These meteorologic parameters are determined by short- and long-termed changes because of atmospheric processes; they depend on solar radiation directly or indirectly which leads to characteristic daily and annual courses.

For the archiving and processing of these data the meteorological database of the Alfred-Wegener-Institute „MISAWI" (Meteorological Information System of the AWI) is used. The 5-minutes data recording started in August 1992 (radiation data) and August 1993 (meteorological data) and ended in 13th July 1998. Starting from July 14th, 1998 the measurements in the actual resulution of the instrument and the transmitting frequency could be substantially increased by the usage of a new logging system, and starting from this time average values per minute are able to be stored. For the meteorological parameters weighted average values were formed by the data rows of the 5- and 1-minute means.
During the evaluation of the measured values an error could be recognized with the computation of the sun altitude within the data base. Therefore for the radiation data the incorrect daily means were not used, where a weighting was not necessary for the formation of the monthly and annual means. The data row of the observation period 1993 - 2001 for the radiation parameters and from 1994 to 2001 for the meteorological parameters is called Koldewey row.

A good cooperation with the Norwegian Polarinstitute and the Norwegian Meteorologic Institute (DNMI) made a comparison of data of the Koldewey-row with long yearly means possible. For such a trend analysis the radiation data were made available for the period of 1974 to 1992 by Norwegian Polarinstitut as well as the WMO standards for the meteorological parameters of the periods 1931 - 1960 and 1961 - 1990 for Ny-Ålesund by the DNMI. These long-time data rows are the condition for secured statements about the climatic development in Ny-Ålesund.

The radiation in Ny-Ålesund is determined by polar day, polar night and the transitional phases with a day-night rhythm. In the south of the village the 554m high Zeppelin Fjellet is situated, that causes a delay of the direct solar radiation in spring and in fall its shade darkens the village earlier. During this time the net radiation balance lies in the positive range and is controlled by the global radiation. The global radiation depends on the solar altitude and on the coverage of the sky with clouds. During the observation period the most sunshine duration is occurred in April and May. From June to September the

coverage with low and medium high clouds exceeded 80 %. In this time the sky is mainly covered with cloudfields of large horizontal extent (especially Stratus, Stratocumulus and Altocumulus). In the range of March to June multiple reflexions occurred frequently between the snow surface and the clouds bottom, which caused an increase of the global radiation. A decrease of the global radiation can be caused by atmospheric aerosols and climatic relevant gases, like CO_2, originating from the major industrial zones in North America, Europe and East Asia. (JAWOROWSKI 1989, KLAUS 1999) (see Fig. 5.1).

Aerosols of natural sources, like from the volcano Mt. Pinatubo, were detected in the Arctic even three years after its eruption in 1991 by HERBER et al. (1996). During the months March and May the concentration of aerosols is especially high in the Arctic atmosphere. This phenomenon is called Arctic Haze and the possibility of appearance of Arctic haze occurence is around 40 % during these months. A slight but significant increase of the aerosol content which can be examined by the optical thickness of atmospheric aerosols, was proved by HERBER, et al. (2002) for the years between 1991 and 1999. This increased aerosol content did not show any changes in the mean values for global radiation during the observation time.

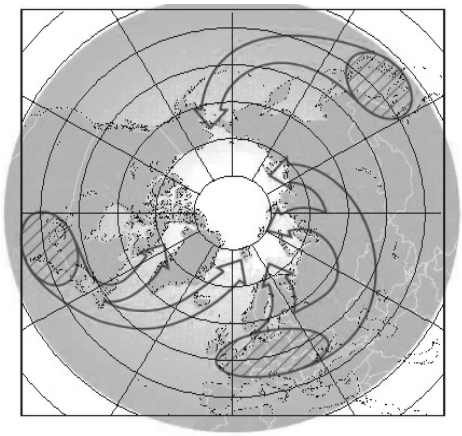

Fig. 5.1: Entry of anthropogic aerosols from the industrial centres of Europe, North America and Eastern Asia into the Arctic region (HERBER et al. 2002: 11)

A significant figure for the radiation balance is the decrease of the reflex radiation and of the related albedo determined by the snow melting processes in June. The yearly mean for the albedo was calculated with 51.9 % for the observation time. Characteristic are the fast reduction of the albedo from over 60 % down to 20 % and less within just a few days in June. The snow melt is mainly determined by the radiation and the increasing temperature over the 0 °C – mark. Shortly after the snow melt the radiation balance reaches its climax. The dense cloud coverage causes a higher downward longwave radiation during the summer months. The long wave radiation that gets absorbed by the clouds and reflected by the earth's surface leads to an increase of the radiation balance and thus the temperature (natural greenhouse effect). Nevertheless, long wave energy losses arise by radiant emittance during summer, in particular on clear days with inversion weather conditions. During the long-term view of the short wave radiation it is further to note that the regarded period fell into a phase of particularly strong solar activity. An intensified luminosity of the sun, which occurs in an 11-year rhythm, leads to a reinforcement of the natural greenhouse effect, which is additionally increased by the entry of anthropogen emissions into the Arctic (ORVIG 1970, FLIGGE und SOLANKI 2002).

In winter the difference between warm air masses from south and cold air masses from the north influence the weather in Ny-Ålesund. Cold and dry air is transported to Spitsbergen with high-pressure areas originating from the polar sea. Due to the missing Sun, the polar night from end of October till end of Februar is characterisized by energy loss. Dry air leads to big radiation losses during the months of December and January, where the most clear days and nights of the year occur.

The loss of energy in winter is slightly less than the energy gain in summer, so that the yearly mean of the energy budget is positive with 1,4 W/m². It clearly lies under the value for the lengthened period between 1976 and 2001 with 5,7 W/m². An increase of the short-wave irradiation was detected during the observation period, which went along with a rise of energy-loss and a reduction of the radiation balance. The trend-analysis showed that the decrease of the balance in the Koldewey-row is equal to the reduction of the balance during the years between 1974 and 2001.

During the polar night, the temperature in Ny-Ålesund showed fluctuations between 7 and -35 °C due to high pressure – and temperature differences, while the summer months showed pretty constant temperatures around 5 °C. The yearly mean temperature in Ny-Ålesund is –5,1 °C, and 0,7 °C higher than the mean of the standard row 1961 – 1990, but 0,8 °C lower than the mean of the standard row 1931 – 1960. A significance of this temperature trend was not found. The balance that decreased during the years 1974 and 2001 cannot be the reason of the slight temperature rise. Possible causes for the warming could be dynamic processes, like the transport of warm air- and ocean currents towards Spitsbergen or the Kongsfjord that stayed icefree for a longer time. There could be found a conspicuous temperature rise during the winter months of the latest years where the January mean value increased 5,9 °C during the observation time. However, because of these high fluctuations in winter this is not a representative figure. Since the nineteen 20ies regular changes of the temperature tendencies have been observed. Already between 1915 and the mid nineteen 20ies an increase of the winter temperatures of 8 °C was found. Especially obvious are the decadical variations of the temperature tendencies which can be followed back until the nineteen 30ies (HISDAL 1985, FØRLAND et al. 1997). According these evaluations the temperature increased again during the nineteen 90ies.

These rhythmic temperature tendencies may be based on the different extend of the Arctic oscillation (AO). There is a zyclonal stream around the northern polar cap in about >2 km height. In winter this stream is strengthened by the cold temperatures in the hight between 17 and 40 km. This leads to the formation of a polar vortex. At a strong development it causes a rise of the wind velocity close to the surface. Through that, warm, humid air can be brought to Svalbard from the south (positive phase). With a warming of the stratosphere over the northpole it may occur that this stream breaks down and cold air anticyclonally flows down to Svalbard from the polar basin (negative phase). These phases alternate in unregular intervals reaching from a few days to some months. But when the phenomenon is watched over years and decades, there is always one of the states dominating, which may explain the decadic fluctuations of the temperature. (HISDAL 1985, LIPPSETT 2002, DORN 2002). This decadal variation of the phases of the AO is standing in significant relationship with the 11-year cyclus of high and low intensity of solar activity (SCHULZ 2001).

The Kongsbreen (Kings Glacier) is situated about 15 km east to southeast of the village and has a big regional influence. Air masses cool down over this huge glacier and cold and fast katabatic winds blow down from it. Through the location of the Kongsfjord in NW–SE direction these winds get canalised additionally. However the strongest winds measured in the village originate directly from the Kongsbreen in eastern direction. This makes an exact measurement of precipitation at standard hight in Ny-Ålesund very complicated. The yearly mean of precipitation was defined by the DNMI with 365 mm for the WMO standards of the period between the years 1961 and 1990. Most of the precipetation is detected as snow in March and September. With the data evaluated there could not be given an exact time for a rebuilt of a closed snow cover in September,

because of the low amount of irradiation from a dense cloud cover and the low solar altitude.

An evaluation of the meteorologic and radiation parameters in the observation period of 8 and 9 years is too short for a detailed climatologic analysis. Nevertheless, with the help of historic data, there can be detected and observed climatologic tendencies.

References

Akademie der Wissenschaften der DDR - Nationalkommitee für Geodäsie und Geophysik [Hrsg.] (1962, 1965 1966): Deutsche Spitzbergen Exkursion.- Exkursionsberichte. - Potsdam, Berlin.

BLÜMEL, W.D. und EBERLE, J. (2001): Global Warming in Permafrostgebieten.- Geographische Rundschau 53, Heft 5: 48-53.

BOIKE, J., ROTH, K., IPPISCH, O. (2003): Seasonal snow cover on frozen ground: Energy balance calulations of a permafrost site near Ny-Ålesund, Spitsbergen.- Journal of Geophysical Research, Vol.108, No. D2: 8163-8173.

DEHNE, K. et al. (1995): BSRN – ein hochgenaues Strahlungsmeßnetz des Weltklimaforschungsprogramms der WMO.- Annalen der Meteorol. 31 (1995): 62-63.

DORN, W.(2002): Natürliche Klimavariationen in der Arktis in einem regionalen hochauflösenden Atmosphärenmodell.- ALFRED WEGENER INSTITUT für Polar- und Meeresforschung: Berichte zur Polarforschung 416/2002.-Bremerhaven

DWD (1982): Wetterschlüsselhandbuch VuB2, Band A+B.- Offenbach.

DWD (1987³): Allgemeine Meteorologie – Leitfaden für die Ausbildung im Deutschen Wetterdienst.- Offenbach.

FLIGGE, M. und SOLANKI, S.K. (2002): Sonnenhelligkeit und Klima- Spektrum der Wissenschaft – Dossier Klima: 32 –33.

FØRLAND, E.J., HANSSEN-BAUER, I., NORDLI, P.Ø. (1997): Climate Statisticvs & longterm series of temperature and precipitation at Svalbard and Jan Mayen.-DNMI: Det Norske Meteorologiske Institutt: Klima.- Report No.21/97 Klima

FØRLAND, E.J. and HANSSEN-BAUER, I. (2000): Increased prtecipitation in the norwegian arctic: True or false?.- Climatic Change 46: 485 – 509.

HANSSEN-BAUER, I., KRISTENSEN SOLÅS, M., STEFFENSEN, E.L. (1990): The Climate of Svalbard.- DNMI: Det Norske Meteorologiske Institutt: Klima.- Report No.39/90 Klima.

Haenni Solar 111 technical mannual

HELMES, L. (1989): The Meteorological Data of the Georg-von-Neumayer-Station (Antarctica) for 1985, 1986 and 1987.- ALFRED WEGENER INSTITUT für Polar- und Meeresforschung: Berichte zur Polarforschung 64/1989.-Bremerhaven.

HERBER, A. et al. (1996):Volcanic perturbation of the atmosphere in both polar regions: 1991 – 1994.- J. Geophys. Res. Vol. 101, 3921 - 3928.

HERBER, A.. et al. (2002): Continious day and night aerosol optical depth observations in the Arctic between 1991 and 1999.- J. Geophys. Res. Vol. 107, No. 10.1029: AAC 6 1-14.

HISDAL, V. (1985²): Geography of Svalbard.- Norsk Polarinstitutt.- Oslo.

HISDAL, V., FINNEKÅSA, Ø., VINJE, T. (1992): Radiation Measurements in Ny-Alesund, Spitzbergen 1981 – 1987.- Norsk Polarinstitutt: Meddelelser Nr. 118.-Oslo

HISDAL, V. and FINNEKÅSA, Ø. (1996): Radiation Measurements in Ny-Alesund, Spitzbergen 1988 – 1992.- Norsk Polarinstitutt: Meddelelser Nr. 142.-Oslo

HISDAL, V. (1998): Svalbard- Nature and history.- Norsk Polarinstitutt.- Oslo.

HUPFER, P. und KUTTLER, W. (1998[10])[Hrsg.]: Witterung und Klima.- Stuttgart, Leipzig.

Impulsphysik LD-25/LD-40 technical manual

IQBAL, M. (1983): An Introduction to Solar Radiation.- Toronto, New York, London.

JAWOROWSKI, Z. (1989): Pollution of the Norwegian Arctic: A review.- Norsk Polarinstitutt - Rapportserie No.55- Oslo.

Kipp & Zonen CM11 technical manual

Kipp & Zonen: Standard CM Pyranometer Series Specifications

KLAUS, D. (1999): Neue Ansätze und Erkenntnisse in der Klimaforschung.- Geogr. Rundsch. Heft 9: 448 – 453.

KOENIG-LANGLO, G. (1992): The Meteorological Data of the Georg-von-Neumayer-Station (Antarctica) for 1988, 1989, 1990 and 1991.- ALFRED WEGENER INSTITUT für Polar- und Meeresforschung: Berichte zur Polarforschung 116/1992.-Bremerhaven.

KOENIG-LANGLO, G. and HERBER, A. (1996): The Meteorological Data of the Neumayer Station (Antarctica) for 1992, 1993 and 1994.- ALFRED WEGENER INSTITUT für Polar- und Meeresforschung: Berichte zur Polarforschung 187/1996.-Bremerhaven

KOENIG-LANGLO, G. and MARX, B. (1997): The Meteorological Information System at the Alfred-Wegener-Institute.- LAUTENSCHLAGER, M., REINKE, M. [Ed.]: Climate and Environmental Database Systems.– Norwell

KORSNES, (1998): Summary of ice maps – The Barents Sea 1966 – 1989. – Univ. of Leeds. – unpublished.

LANGE, G.(2001)[Hrsg.]: Eiskalte Entdeckungen.- Bad Oeyenhausen.

LAUER, W. (1993): Klimatologie.- Braunschweig.

LILJEQUIST, G. H. und CEHAK, K. (1994³): Allgemeine Meteorologie.- Braunschweig, Wiesbaden.

LIPPSETT, L. (2002): El Niño und seine Verwandten.- Spektrum der Wissenschaft – Dossier Klima: 18 –25.

McARTHUR, L.J.B. (2000[2]): World Climate Research Programme - Baseline Surface Radiation Network (BSRN)- Operations Manual: WMO/TD-No.579.

MONKA, M. und VOSS, W.(2002): Statistik am PC.- München, Wien.

ORVIG, S. (1970): World survey of Climatology – Climates of Polar regions; Vol. 14.- Amsterdam, London, New York.

PAROSCIENTIFIC, INC. (2002): Digiquartz-Precision Pressure Measurements – Programming and Operations manual. Doc.No.8107-001.

ROTH, K. and BOIKE, J.(2001): Quantifying thermal dynamics of a permafrost site near Ny-Aalesund, Svalbard.- Water Resources Research, Vol.37, No.12: 2901-2914.

SCHMIDT, T. and KÖNIG LANGLO, G. (1994): Radiation Measurements at the German Antarctic Station Neumayer 1982-1992.- ALFRED WEGENER INSTITUT für Polar- und Meeresforschung: Berichte zur Polarforschung 146/1994.-Bremerhaven.

SCHÖNWIESE, C.-D. (2000³) : Praktische Statistik für Meteorologen und Geowissenschaftler .- Berlin, Stuttgart.

SCHULZ, A. (2001): Bestimmung des Ozonabbaus in der arktischen und subarktischen Stratosphäre. - ALFRED WEGENER INSTITUT für Polar- und Meeresforschung: Berichte zur Polarforschung 387/2001.-Bremerhaven

STONEHOUSE, B. (1989): Polar Ecology.-Glasgow, London.

Thies 1.1000.50 technical manual

Thies 2.1265.10 technical manual

Thies 4.3323.21 technical manual

VAISALA technical manual: Humicap- Sensor

VDI 3786 Bl.5 (1986): Meteorologische Messungen für Fragen der Luftreinhaltung; Globalstrahlung, direkte Sonnenstrahlung und Strahlungsbilanz.

VDI 3786 Bl.16 (1996): Umweltmeteorologie: Messen des Luftdrucks.

VINJE, T.E. (1974 - 79): Radiation conditions in Spitsbergen.- Norsk Polarinstitutt Årbok 1974 -79.

VINJE, T.E. (1984): Frequency distribution of sea ice, ridges and water openings in the Greenland and Barents Seas.- A preliminary report on 'Birds Eye' observations.- Norsk Polarinstitutt - Rapportserie No.15.- Oslo.

VINJE, T. 2000. Anomalies and trends of sea ice and atmospheric circulation in the Nordic Seas during the period 1864-1998. J. of Clim., 14(3), 255-267.

WMO (1981): Meteorological Aspects of the Utilization of Solar Radiation as an Energy Source; No.:557.- Geneva.

WMO (1991): Radiation and Climate.- WCRP-64.

URL:

[Web1] http://www.traveljournals.net/countries/maps/?cc=sv&cn=Svalbard

[Web2] US Naval Observatory
http://aa.usno.navy.mil/data/docs/AltAz.html

ROESCH, A., WILD, M. (2002): http://bsrn.ethz.ch

KÖNIG-LANGLO (2002): http://www.awi-bremerhaven.de/MET/Ny-Alesund/index.html

MISU (2003): www.misu.su.se/~baseline

Maps:

Svalbard 1:100.000, Blad A7 Kongsfjorden, Norsk Polarinstitutt Oslo 1990

Svalbard 1:30.000, Brøggerhalvøya, Norsk Polarinstitutt Tromsø 2000

A P P E N D I X

Appendix Index

A 2 Map – Brøggerhalvøya with Ny-Ålesund

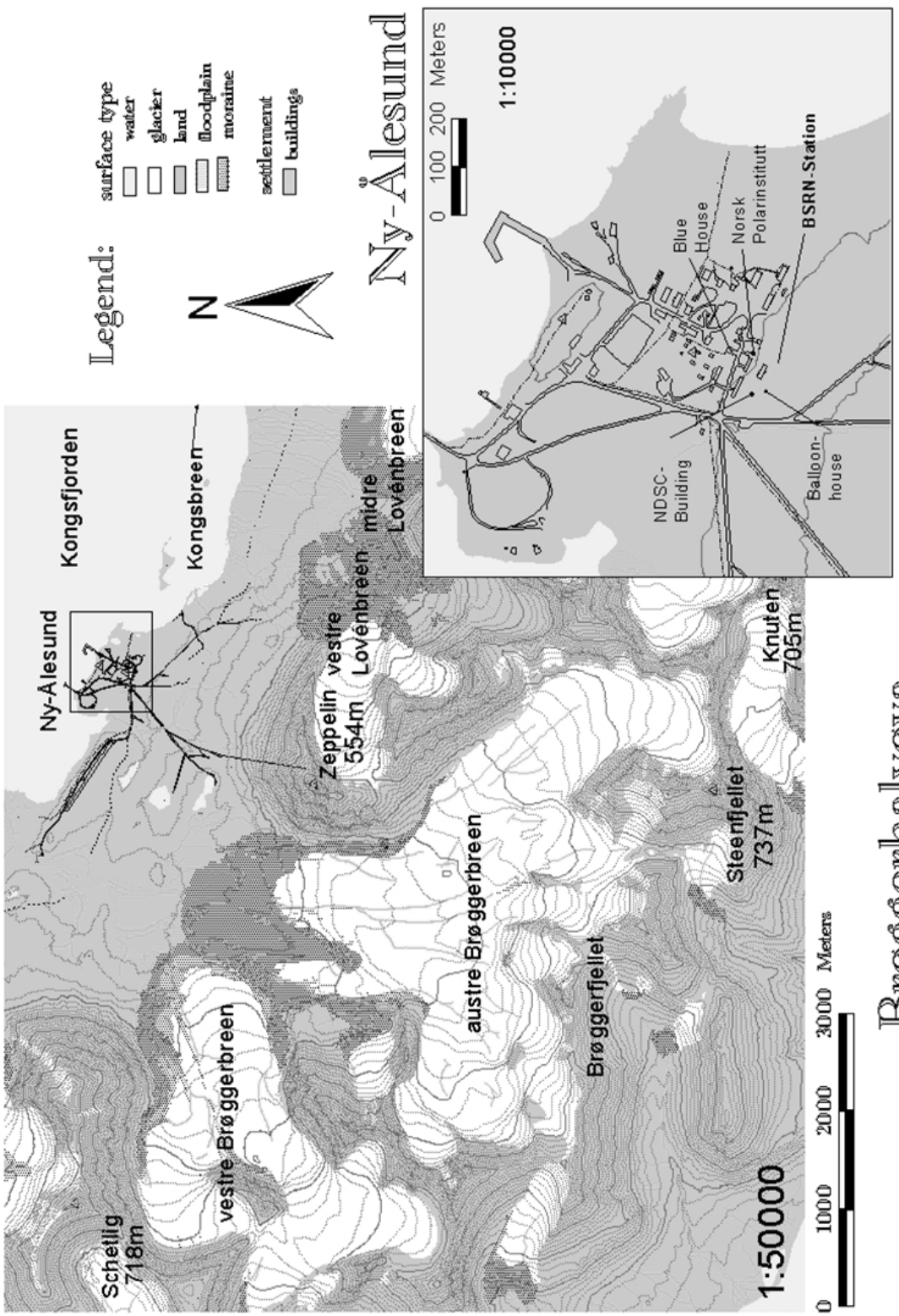

A 3 Coordinates of the BSRN-Station

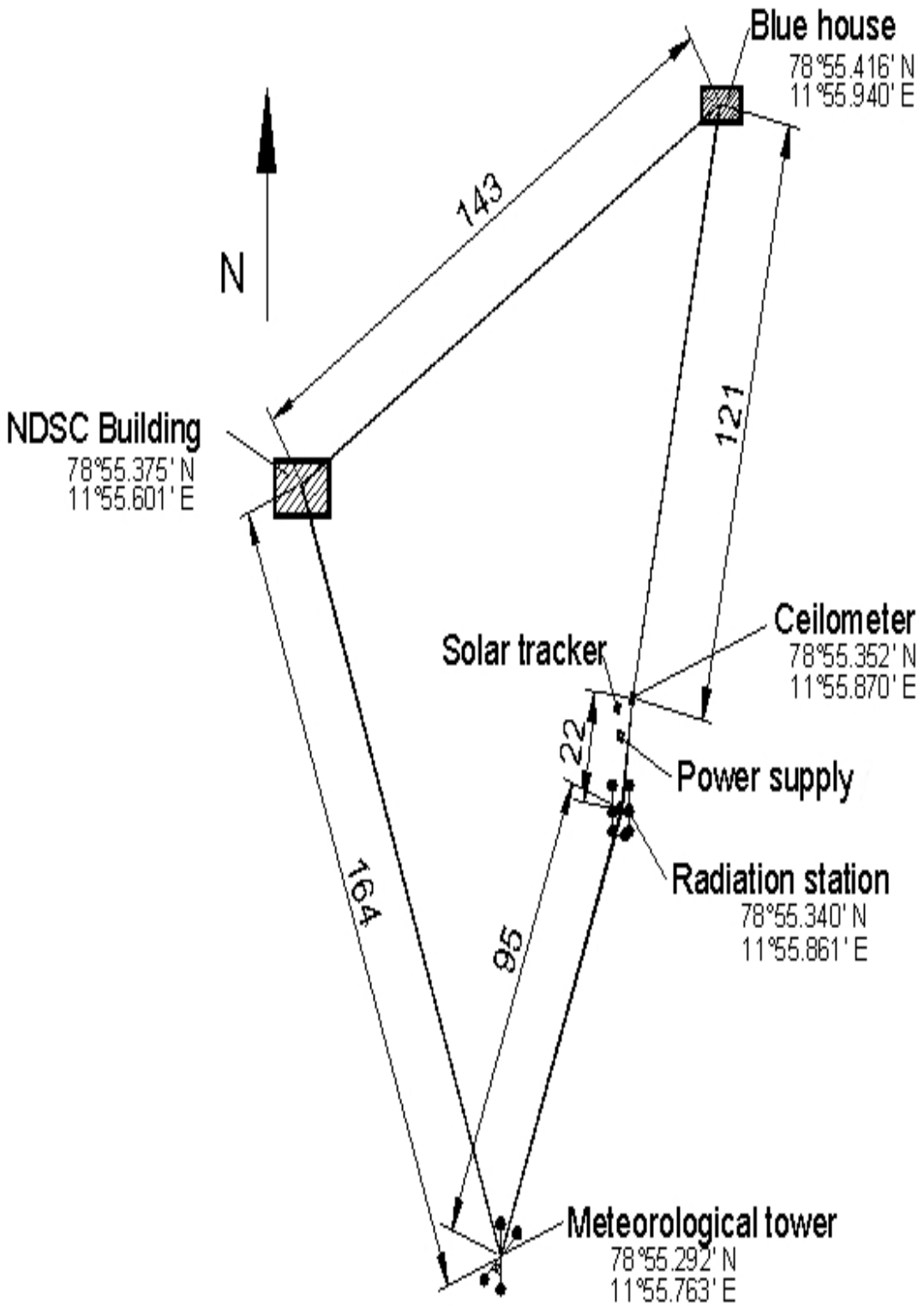

Positions of the BSRN-Station and distances

A 4.1 Monthly Light Conditions in Ny-Ålesund

Pictures of the webcam of the Zeppelin-station

Fig. 1: January

Fig. 2: February

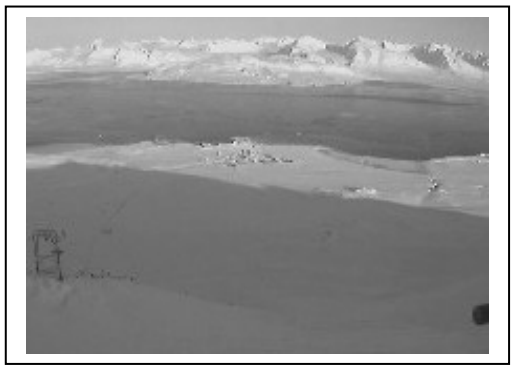

Fig. 3: March

Fig. 4: April

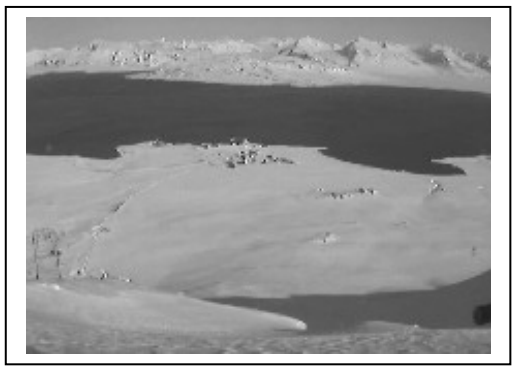

Fig. 5: May

Fig. 6: June

Fig. 7: July

Fig. 8: August

Fig. 9: September

Fig. 10: October

Fig. 11: November

Fig. 12: December

Source: MISU, Zeppelin Stasjonen Ny-Alesund: http://www.misu.su.se/~baseline

A 4.2 Sunshine Duration

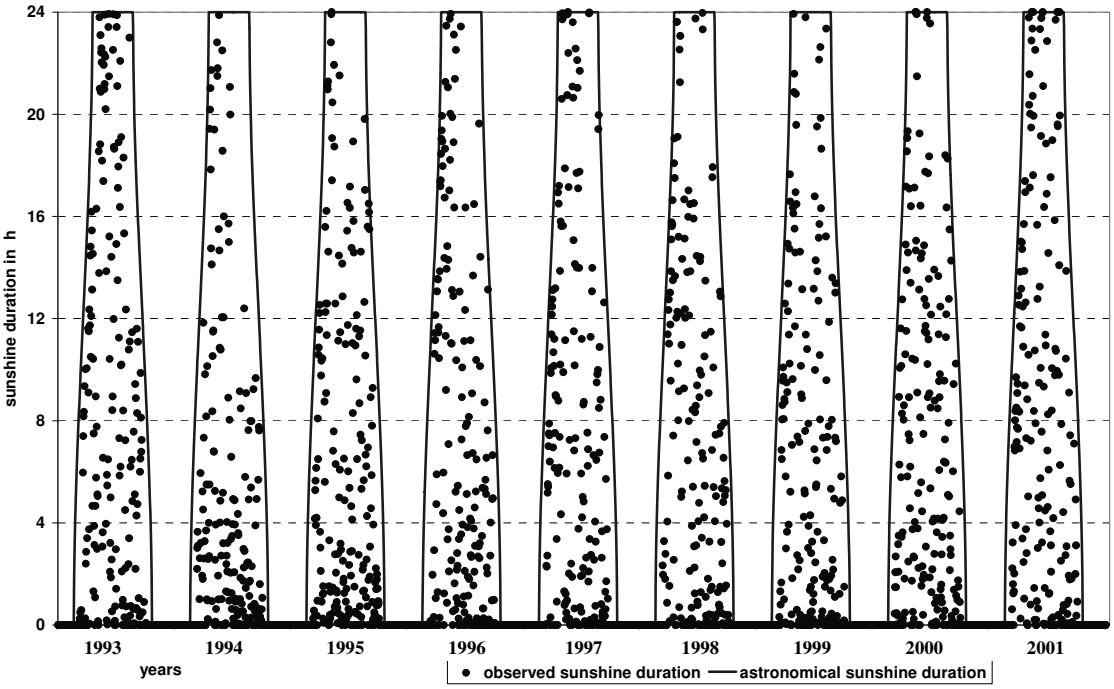

Fig.1: Observed and astronomical sunshine duration for Ny-Ålesund 1993 – 2001

A 4.3 Cloud Ceiling

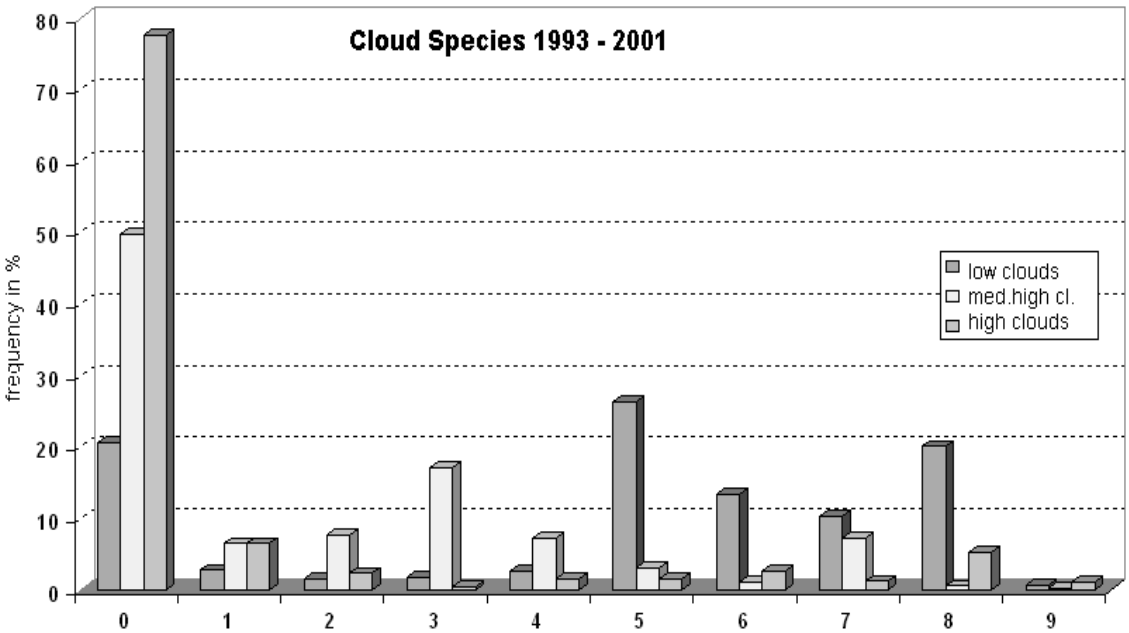

Fig. 1: Frequency of the coverage: clear sky, low clouds (C_L), medium high clouds (C_M) and high clouds (C_H) for Ny-Ålesund for the months March till October between 1993 and 2001 [For the differentiation of the cloud types, every layer was seperated into 10 different classes (class 0: no detected clouds in the respective layer, class 1-8: according the coverage eighths, class 9: failtures or no detection because of precipitation or fog)].

A 4.4.1 Direct Radiation

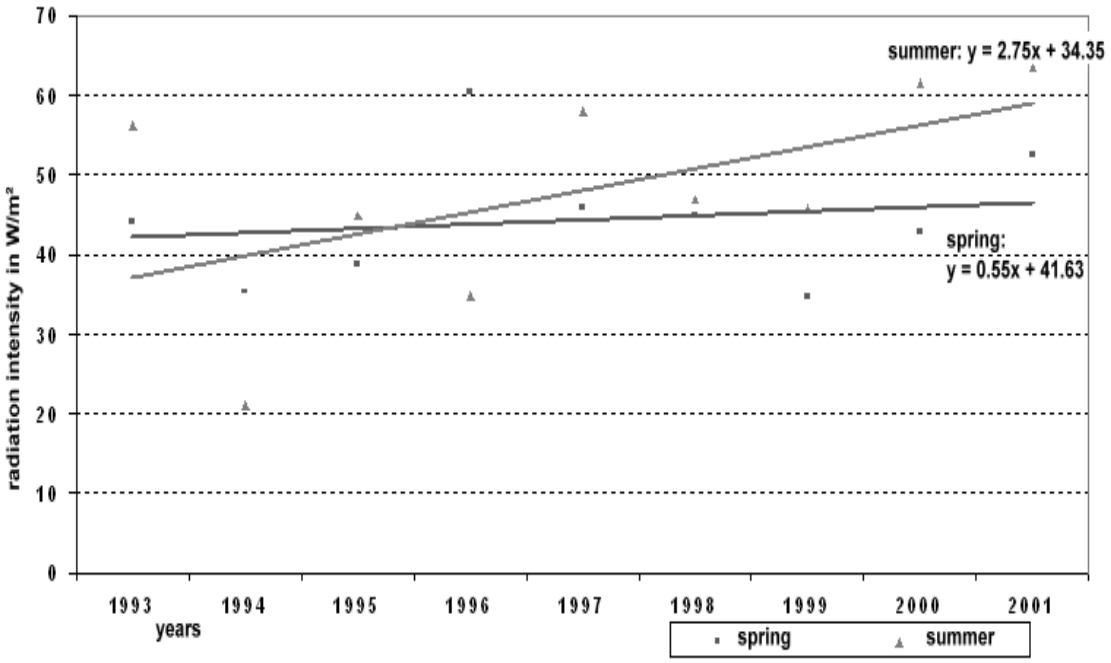

Fig. 1: Seasonal trends of the direct-horizontal radiation between 3/1993 and 8/2001

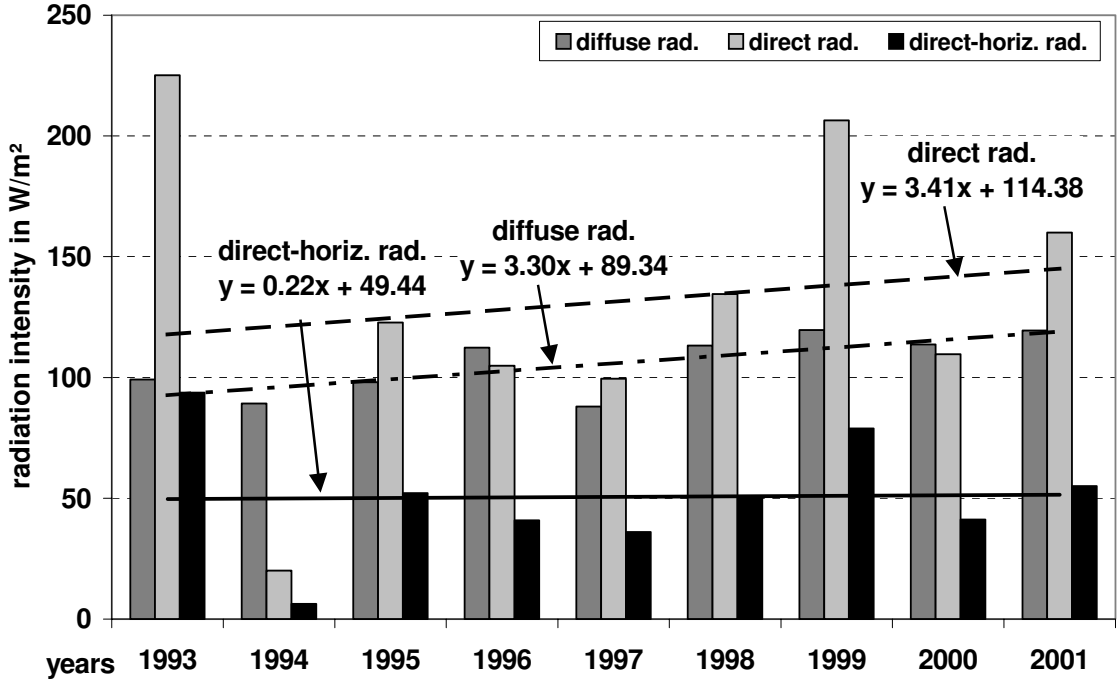

Fig. 2: July-mean of the direct, direct-horizontal – and diffuse radiation 1994 – 2001

A 4.4.2 Diffuse Radiation

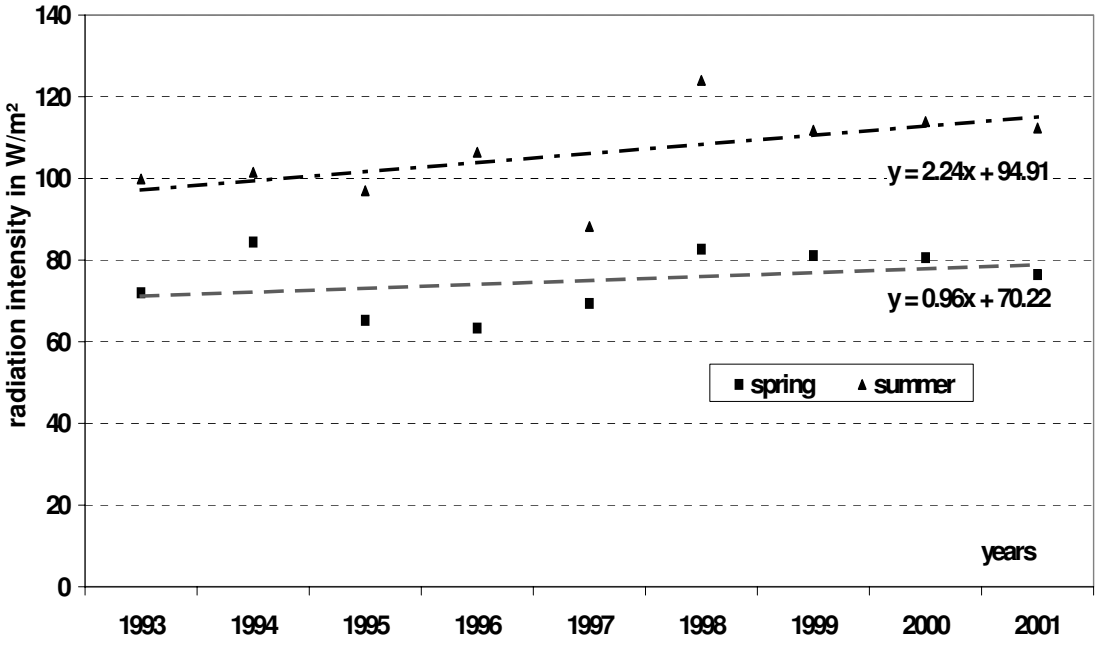

Fig. 1: Seasonal trends of the diffuse radiation in a period of 3/1993 – 8/2001

A 4.4.3 Global Radiation

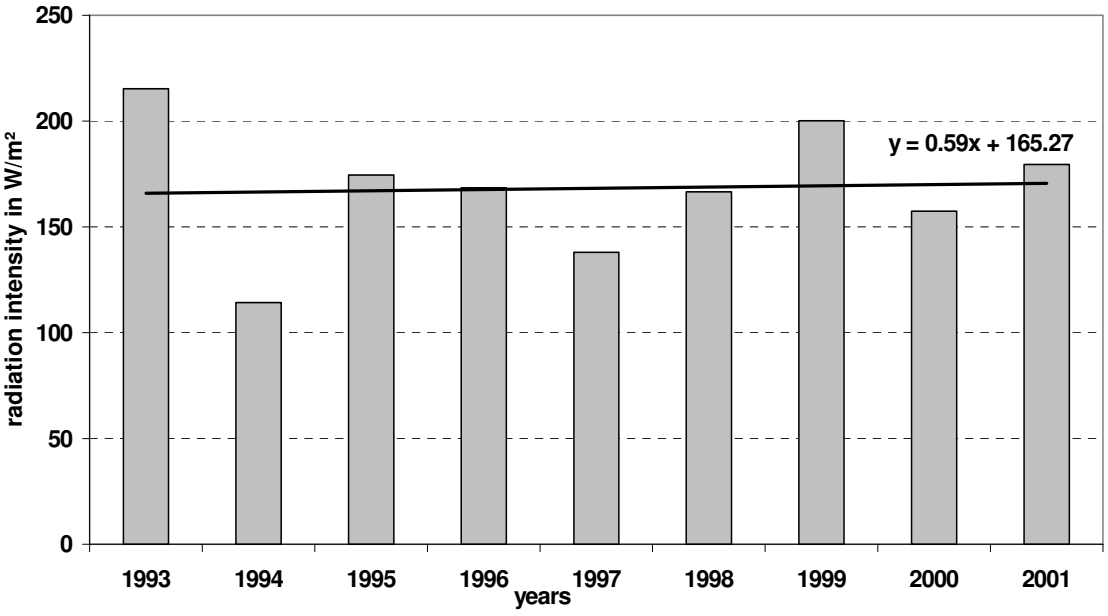

Fig. 1: July-mean of the global radiation between 1993 and 2001

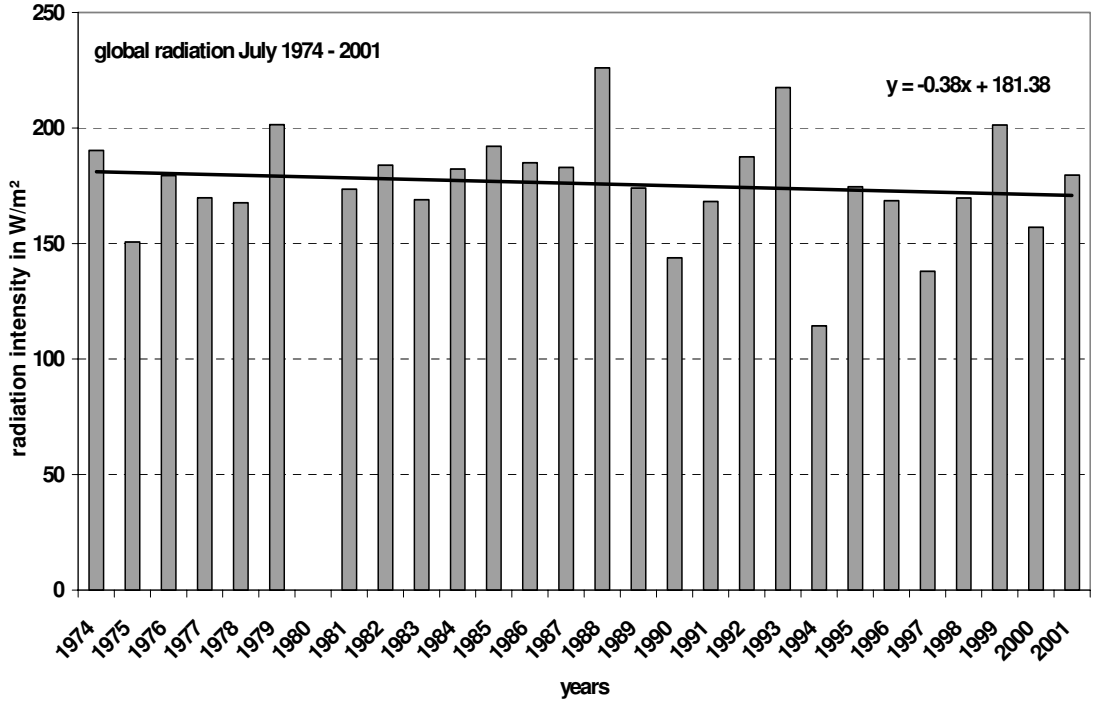

Fig. 2: Seasonal trends of the global radiation between 3/1993 – 8/2002

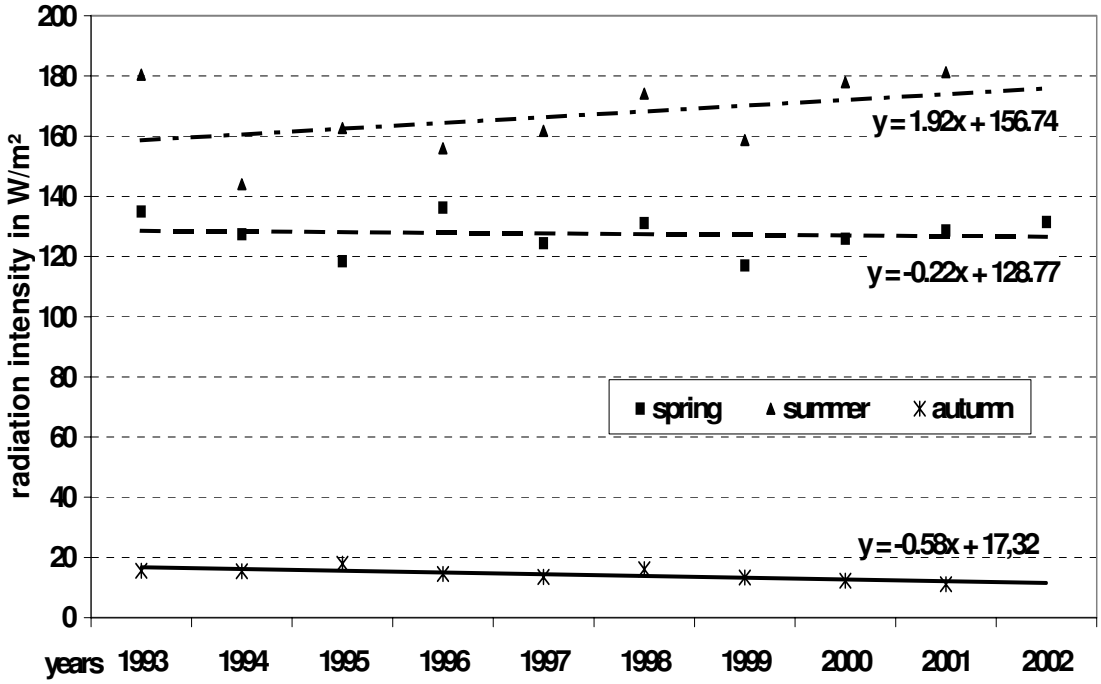

Fig. 3: Seasonal change of the global radiation from 1974 – 2001 (Norsk Polarinstitutt: 1974 – 1979/ 1981 - 1992 and the Koldewey-data series 1992 – 2001)

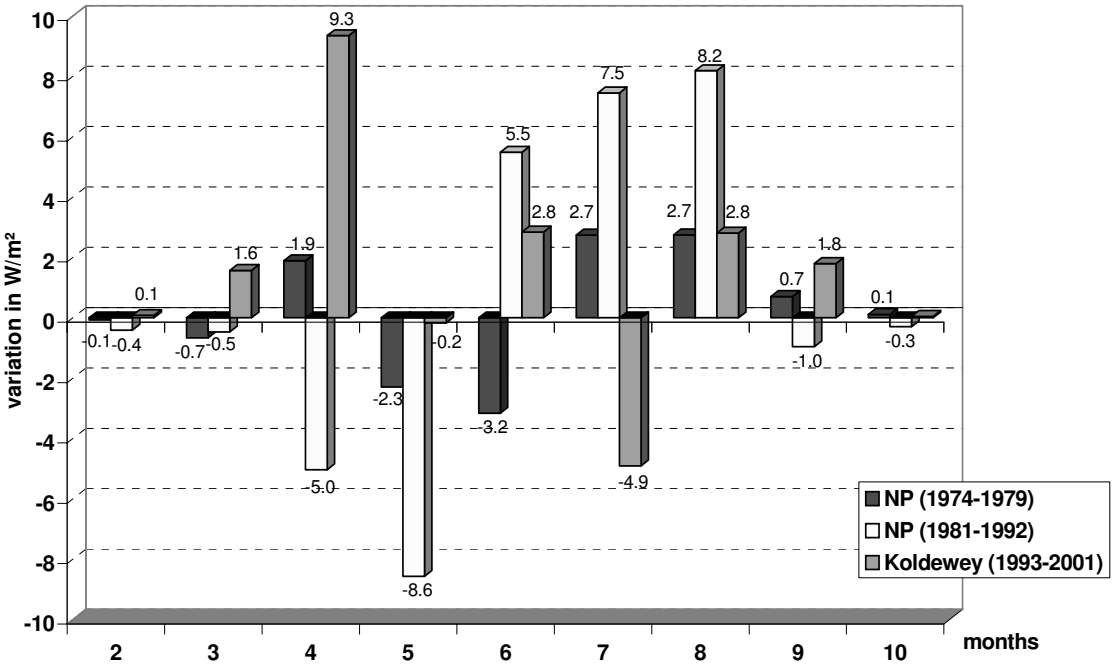

Fig. 4: Variations of the monthly means of the global radiation: Koldewey data series 1993 - 2001 and NP data series 1974 – 1979/ 1981-1992 from the WMO-normals 1931 - 1960

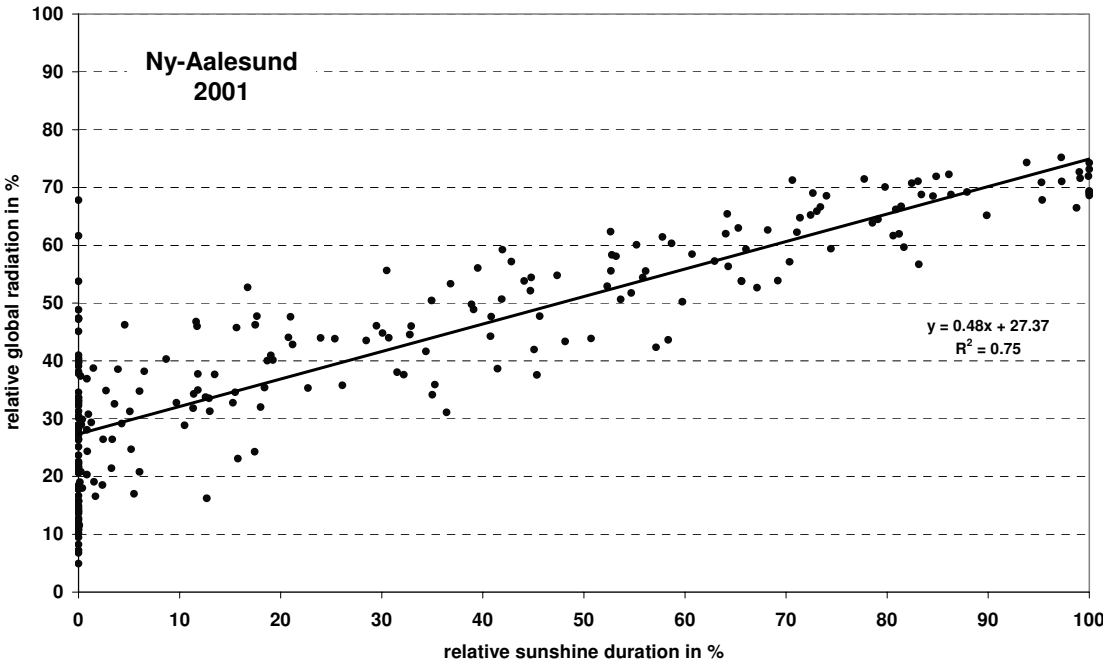

Fig. 5: Relative global radiation (ratio of recorded global radiation to calculated extraterrestrical radiation) as a function of the relative sunshine duration (ratio of observed sunshine duration to astronomical sunshine duration)

A 4.4.4 Albedo

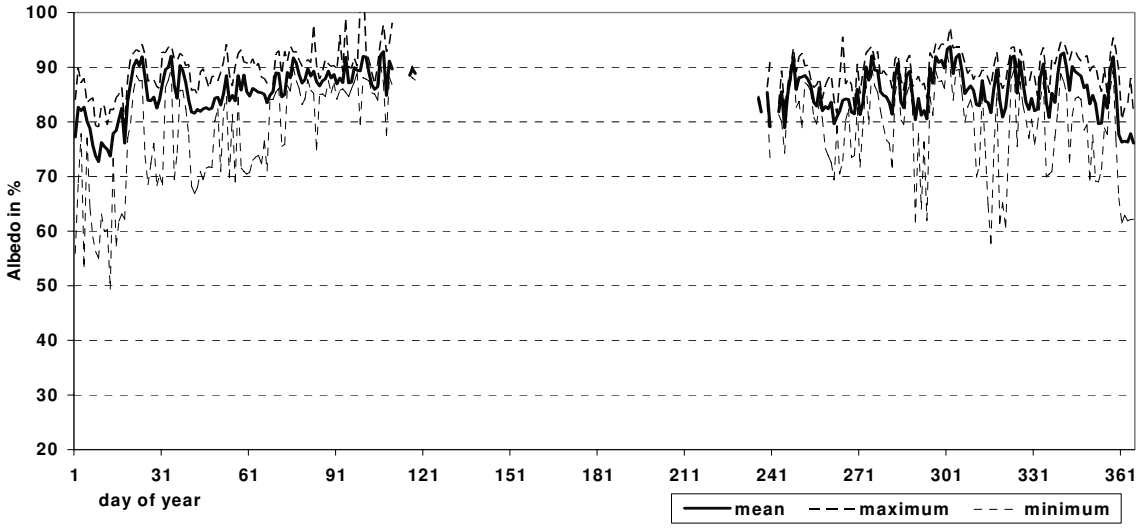

Fig. 1: Daily mean of the albedo for the Neumayer –Station (Antarctica) in 2001

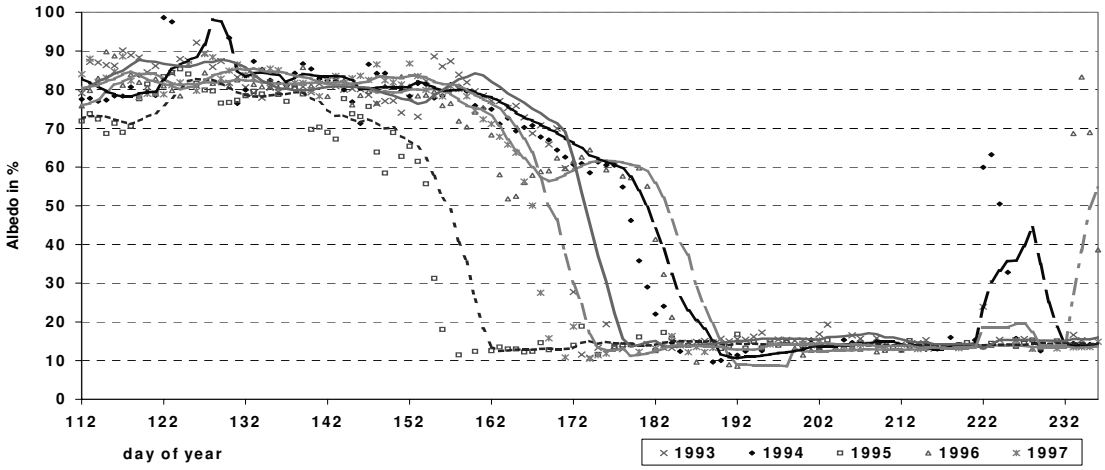

Fig. 2: 7-day running mean of the albedo between 21st Apr. - 23th Aug. of 1993 and 1997

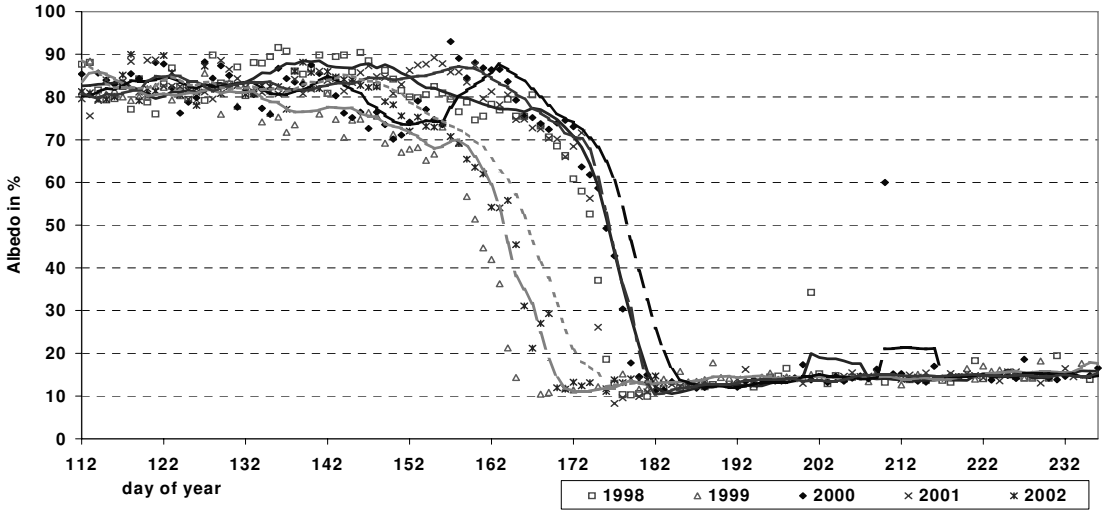

Fig. 3: 7-day running mean of the albedo between 21st Apr. - 23th Aug. of 1998 and 2002

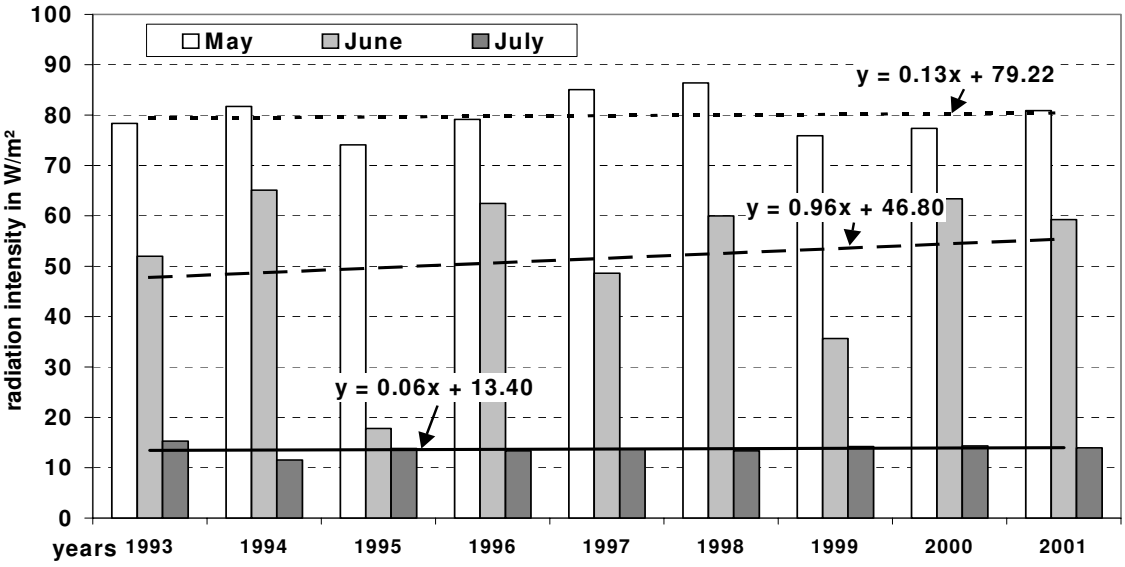

Fig. 4: Monthly trends of the Albedo for May, June and July between 1993 and 2001

A 4.4.5 Long-wave Radiation

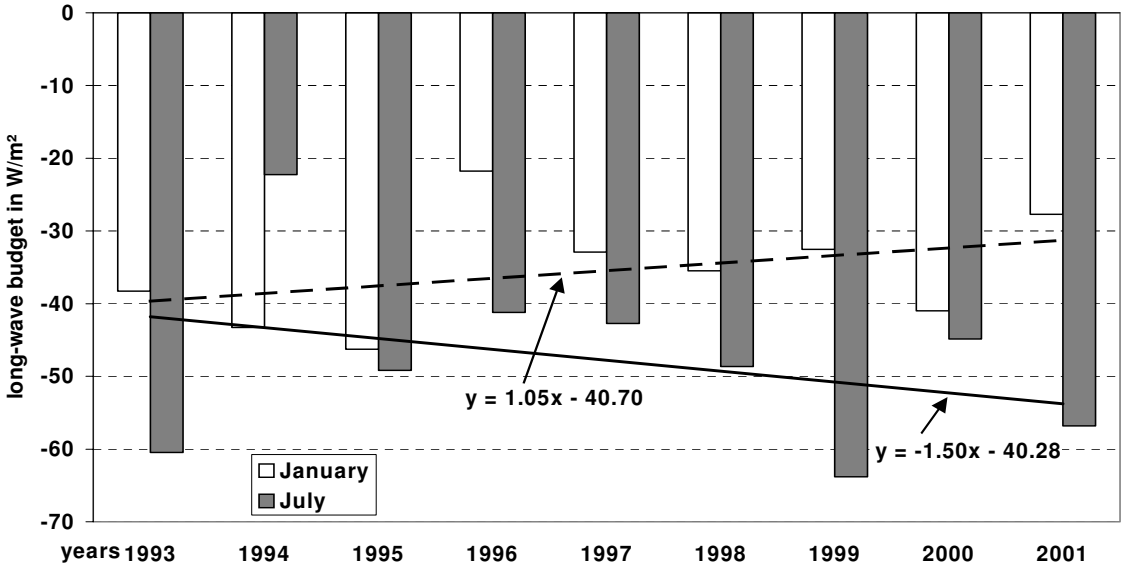

Fig. 1: January- and July-mean of the long-wave radiation budget between 1993 and 2001

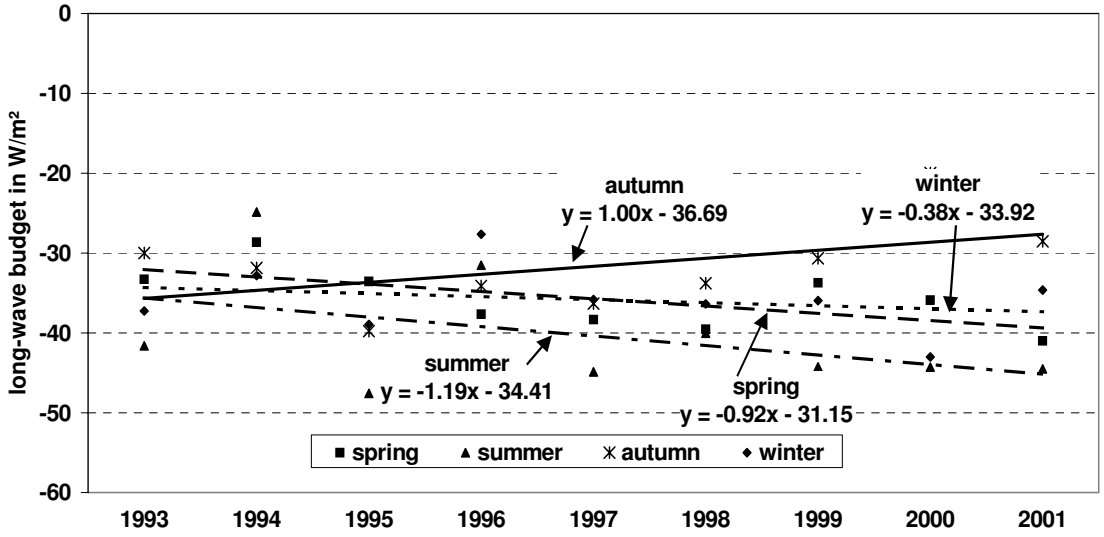

Fig. 2: Seasonal trends of the longwave radiation budget between 12/1992 and 11/2001

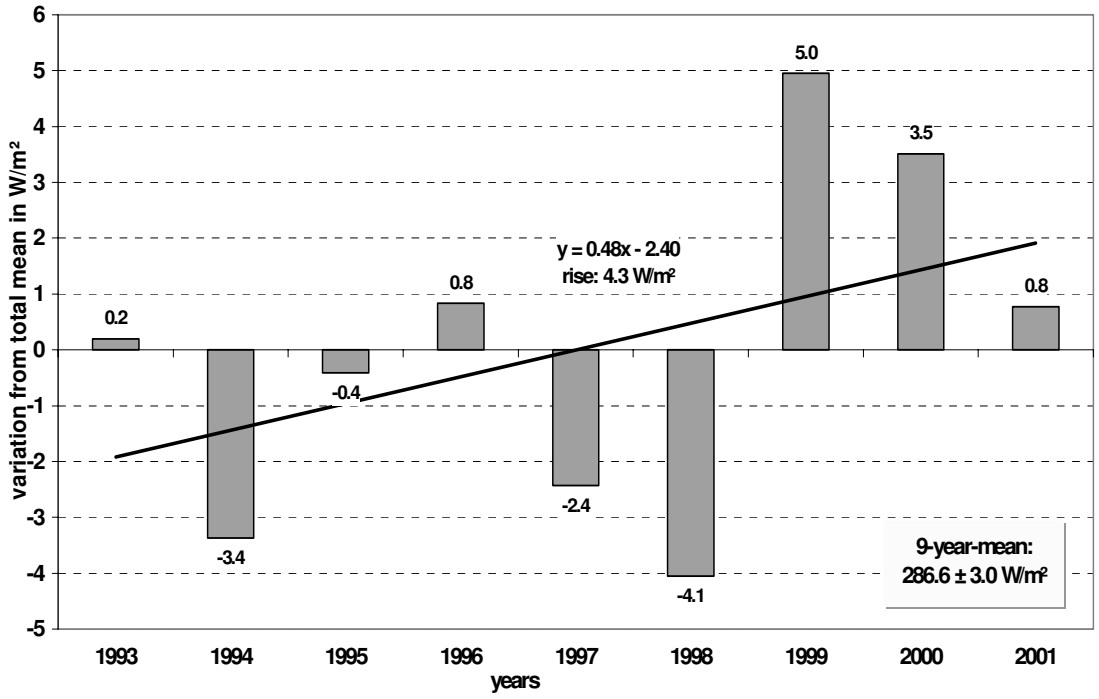

Fig. 3: Variations of the annual means of the emitted longwave radiation from the 9-year-mean (1993 - 2001)

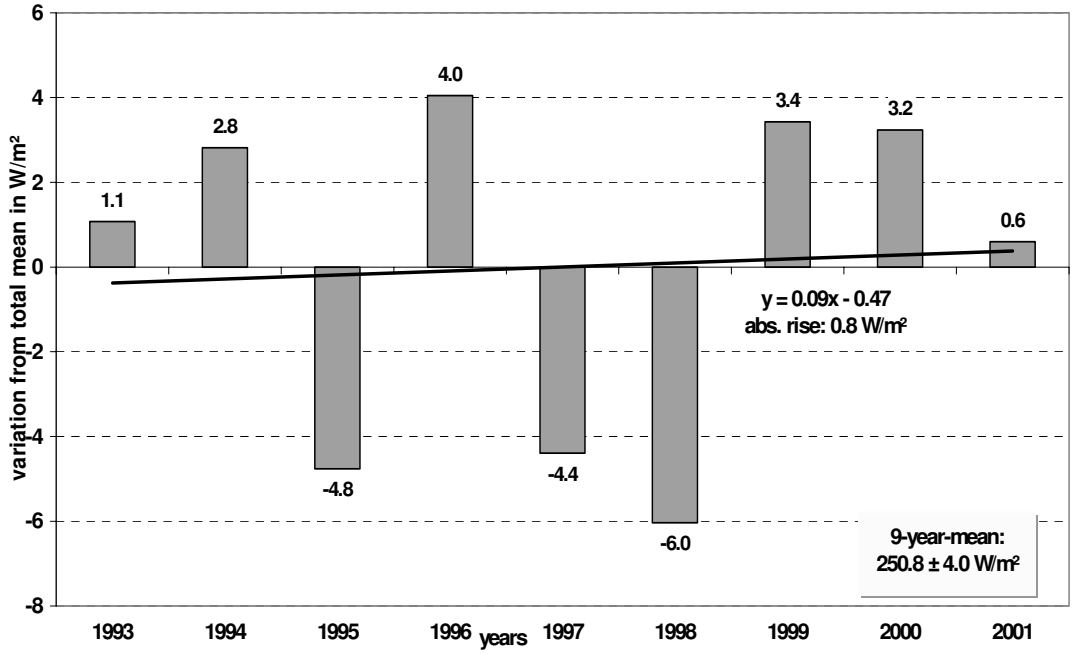

Fig. 4: Variations of the annual means of the reflected longwave radiation from the 9-year-mean (1993 - 2001)

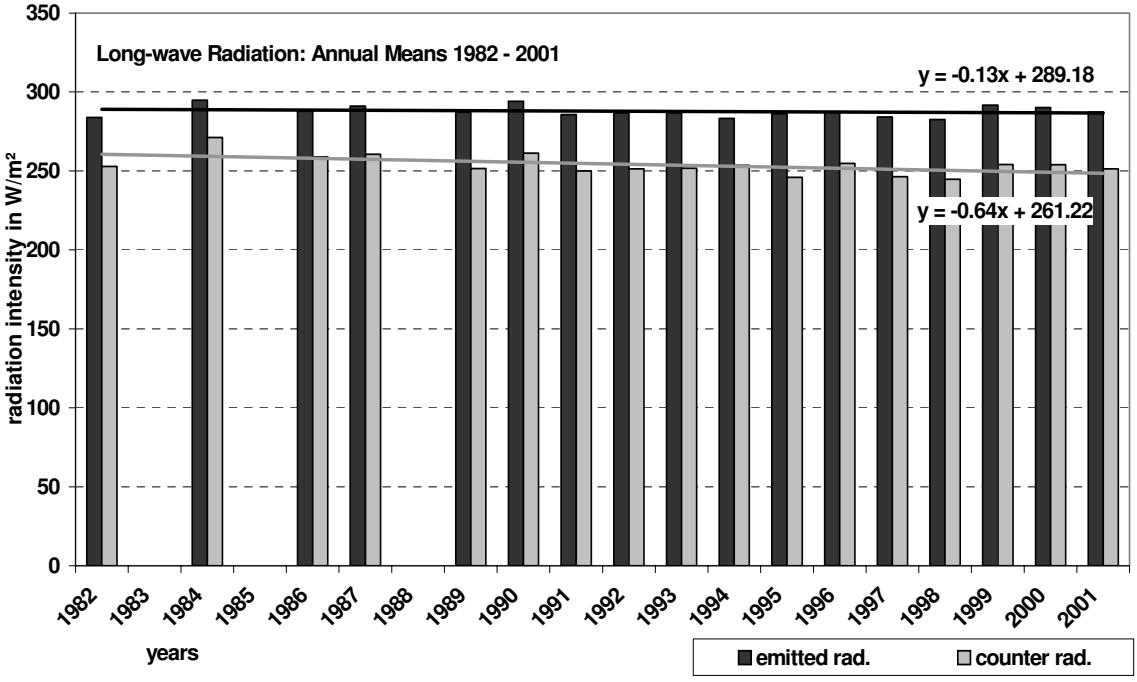

Fig. 5: Annual means of the longwave radiation between 1982 and 2001

A 4.4.6 Net Radiation Budget

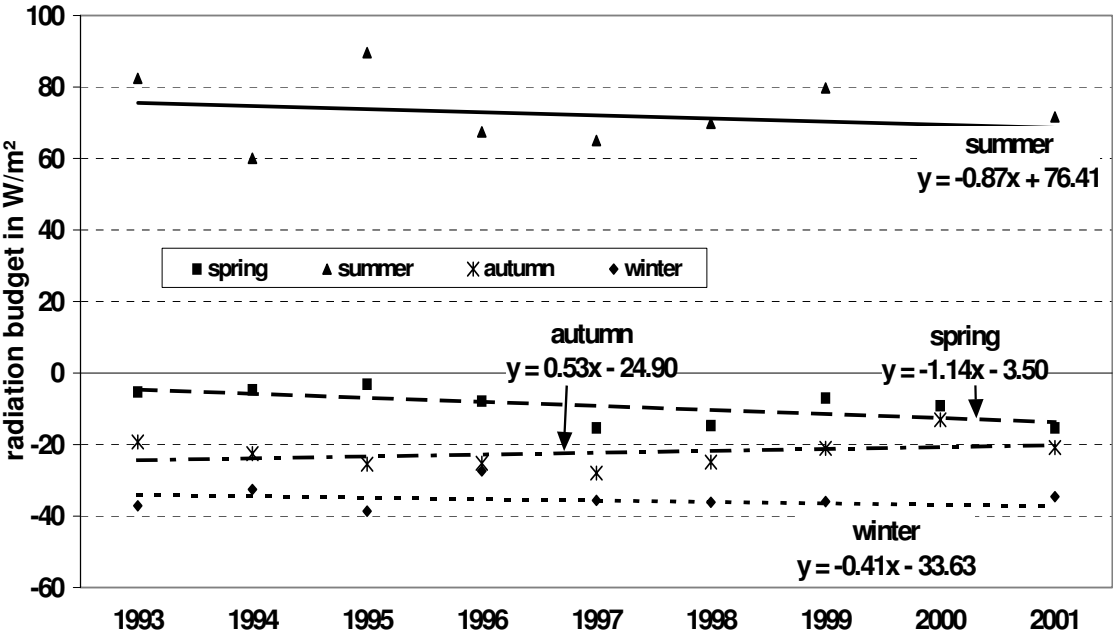

Fig. 1: Seasonal trends of the net radiation budget between 12/1992 and 11/2001

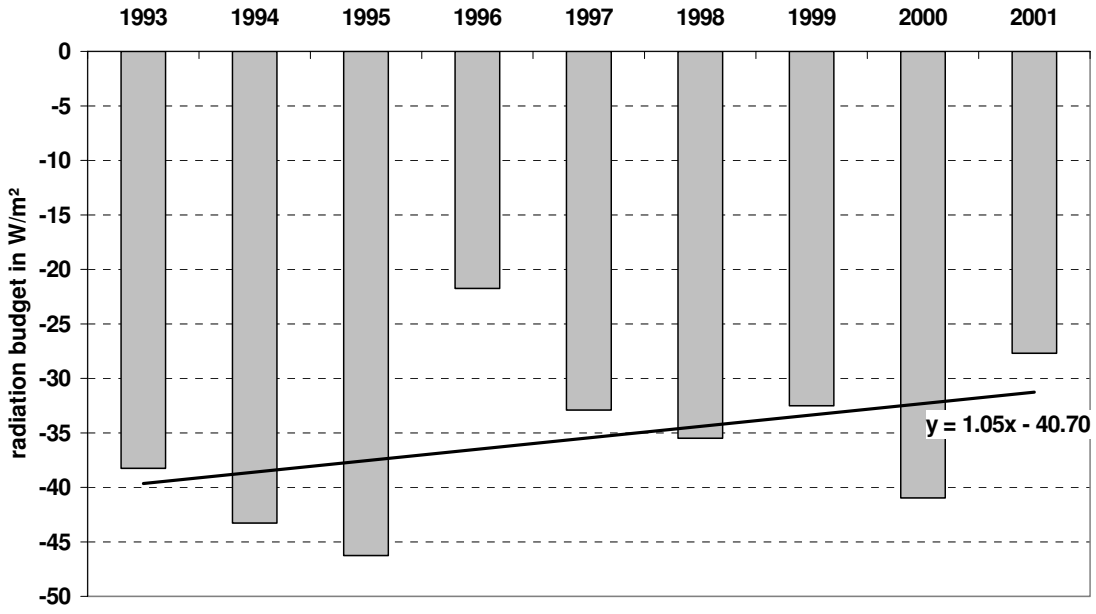

Fig. 2: January-mean of the net radiation budget between 1993 and 2001

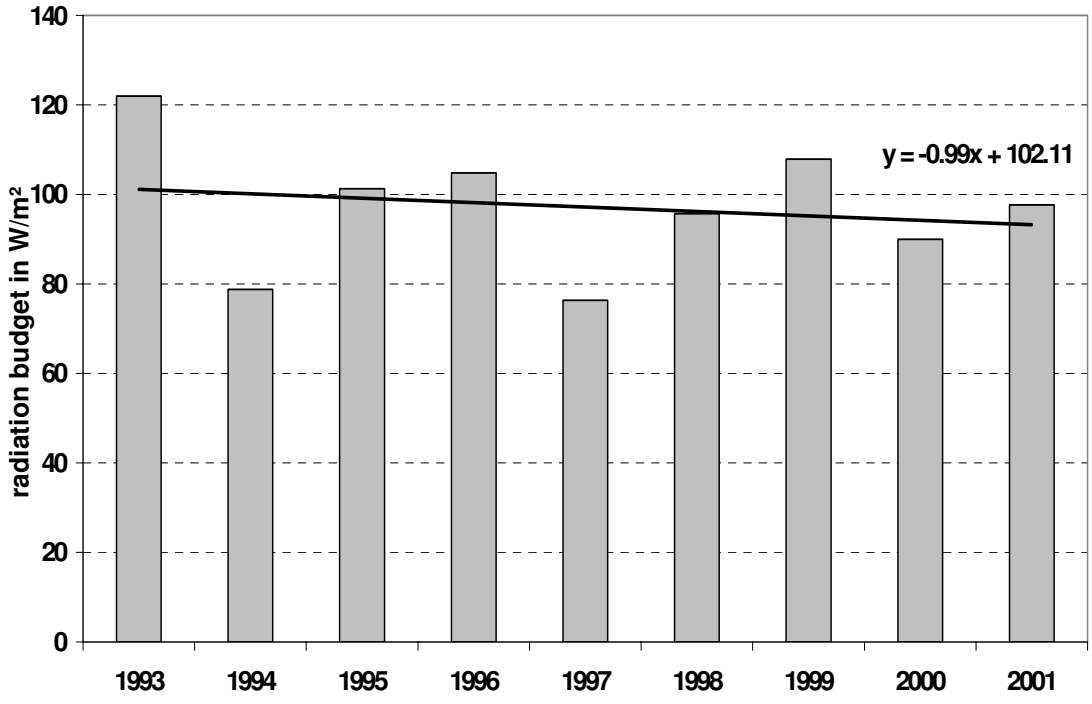

Fig. 3: July-mean of the net radiation budget between 1993 and 2001

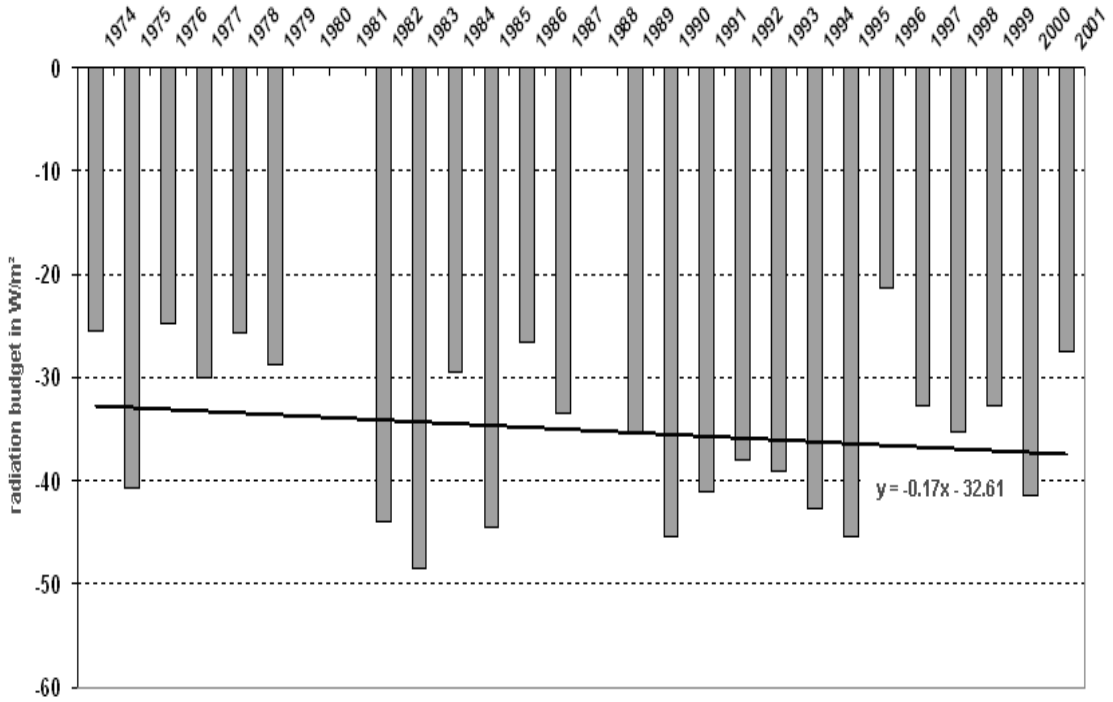

Fig. 4: January-mean of the net radiation budget between 1993 and 2001 (NP data series: 1974 - 1992; Koldewey data series: 1993 - 2001)

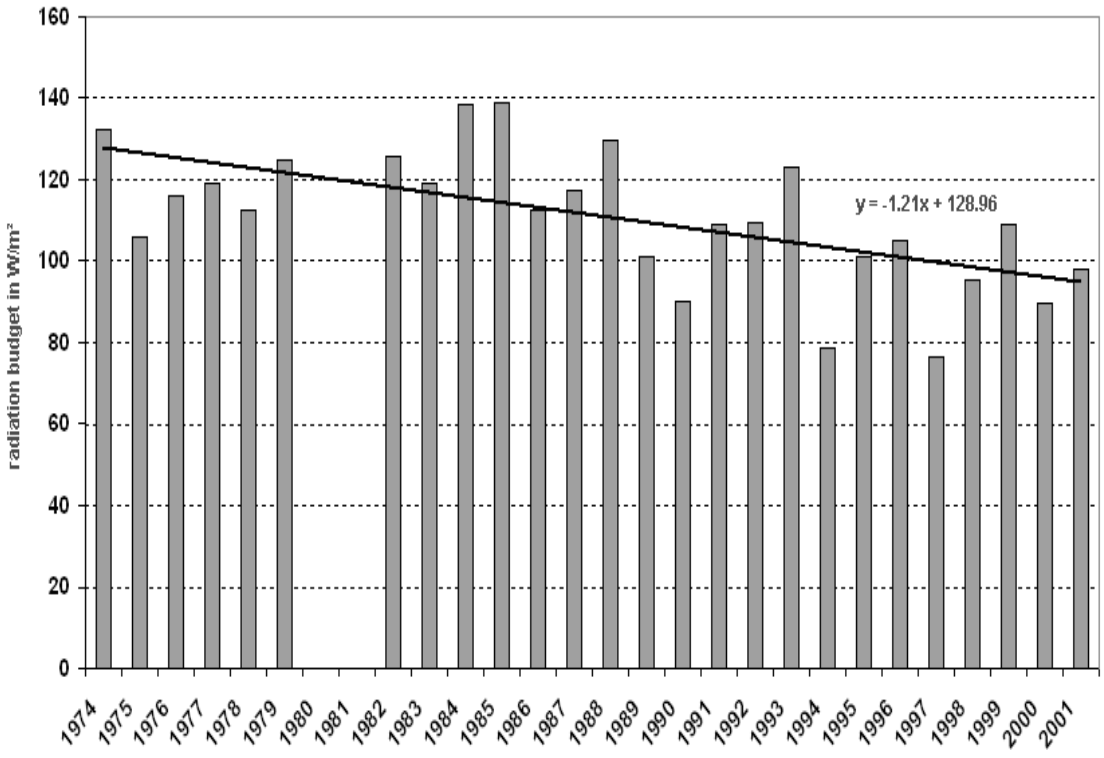

Fig. 5: July-mean of the net radiation budget between 1993 and 2001 (NP data series: 1974 - 1992; Koldewey data series: 1993-2001)

A 4.5.1 Air Temperature

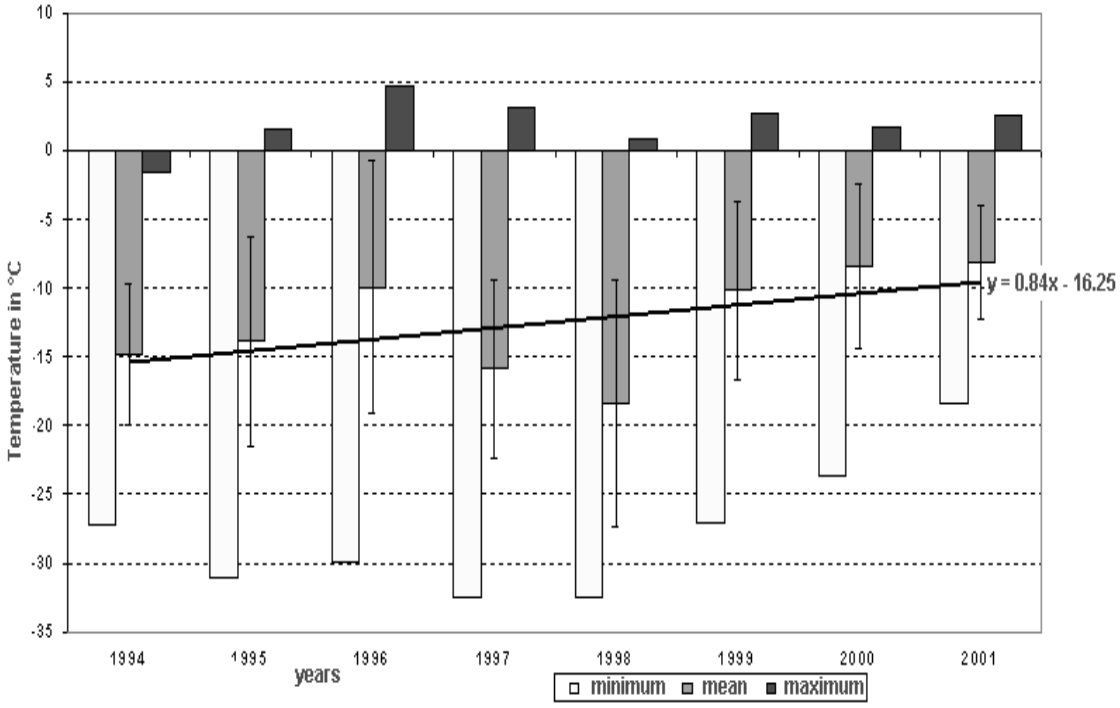

Fig. 1: January-mean and extreme values of the air temperature between 1994 and 2001

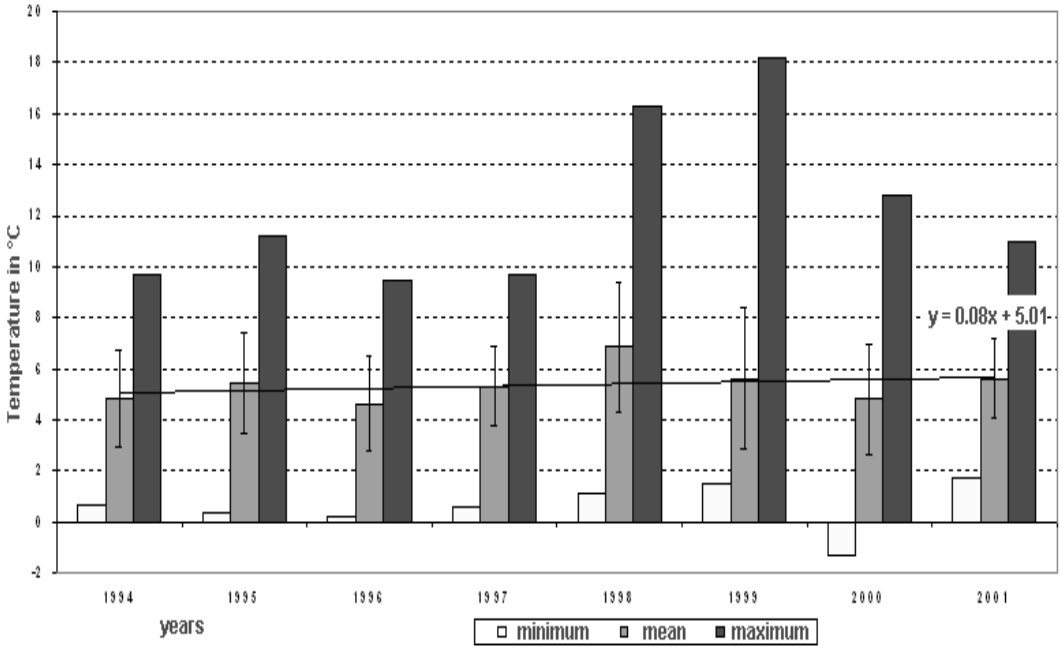

Fig. 2: July-mean and extreme values of the air temperature between 1994 and 2001

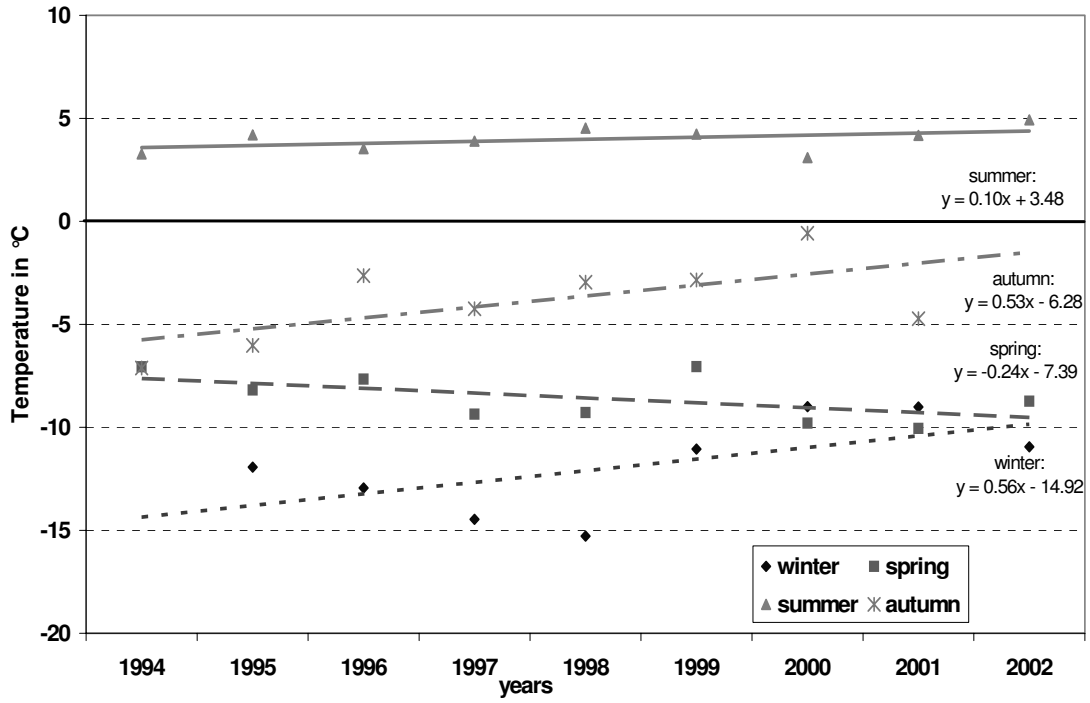

Fig. 3: Seasonal trends of the air temperature between 12/1993 and 8/2002

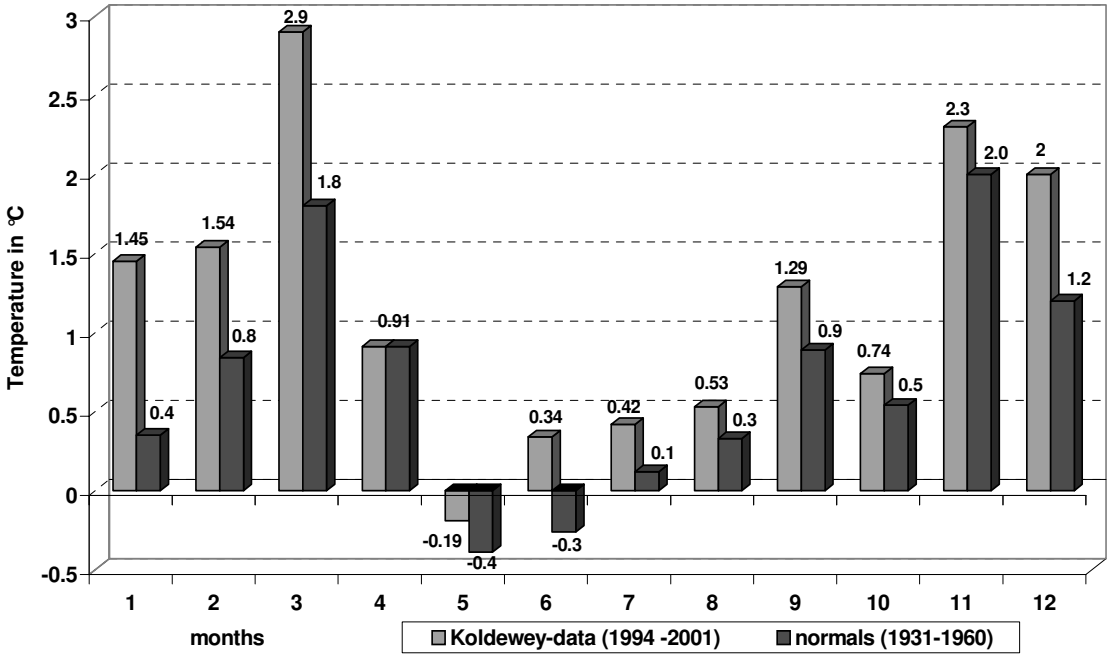

Fig. 4: Variations of the monthly means of the air temperature: Koldewey data series 1994 - 2001 and WMO-normals 1931 – 1960 from the WMO-normals 1961 – 1990

A 4.5.2 Relative Humidity

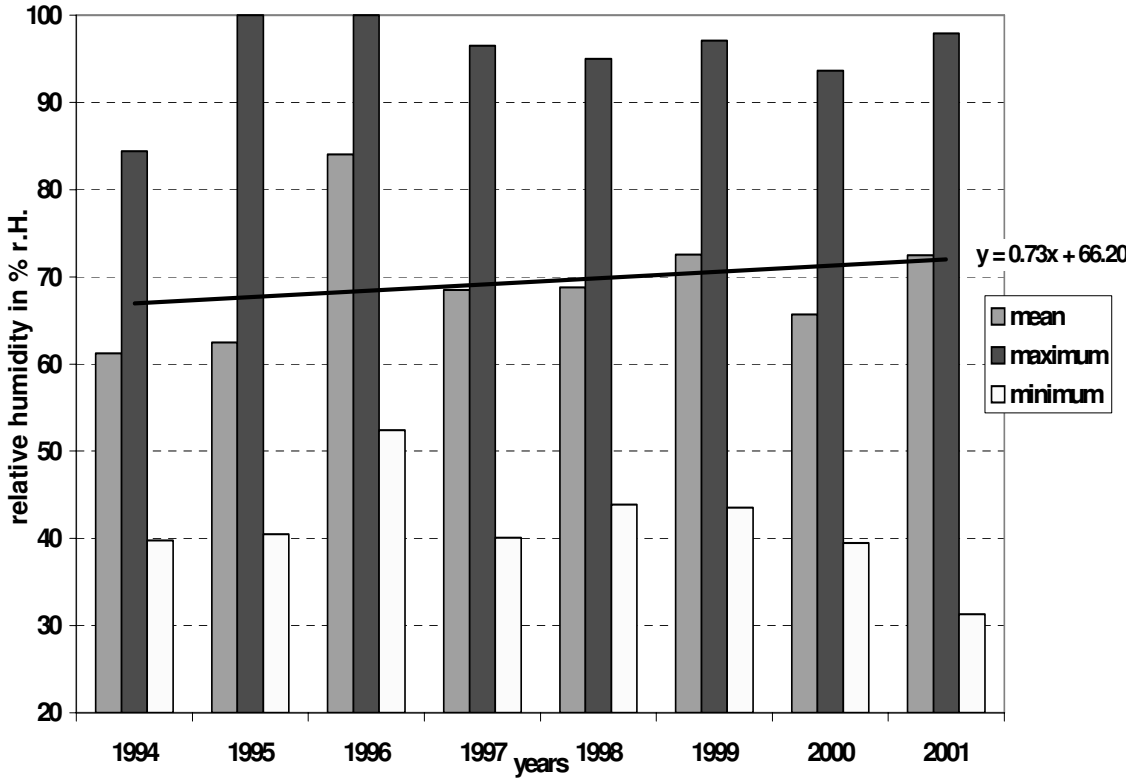

Fig. 1: January-mean and extreme values of the relative humidity between 1994 and 2001

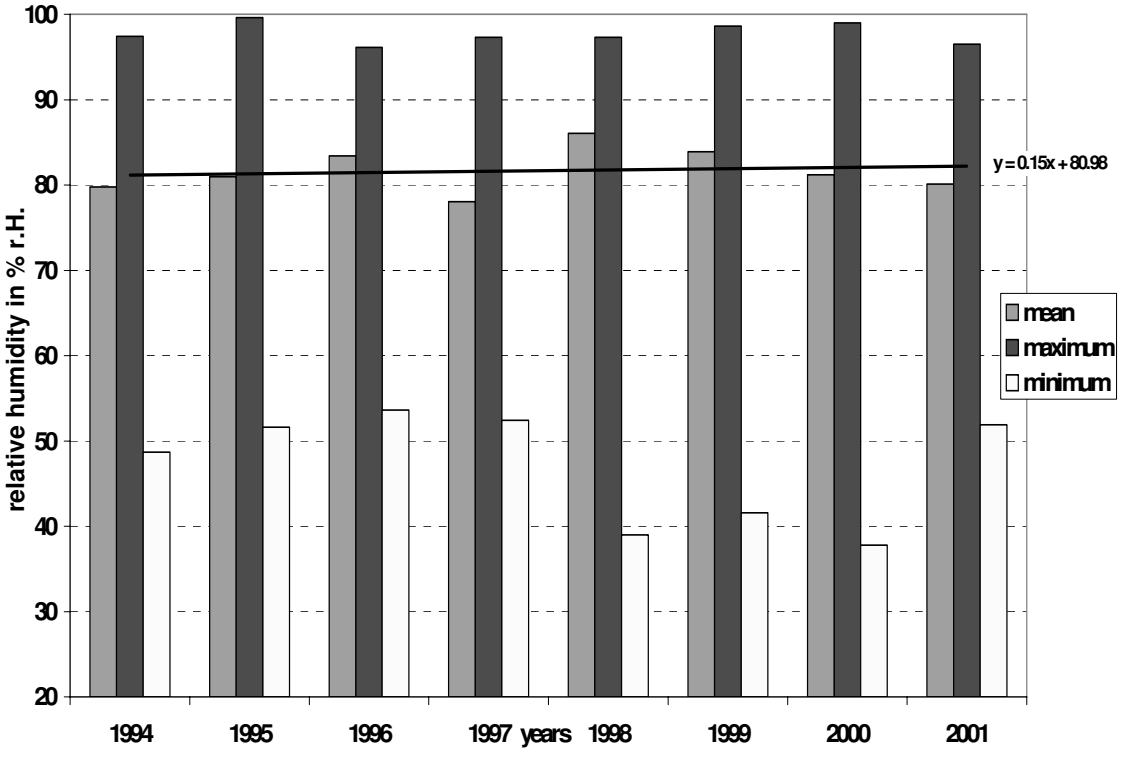

Fig. 2: July-mean and extreme values of the relative humidity between 1994 and 2001

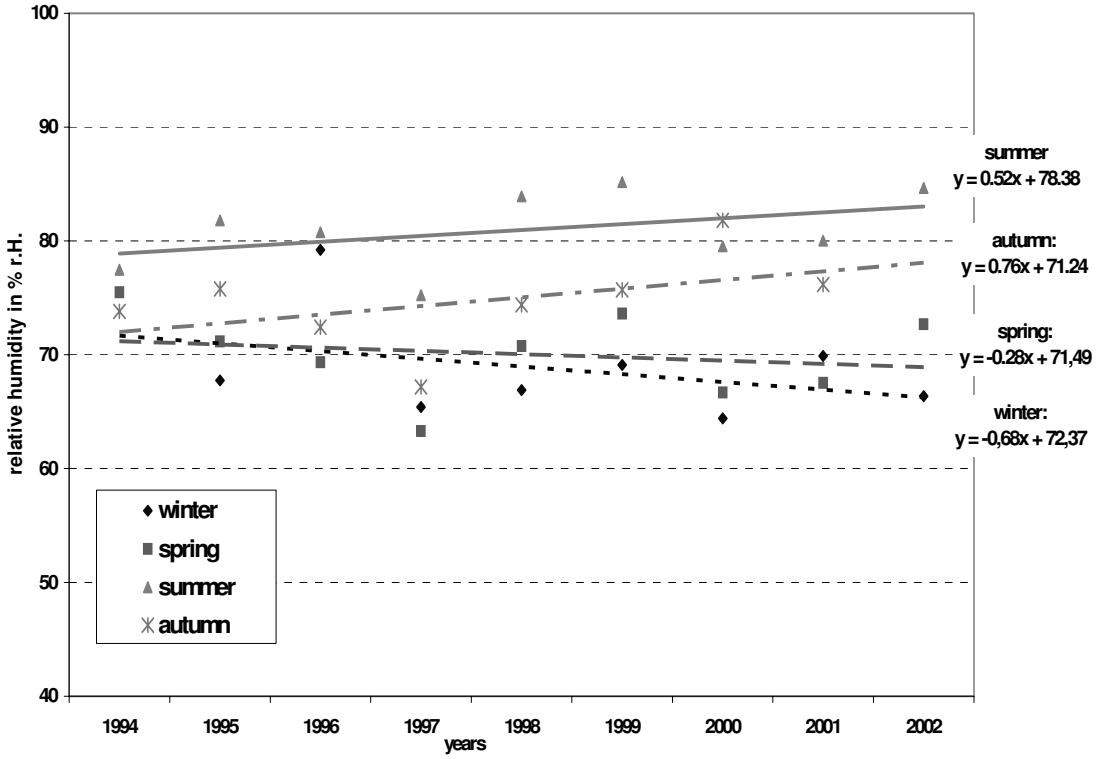

Fig. 3: Seasonal trends of the relative humidity between 12/1993 and 8/2002

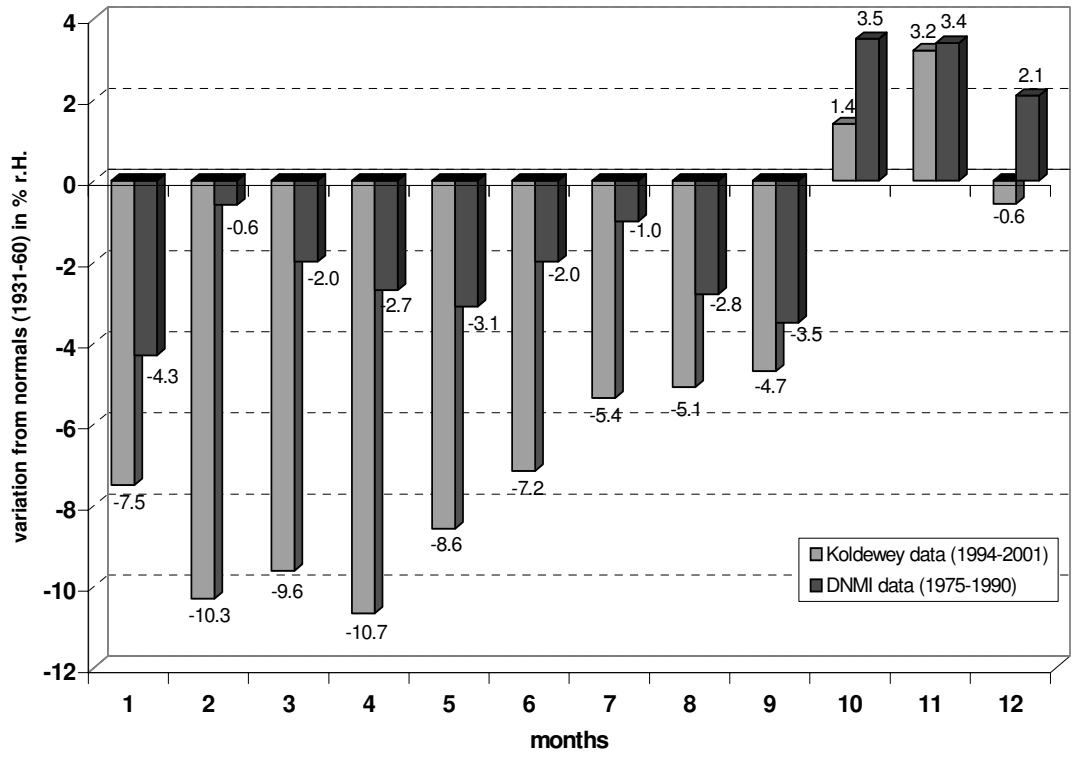

Fig. 4: Variations of the monthly means of the relative humidity: Koldewey data series 1994 - 2001 and DNMI data series 1975 – 1990 from the WMO-normals 1931 - 1960

4.5.3 Air Pressure

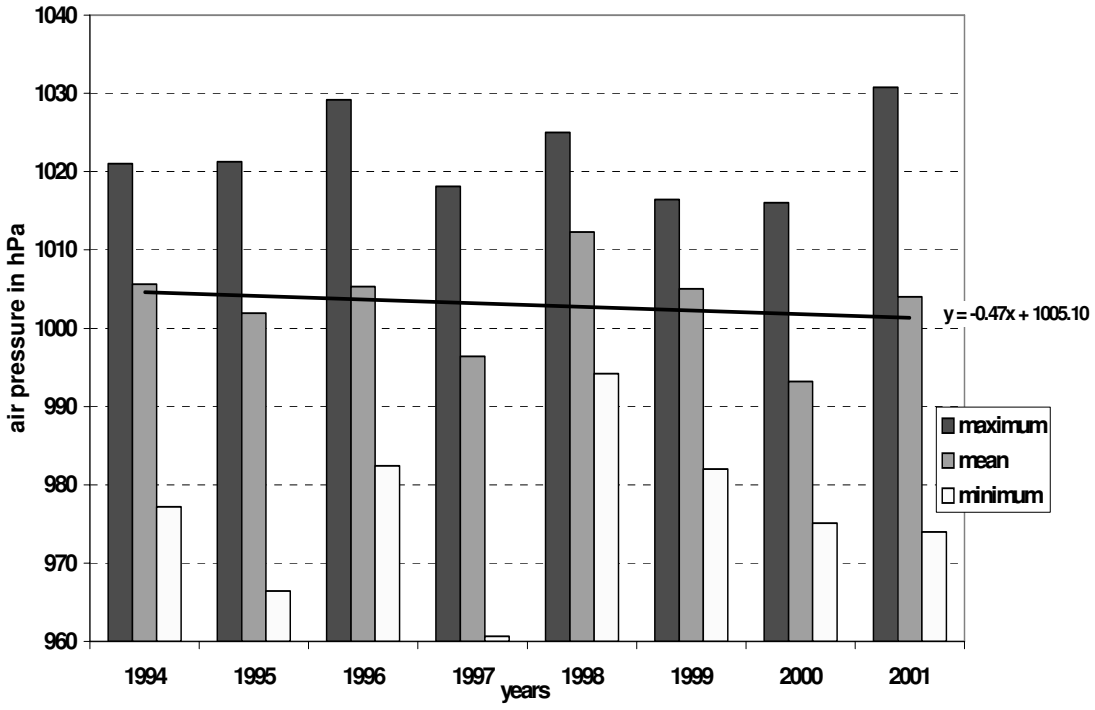

Fig. 1: January-mean and extreme values of air pressure between 1994 and 2001 (11 m above sea level)

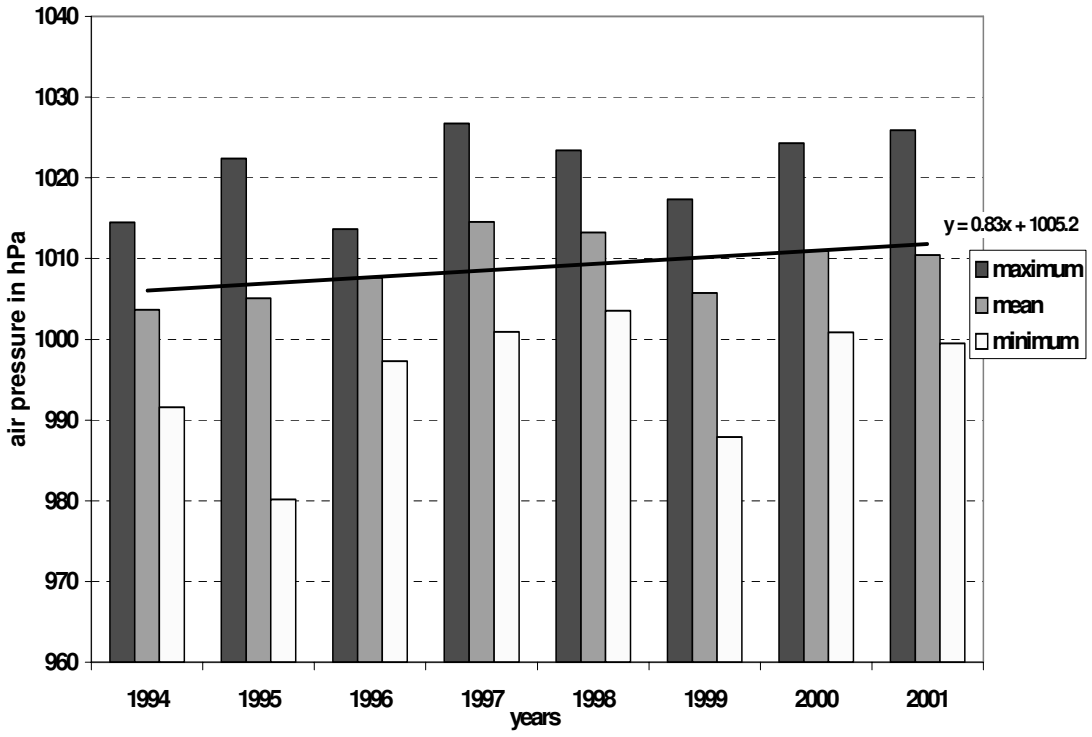

Fig. 2: July-mean and extreme values of air pressure between 1994 and 2001 (11 m above sea level)

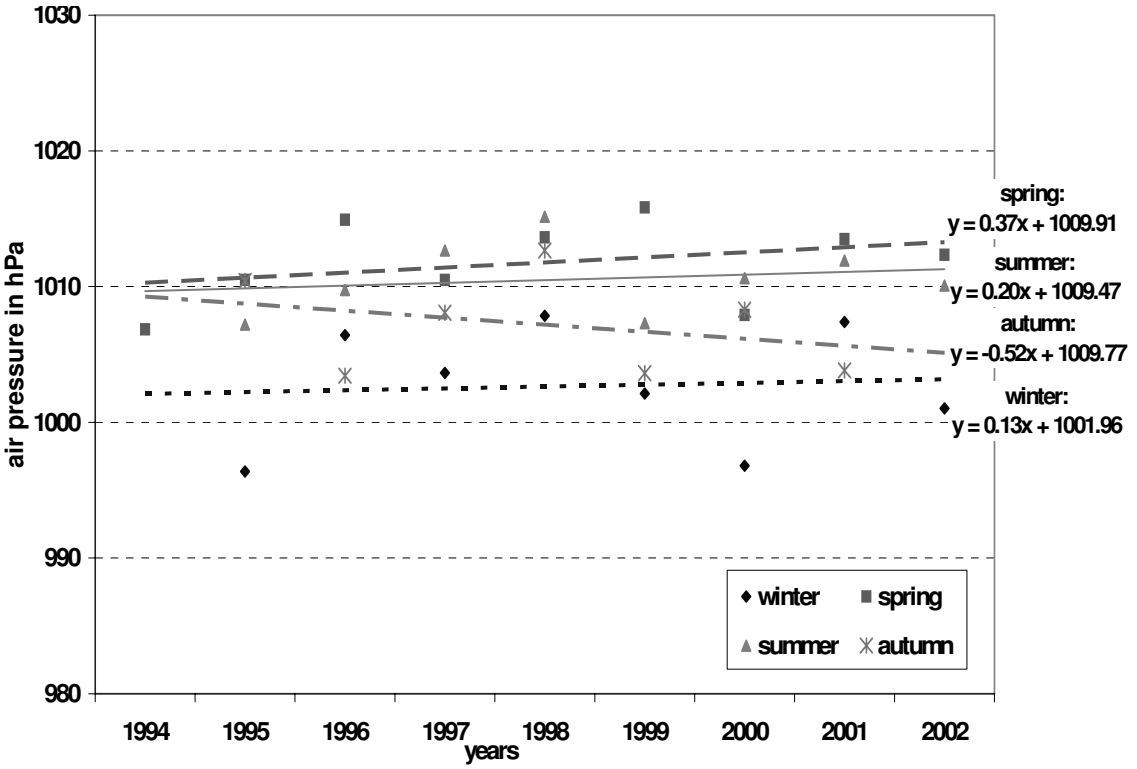

Fig. 3: Seasonal trends of the air pressure (11 m above sea level) between 12/1993 and 8/2002

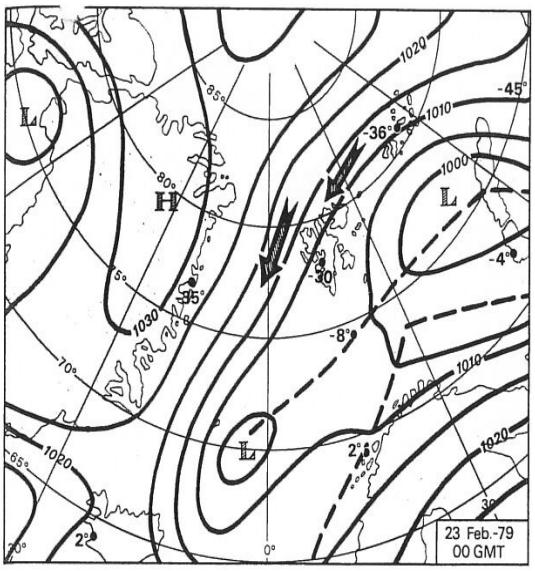

Fig. 4: Cold polar air streams towards Svalbard between lows in the south and a high over Greenland

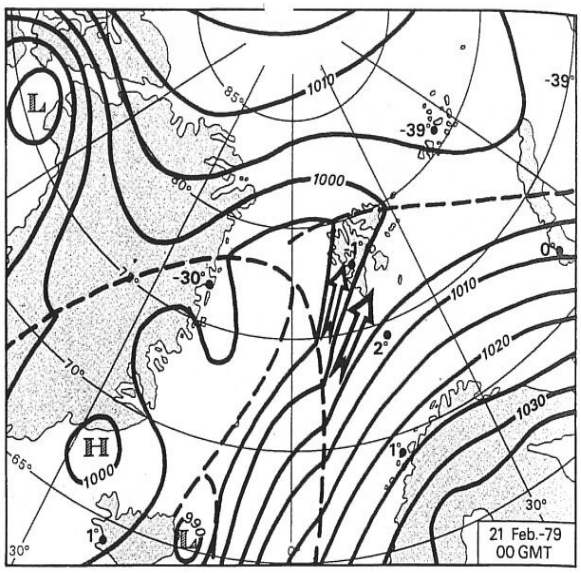

Fig. 5: An intense low with mild maritim air moves towards Svalbard

4.6 Comparison of a clear and a cloudy day

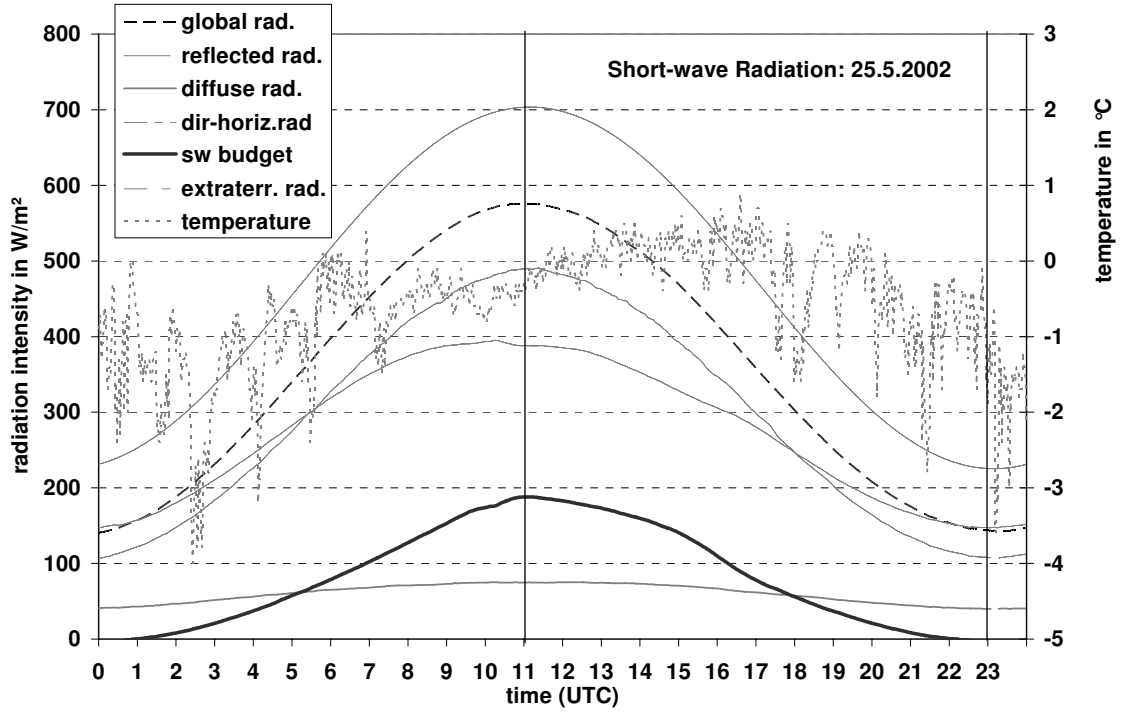

Fig. 1: Daily trends of the air temperature and the shortwave radiation on 25th of May 2002

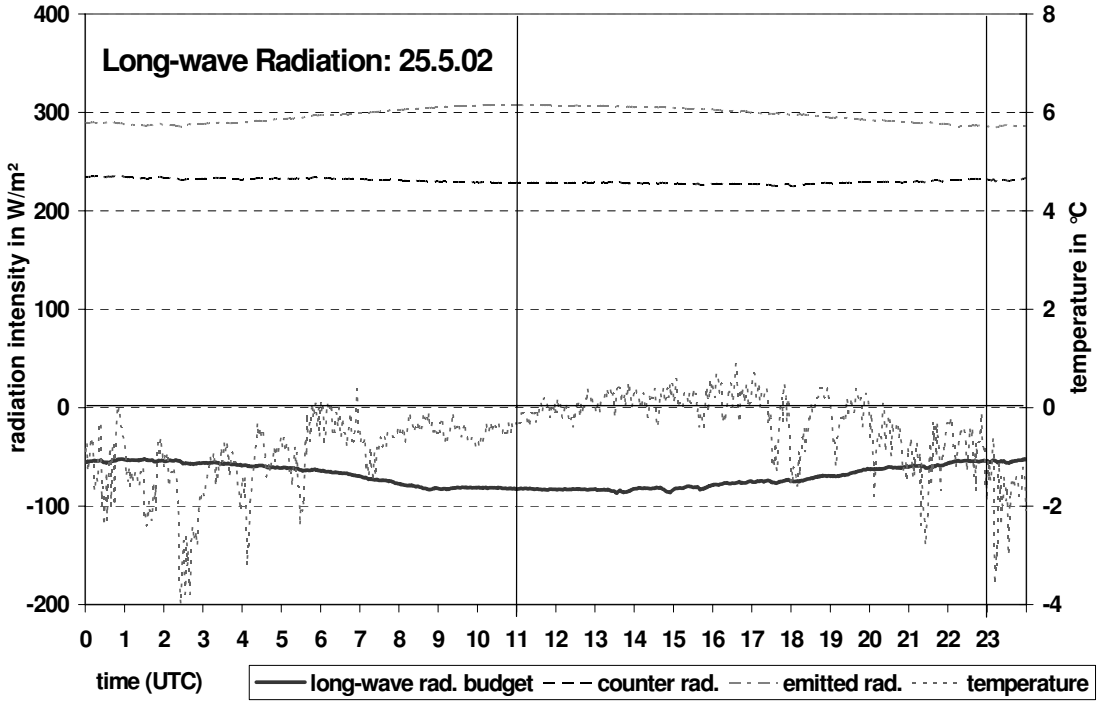

Fig. 2: Daily trends of the air temperature and the longwave radiation on 25th of May 2002

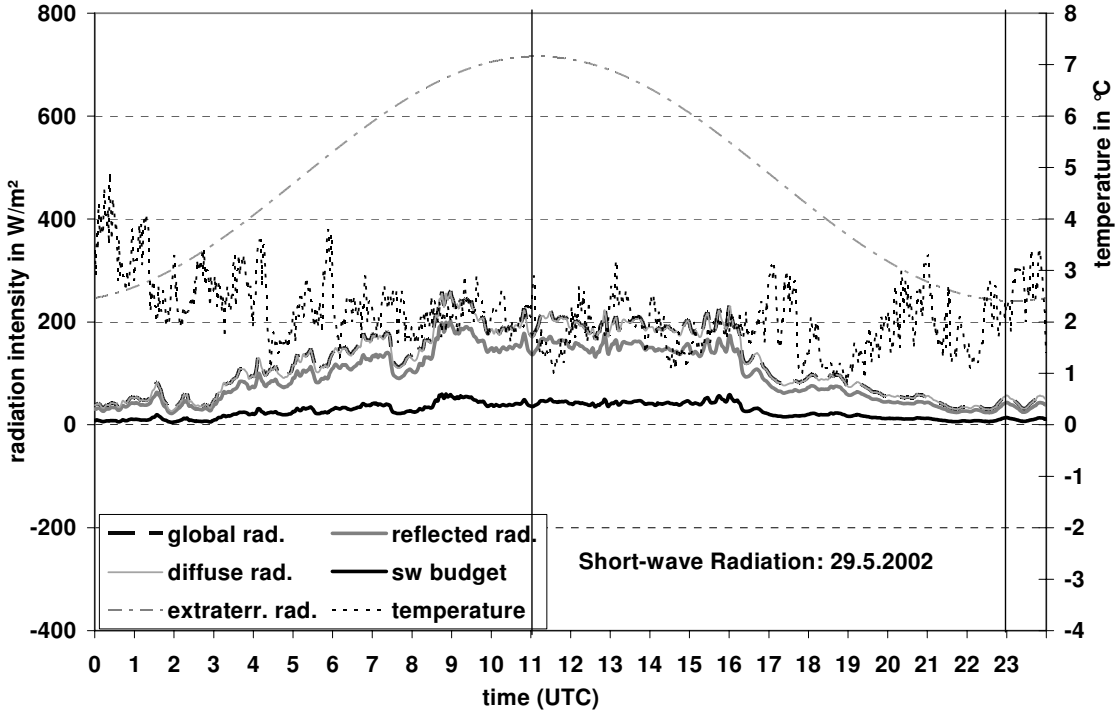

Fig. 3: Daily trends of the air temperature and the shortwave radiation on 29th of May 2002

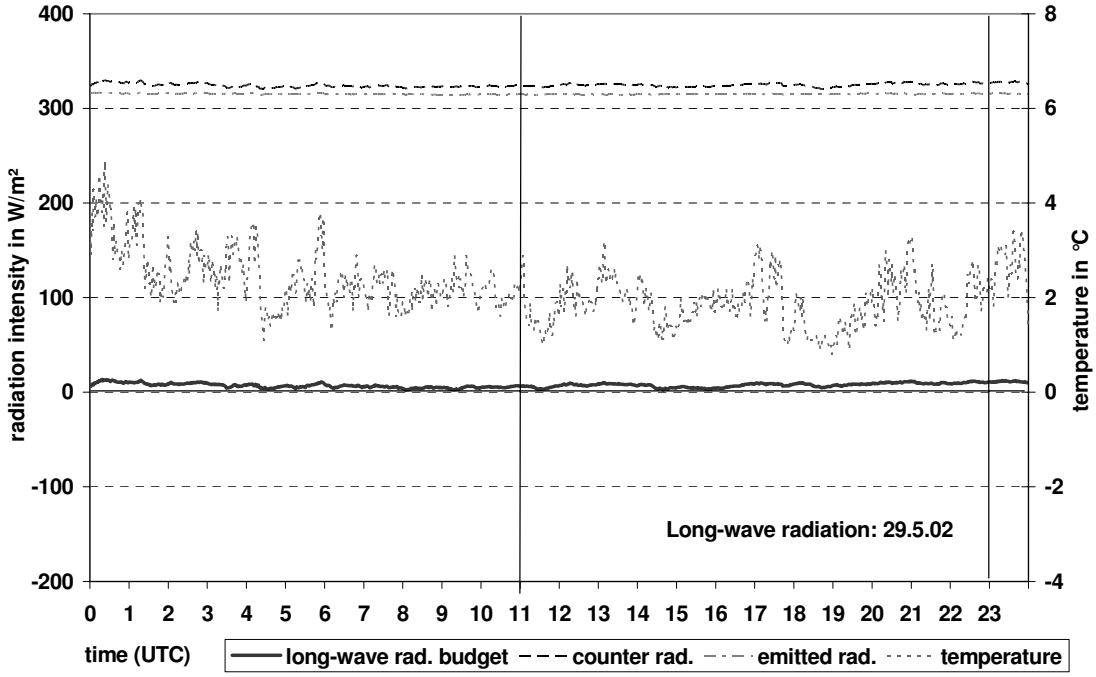

Fig. 4: Daily trends of the air temperature and the longwave radiation on 29th of May 2009

A 4.6 Picture Dokumentation for the Light Conditions on 25th and 29th May 2002

Fig. 5: 25th May 2002 at 00:03

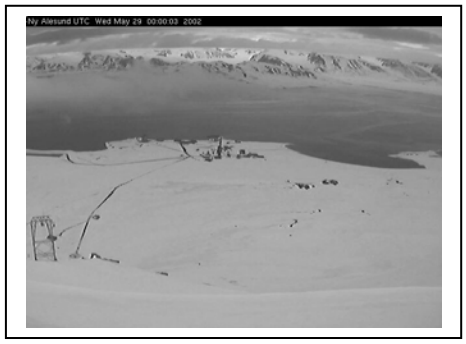

Fig. 6: 29th May 2002 at 00:03

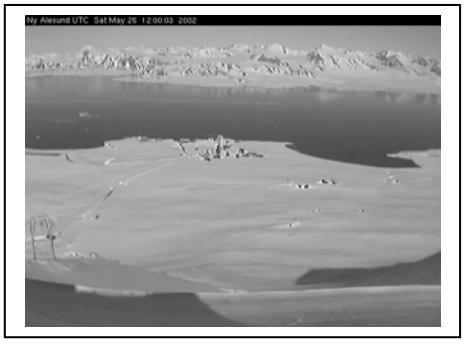

Fig. 7: 25th May 2002 at 06:03

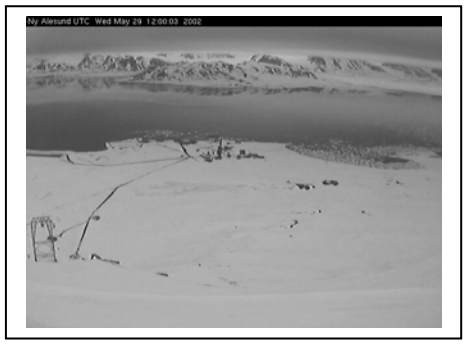

Fig. 8: 29th May 2002 at 06:03

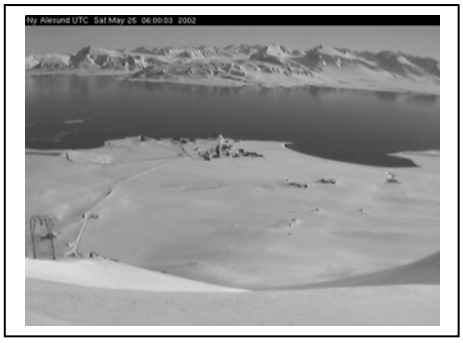

Fig. 9: 25th May 2002 at 12:03

Fig. 10: 29th May 2002 at 12:03

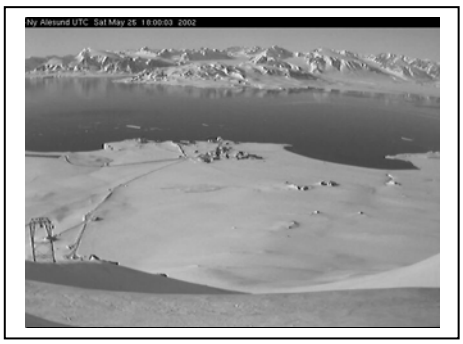

Fig. 11: 25th May 2002 at 18:03

Fig. 12: 29th May 2002 at 18:03

source: MISU, Zeppelin Stasjonen Ny-Alesund: http://www.misu.su.se/~baseline